

Complement-3a receptor involvement in peripheral and central neuropathic pain

A DISSERTATION SUBMITTED TO THE FACULTY OF UNIVERSITY OF MINNESOTA
BY

Jennifer Leigh Cook

IN PARTIAL FULFILLMENT OF THE REQUIREMENTS FOR THE DEGREE OF
DOCTOR OF PHILOSOPHY

Advisor: Lucy Vulchanova

September 2019

© Jennifer L. Cook 2019

ACKNOWLEDGEMENTS

My entire scientific career has been shaped by amazing, brilliant, and fierce female mentors, and I would not be where I am without them.

Firstly, I'd like to thank the members of the Meagher lab. The basement of the Psychology building at Texas A&M is where I fell in love with Neuroscience, and my life forever changed. I owe a debt of gratitude to the scientific mentorship and deep friendship provided by Dr. Erin Young and Dr. Elisabeth Vichaya. I thank Dr. Mary Meagher for giving me a chance to be the lab tech wunderkind and feel like science is where I belong.

Next, I thank Dr. Xiaoying Bai at UT Southwestern, who was my second main scientific mentor. She allowed me to grow as a scientist, and was extraordinarily supportive while I was applying to and interviewing for graduate schools.

My biggest thanks is to Dr. Lucy Vulchanova. You are everything I could have asked for in a mentor and more. You are one of the most brilliant people I've ever met, and I am so honored to have been your student. Your kindness, empathy, and love for your students is unmatched. I am forever grateful for the wonderful graduate experience you created for me. You taught me how to be a scientist, and you supported me while I found what my calling was. I am privileged to call you a mentor and a friend.

I'd like to thank Dr. Carolyn Fairbanks, the chair of my thesis committee and an important collaborator. What I admire most about you is your passion, and your genuine love of science and for the work that you do. You are the person everyone should have in their corner. I have benefitted greatly from your career mentorship, and your support. i.

I'd like to thank my committee members – Dr. Ann Parr, Dr. Yasushi Nakagawa, and Dr. Bradley Taylor. Your feedback, assistance, and support have been invaluable over the past five years. Thank you for giving your time and mentorship, this thesis wouldn't have taken shape without you.

I'd like to thank the Graduate Program in Neuroscience – for providing a stellar foundation, endless support, and a built-in science family. This community is seriously like no other, and visiting Lake Itasca will always feel like coming home.

To the wonderful members of the Vulchanova Lab Family – thank you for your support and friendship. A special thanks to Amy Chan, with whom I owe my sanity for the past few years. Also, my work wouldn't have been possible without the help from Dr. Maureen Riedl, Kelley Kitto, and Galina Kayuzhnaya. Thank you to Reshma, Alex, and Roman for being the best lab brothers and sisters.

Lastly I'd like to thank my family and friends. Grad school is hard, but man is life so much better with all of you in it. Thank you to my parents Kevin and Janet for your endless support, and my brother Kyle and sister Steph for your love and friendship. Thank you to my friends that are like family – Kellie, Adele, and Carrie. I love you all.

DEDICATION

This thesis is dedicated to my parents, Kevin and Janet Cook. You may not understand a word of it, but it wasn't possible without you.

ABSTRACT

VGF (non-acronymic), a neuropeptide precursor protein related to the chromogranin family, has been implicated in neuroplasticity associated with depression, learning and memory, and chronic pain. The Vulchanova lab has previously demonstrated that the VGF-derived peptide TLQP-21 contributes to both the development and maintenance of hypersensitivity after peripheral nerve injury and inflammation. The receptor for TLQP-21 is the complement-3a receptor C3aR1. Although the complement system has been implicated in mechanisms of neuropathic pain, the potential relevance of C3aR1 in these processes has not been addressed. This thesis examines the involvement of C3aR1 signaling following spared nerve injury (SNI) and spinal cord injury (SCI). I hypothesized that C3aR1 located on microglia are a key signaling mediator in neuropathic pain following peripheral and central injury. In this thesis, I show that C3aR1 is localized to microglia in both naïve mice, and mice following SNI and SCI. Following SNI, an antagonist to C3aR1 was able to transiently attenuate mechanical hypersensitivity. Additionally, I found that TLQP-21 specifically activates C3aR1 located on microglia. I identified that there was upregulation of C3aR1 in a time-dependent manner following SNI and SCI. The early increase of receptor expression indicates a potentially important role of C3aR1 signaling throughout the acute stages of peripheral and central nervous system injury. Prior to this thesis work, there were limited studies examining sensory changes occurring in male mice following SCI. I provide the most thorough characterization of behavior following SCI in male mice to date, and show for the first time that SCI mice exhibit a dramatic loss of light touch sensitivity. Utilizing an antisense oligonucleotide, I show a potentially protective effect of knocking down the C3aR1 receptor during the acute phase of spinal cord injury. I found that knockdown attenuated the loss of light touch sensitivity seen in spinal cord injury animals. Overall, this thesis highlights the potential relevance of

iv.

C3aR1 as a therapeutic target following injury, and uncovers the complex role complement receptor-mediated immune signaling has in neuropathic pain.

TABLE OF CONTENTS

List of Tables	vii.
List of Figures	vii - viii.
Introduction	Pg. 1-12
Chapter 1 – Expression and function of the Complement-3a receptor following peripheral nerve injury	Pg. 12 - 33
Chapter 2 – Comprehensive characterization of sensory behavior following a mouse model of spinal cord injury	Pg. 34 - 65
Chapter 3 – Antisense oligonucleotide-mediated knockdown of Complement-3a receptor: Effect on peripheral and central models of neuropathic pain	Pg. 66 - 102
Discussion	Pg. 103 - 109
References	Pg. 110 - 122

Tables

Table 2.1: Experimental groups in chapter 2	37
Table 2.2: BMS Scores	42
Table 3.1: Experimental groups in chapter 3	70

Figures

Figure 1.1: Spinal localization of C3aR1.	20
Figure 1.2: TLQP-21 activates C3aR1 in cultured primary microglia.	23
Figure 1.3: C3aR1 mediates peripheral nerve injury-induced hypersensitivity.	25
Figure 1.4: Spinal expression of C3aR1 increases after nerve injury.	27
Figure 1.5: Spinal C3aR1-ir is localized in microglia after nerve injury.	29
Figure 2.1: Male ICR mice recover locomotion following mild and moderate thoracic contusion spinal cord injury in a reproducible manner	43
Figure 2.2: Analysis of mild 50 kdyn thoracic contusion spinal cord injury effects on fine motor coordination in male ICR mice	45
Figure 2.3: Mechanical withdrawal thresholds are not altered following mild and moderate thoracic contusion spinal cord injury in male ICR mice	48
Figure 2.4: Following mild or moderate thoracic contusion spinal cord injury, injury severity measured on day one affects whether male ICR mice develop heat hyperalgesia	51
Figure 2.5: Following mild or moderate thoracic contusion spinal cord injury, injury severity measured on day one affects how much male ICR mice burrow	54
Figure 2.6: Mild and moderate thoracic contusion spinal cord injury induces a dramatic loss of light touch sensitivity in male ICR mice	57

Figure 3.1: Treatment with C3aR1 ASO significantly knocks down expression of C3aR1 in the spinal cord.	74
Fig. 3.2: Treatment with C3aR1 ASO has no effect on the development or maintenance of hypersensitivity following peripheral nerve injury	76
Figure 3.3: Spinal expression of C3aR1 and Iba1 is increased 6 days after spinal cord injury.	78
Figure 3.4: Iba1 and C3aR1 are present in the dorsal columns of SCI mice.	79
Figure 3.5: Treatment with C3aR1 ASO 3 days following a mild 50 kdyn contusion SCI has variable effect on pain-related behaviors.	84
Figure 3.6: Treatment with C3aR1 ASO 3 days following moderate 75 kdyn thoracic contusion SCI has a variable effect on behavior in male ICR mice	88
Figure 3.7: Control ASO induces thermal hypersensitivity in injured subjects.	91
Figure 3.8: Control ASO-induced changes in expression of C3aR1 in injured subjects	94

INTRODUCTION

Chronic pain overview

Pain is defined as “an unpleasant sensory or emotional experience associated with actual or potential tissue damage, or described in terms of such damage” (International Association for the Study of Pain, 2017). Chronic pain affects approximately 20 percent of the worldwide population, or around 1.5 billion people. Chronic pain is one of the leading causes of disability (Nahin, 2015). Over 100 million people in the United States suffer from chronic pain (Johannes, Le, Zhou, Johnston, & Dwor kin, 2010; Nahin, 2015), with economic costs equaling 600 billion dollars per year in treatment and lost productivity (Gaskin & Richard, 2012). Chronic pain was added to the most recent International Classification of Diseases (ICD-11) released in May 2019, where it was defined as “pain that lasts or recurs for more than three months” (Benoliel et al., 2019; Treede et al., 2015).

Why and how do we have pain?

Pain is an important protective mechanism, alerting us to potential bodily damage in addition to encouraging us to guard injured areas from further damage. Pain information is sent by primary afferents called nociceptors. Nociceptors fall into two major classes, including thinly myelinated a-delta fibers and small diameter unmyelinated c-fibers (Dubin & Patapoutian, 2010). The types of stimuli that nociceptors respond to include temperature, mechanical stimuli, and chemical stimuli. Nociceptors respond within a narrow physical range. The specific stimuli nociceptors are activated by depend on the receptors expressed at the peripheral terminals. Nociceptors innervated by a-delta fibers produce short latency pain that is described as sharp or pricking, whereas C-fibers

produce dull, burning pain that is diffusely localized and poorly tolerated (Ringkamp & Meyer, 2010).

Chronic Pain: Peripheral and Central Sensitization

Chronic pain can occur due to maladaptive changes transpiring at both the peripheral and central levels. Peripheral sensitization occurs at the level of the nociceptors, at the terminals located in the target organs that have undergone injury. Sensitization of the nociceptive afferents leads to lowered thresholds. These thresholds are lowered in response to the release of various chemicals generated during tissue injury and inflammation (Stein et al., 2009). Immune cells in the periphery can release some of these factors, including cytokines, prostaglandins, chemokines, and growth factors (Ren & Dubner, 2010). Other chemicals, such as ATP and glutamate, are released from the damaged cells at the location of the injury (Millan, 1999).

Central sensitization occurs at the level of the spinal cord, through a phenomenon called Wind Up. Dorsal horn neurons can present with enhanced excitability due to sustained C-fiber firing. The consistent action potentials lead to post-synaptic depolarization which activates NMDA receptors. This causes long-term changes in cellular excitability, referred to as spinal long term potentiation (LTP), and this can lead to spontaneous firing of dorsal horn neurons (D'Mello & Dickenson, 2008; Ji, Kohno, Moore, & Woolf, 2003). Another mechanism leading to central sensitization is a reduction of inhibitory drive. The majority of neurons in the spinal cord dorsal horn are interneurons, with a number of these being inhibitory (Peirs & Seal, 2016). Inhibitory neurons play an important role in the "gate theory" of pain, developed by Melzack and Wall in the 1960s (Melzack & Wall, 1965). The way that the central nervous system normally controls the perception of pain is through local circuits in the spinal cord dorsal horn, necessary to balance incoming nociceptive

and non-nociceptive input. There is a convergence of these two in the dorsal horn, coming from nociceptive C-fibers and non-nociceptive A-beta fibers. Activation of non-nociceptive fibers inhibits the transmission of nociceptive input to the brain, but a delicate balance of the system is necessary. During central sensitization, there is an increase of intracellular chloride that occurs as a result of downregulation of potassium-chloride co-transporters. This can lead to reduced inhibitory (GABAergic and glycinergic) transmission, known as disinhibition, or even a reversal of inhibitory activity to excitatory (Meisner, Marsh, & Marsh, 2010a; Price, Cervero, & de Koninck, 2005; Price & Prescott, 2015; Zeilhofer, Benke, & Yevenes, 2011).

Central sensitization occurring in the spinal cord leads to two behavioral phenomena known as allodynia and hyperalgesia. Allodynia is when a stimulus that is normally not painful, such as a normal touch, is perceived as painful. Hyperalgesia is when a normally painful stimulus elicits an enhanced painful sensation. These two behavioral consequences in particular are hallmarks of neuropathic pain (Eide, Jørum, & Stenehjem, 1996; Jensen & Finnerup, 2014).

Chronic Pain: Immune System Involvement

The immune system's role in chronic pain has been investigated with great interest over the past few decades. Historically, many believed the immune system only played a role in pain arising from inflammation. It has become clear that immune cells are involved at both the peripheral and central levels.

In the periphery, when there is disruption of a barrier, such as the skin, the immune system responds in a stereotypical fashion. Almost immediately following this injury, the cell intrinsic and innate immune system is activated, as a fast and nonspecific response (Kupper & Fuhlbrigge, 2004; Uematsu & Akira, 2008). Cell types involved in the immediate response include complement factors, macrophages, dendritic cells, eosinophils, mast cells, and neutrophils, among others. Around 96 hours after injury, the adaptive immune system is activated, with specific responses that carry a “memory.” Cell types include CD4+ and CD8+ T-cells, and B-cells that secrete antibodies (Bangert, Brunner, & Stingl, 2011; Grice & Segre, 2011). The infiltration of immune cells to the injured barrier are capable of producing inflammatory pain, through the release of DAMPs, or danger associated molecular patterns, aka alarmins (Schaefer, 2014). These can include proinflammatory cytokines such as TNF-alpha and IL-1-beta released by macrophages, CGRP and Substance P released by neurons, or prostaglandins released by mast cells. The influx of inflammatory agents can cause localized swelling, redness, and pain due to activation of nociceptors (Schaefer, 2014; Tang, Kang, Coyne, Zeh, & Lotze, 2012).

In addition to immune activation occurring at the level of the skin, when there are injuries to peripheral nerves, the immune system is a key component of the development of neuropathic pain. Macrophages can respond to chemotactic signals and are recruited to the peripheral nerves and the dorsal root ganglion following injury (Cui, Holmin, Mathiesen, Meyerson, & Linderöth, 2000; T. Liu, Van Rooijen, & Tracey, 2000). Activated macrophages release a number of proinflammatory cytokines capable of binding to cytokine receptors located on peripheral nerves, thus activating them. Interestingly, in addition to the pronociceptive actions of immune cells at the site of peripheral nerve injury, there are also potentially protective roles that can occur in the right conditions. Following

peripheral nerve injury, opioid receptors are upregulated at the site of injury, and activation of leukocytes can induce endogenous opioid release (Sauer et al., 2014). Additionally, macrophages in the M2 (anti-inflammatory) state can also release endogenous opioids to reduce pain-related behavior following peripheral nerve injury (Pannell et al., 2016).

The immune system also plays a critical role in pain at the level of the central nervous system. The resident immune cells in the central nervous system are microglia, which have a monocytic origin, similar to macrophages. Microglia therefore overlap significantly with macrophages in terms of their receptors and factors that they produce (Kreutzberg, 1996; Ransohoff & Brown, 2012). Microglia make up approximately 10 to 15 percent of all cells in the central nervous system. As the resident immune cells, microglia are continually sampling their environment for potential damage. The role of microglia in a healthy central nervous system is to scan for damaged neurons, unnecessary synapses, and infectious agents (Kreutzberg, 1996). They phagocytose damaged tissue, and are responsible for performing as antigen-presenting cells to activate T-cells (Gehrmann, Matsumoto, & Kreutzberg, 1995). Due to the sensitivity of neurons to damage, microglia are sensitive to the slightest change in environmental milieu. Microglial activation is a crucial component of central sensitization and neuropathic pain. In the spinal dorsal horn, microglia surround the spinal terminals of nociceptors. Following peripheral injury, nociceptors are activated, flooding the dorsal horn with pronociceptive peptides such as CGRP and Substance P, in addition to excitatory neurotransmitters such as glutamate (Reichling & Levine, 2009). Microglia express a number of neurotransmitter receptors and become activated by these factors released at the terminals (H. Liu, Leak, & Hu, 2016). Activated microglia then release a number of proinflammatory factors such as TNF-alpha, IL-1beta, ATP, and prostaglandins (Austin & Moalem-Taylor, 2010). These factors are then capable of binding

to receptors located on both the primary afferent terminal and the second order neuron. This soup of proinflammatory factors entering the environmental milieu simultaneously can induce and/or prolong central sensitization. Many mouse and rat studies have blocked the activation of microglia following peripheral and central injury and have been able to attenuate the development of neuropathic pain (Hains, 2006b; Sorge et al., 2011; Staniland et al., 2010; Zhuang et al., 2007).

Neuropathic Pain: Animal Models

There are over forty existing animal models utilized for the study of neuropathic pain that are produced from peripheral or central nervous system injury (Jaggi, Jain, & Singh, 2011). The studies presented in this thesis use a peripheral model, spared nerve injury (SNI), and a central model, spinal cord injury (SCI).

The spared nerve injury (SNI) model is a well-established model of peripheral nerve injury that produces substantial and prolonged changes in mechanical sensitivity and cold responsiveness that closely mimic the cutaneous hypersensitivity associated with clinical neuropathic pain (Decosterd & Woolf, 2000). In this injury, the three branches of the sciatic nerve are exposed, between the hip and the knee. The peroneal and tibial nerves are ligated and cut, and the sural nerve is left intact. Following this injury, subjects develop mechanical hypersensitivity in the ipsilateral hindpaw, in the lateral portion of the hindpaw which is innervated by the sural nerve (Decosterd & Woolf, 2000). This hypersensitivity is long-lasting, and interventions can be administered to disrupt both the development and maintenance of pain behavior following SNI.

The spinal cord injury model isn't necessarily one singular model, but rather a group of injuries that can be elicited by impact, transection, or excitotoxic chemicals (Cheriyian et al., 2014; Jaggi et al., 2011). The work presented in this thesis used a thoracic contusion injury in mice to study pain-related behaviors. The majority of animal studies examining pain behavior following spinal cord injury have been done in rats. Following thoracic contusion spinal cord injury, rats typically develop mechanical allodynia and thermal hyperalgesia (Hains, 2006a; Hama & Sagen, 2007; Peng et al., 2009; Sweitzer, Pahl, & DeLeo, 2006; Zhao, Waxman, & Hains, 2007a). Performing SCI in mice is more complex, due to their smaller size. Mice develop heat hyperalgesia reliably following SCI, but development of mechanical hypersensitivity is more variable (Hoschouer, Basso, & Jakeman, 2010; Kerr & David, 2007; Meisner et al., 2010a).

Granins: VGF

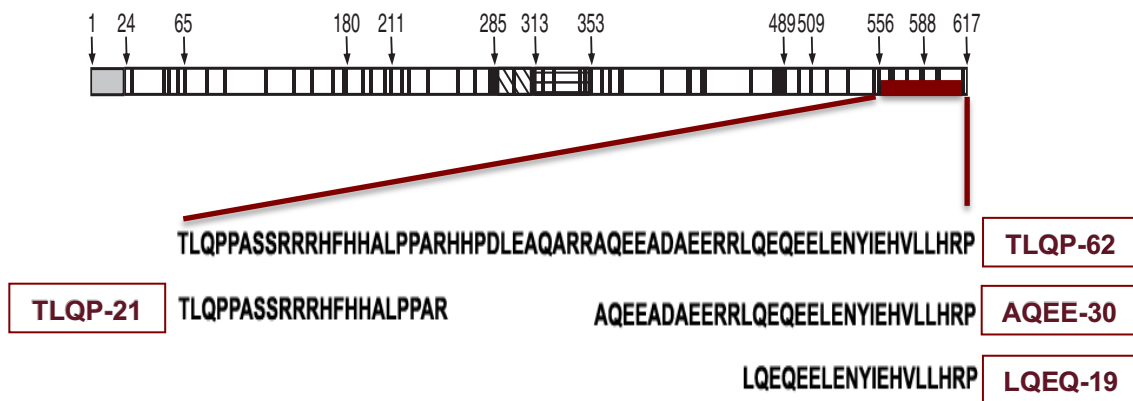
Granins are a family of proteins that are processed into a number of bioactive peptides that are packaged into large dense-core vesicles and secreted via the regulated secretory pathway. The hallmark of granins compared to other secretory proteins is their size and their low isoelectric point. Granins are typically larger than 50 kDa, and have an isoelectric point between 4.5 and 6.1, indicating an acidic composition (Alessandro Bartolomucci et al., 2011; Helle, 2004; Taupenot, Harper, & O'Connor, 2003). Granins are typically expressed in endocrine cells and peptidergic neurons, where they are synthesized in the rough endoplasmic reticulum. Proteins that are released via the regulated secretory pathway must be initially stimulated by a secretagogue, which binds to the cells that produce granins and stimulates the secretion of them. This differs from the constitutive secretory pathway, where proteins can be secreted continuously without stimulation. The

most well-known proteins in the granin family include chromogranin A and B, secretogranin, VGF, and ProSAAS (Alessandro Bartolomucci et al., 2011; Taupenot et al., 2003).

The neurotrophin-inducible protein VGF (non-acronymic) is 617 amino acids long and is expressed in neurons and neuroendocrine cells (Salton, Fischberg, & Dong, 1991). Like other granins, it is proteolytically cleaved into a number of bioactive peptides, which are packaged into large dense core vesicles and released via the regulated secretory pathway. Research on VGF has implicated its involvement in neuroplasticity associated with learning and memory, depression, and chronic pain (A. Bartolomucci et al., 2006; Hunsberger et al., 2007; Lacroix-Fralish, Austin, Zheng, Levitin, & Mogil, 2011; Lin et al., 2015; Moss et al., 2008; Riedl et al., 2009; Thakker-Varia et al., 2007). The Vulchanova lab began researching the involvement of VGF in chronic pain following a proteomic analysis of dorsal root ganglion (DRG) cultures, a model of axotomized neurons. They compared protein levels in cultured DRG at 24 hours utilizing proteomic differential expression analysis (Riedl et al., 2009), and found a 45-fold increase in VGF expression, more than any other protein analyzed. In addition to DRG cultures, the Vulchanova lab examined VGF expression following peripheral nerve injury and inflammation, and found rapid and significant increases in expression at multiple timepoints after injury.

The majority of the Vulchanova lab's work has focused on the C-terminal peptides of VGF. There are a number of cleavage sites within the C-terminus of VGF, producing at least four known bioactive peptides, TLQP-62, TLQP-21, AQEE-30, and LQEQ-19 (Levi, Ferri, Watson, Possenti, & Salton, 2004). These peptides are named for the first four amino

acids in the sequence, followed by the length of the peptide. The largest C-terminal peptide is TLQP-62, which is further cleaved into TLQP-21 and AQEE-30. Previous work from the Vulchanova lab examined the involvement of TLQP-21 in pain following Complete Freund's adjuvant (CFA) induced inflammation and spared nerve injury, a model of long-lasting neuropathic pain (Fairbanks et al., 2014). It was found that an antibody to TLQP-21 (anti-TLQP-21) injected before an intraplantar injection of CFA was able to block the development of CFA-induced tactile hypersensitivity beginning at 2 hours post-CFA injection. Additionally, anti-TLQP-21 injected either before or after spared nerve injury was able to disrupt the development and the maintenance of tactile hypersensitivity. These results indicated that TLQP-21 signaling is a critical component of the pronociceptive cascade occurring following both inflammatory and neuropathic pain models.



Schematic representation of the neuropeptide precursor VGF and its C-terminal peptides. VGF peptides are named for their first four amino acids and the total length.

TLQP-21/C3aR1

TLQP-21 is a particularly interesting peptide to explore, due to the discovery of a receptor for the peptide in 2013. Utilizing CHO-K1 cells and mouse models, it was found that the G-protein coupled receptor complement C3a receptor-1 (C3aR1) is the receptor for TLQP-21 (Hannedouche et al., 2013). The complement pathway is a component of the innate immune system, which is called into action by invading pathogens and endogenous signals indicating injury. The complement 3a receptor-1 (C3aR1) was originally identified as the cognate G-protein coupled receptor for complement component 3a (C3a), a member of the alternative complement pathway (Biryukov & Stoute, 2018; Guo et al., 2010; Harboe & Mollnes, 2008). TLQP-21 and C3a have a competitive relationship at the same binding site within C3aR1 (Cero et al., 2014; Hannedouche et al., 2013). Activation of C3aR1 leads to leukocyte activation and chemotaxis and can mediate apoptotic cell death, demyelination, and activation of resting microglia and astrocytes (Peterson & Anderson, 2014). C3aR1 participates in microglial signaling under pathological conditions including neurodegeneration and virus-induced cognitive impairment (Lian et al., 2015; Vasek et al., 2016). C3aR1 has been localized to neurons, microglia, and cultured astrocytes via *in situ* hybridization (Davoust, Jones, Stahel, Ames, & Barnum, 1999). Although the complement system has been implicated in mechanisms of neuropathic pain, the potential relevance of C3aR1 in these processes has not been addressed.

Purpose of Studies

In summary, previous work from the Vulchanova lab found that the VGF peptide TLQP-21 is involved in the development and maintenance of neuropathic pain following peripheral nerve injury. The relevance of the receptor for TLQP-21, C3aR1, in this process is unknown. The overarching goal of this thesis was to examine the involvement of C3aR1 in peripheral and central models of neuropathic pain. The following chapters include the following goals:

Chapter 1:

Determine the cell type that expresses C3aR1, and characterize the activation of C3aR1 by TLQP-21. Examine the involvement of TLQP-21/C3aR1 signaling in neuropathic pain following peripheral nerve injury, via *in vivo*, *in vitro*, and immunohistochemical approaches.

Chapter 2:

Extensively characterize pain-related behaviors following spinal cord injury in male mice, and establish the relationship between injury severity and sensory changes occurring following spinal cord injury.

Chapter 3.

Examine the involvement of C3aR1 signaling in neuropathic pain following spinal cord injury, via *in vivo* and immunohistochemical approaches. Characterize antisense oligonucleotide mediated knockdown of C3aR1 on pain-related behaviors following peripheral nerve injury and spinal cord injury in mice.

CHAPTER 1

EXPRESSION AND FUNCTION OF THE COMPLEMENT-3A RECEPTOR FOLLOWING PERIPHERAL NERVE INJURY

Chapter 1 contains works previously published in Glia; First published 29 August 2017; <https://doi.org/10.1002/glia.23208>; Title: "Complement 3a receptor in dorsal horn microglia mediates pronociceptive neuropeptide signaling." Only the portions that were performed by the author of this thesis were included in this chapter. Portions of the article reprinted with permission from Wiley Periodicals, Inc.

The complement pathway is a component of the innate immune system, which is called into action by invading pathogens and endogenous signals indicating injury. The complement 3a receptor (C3aR1) was originally identified as the cognate G-protein coupled receptor for complement component 3a (C3a), a member of the alternative complement pathway (Mathern & Heeger, 2015). In addition to C3a, the receptor has another endogenous ligand, the neuropeptide TLQP-21 (Cero et al., 2014; Hannedouche et al., 2013). TLQP-21 is generated from the neurotrophin-inducible protein VGF (nonacronymic), which has been implicated in neuroplasticity associated with learning and memory, depression, and chronic pain (Bartolomucci et al., 2006; Hunsberger et al., 2007; La Croix-Fralish, Austin, Zheng, Levitin, & Mogil, 2011; Lin et al., 2015; Moss et al., 2008; Riedl et al., 2009; Thakker-Varia et al., 2007). TLQP-21 and C3a have a competitive relationship at the same binding site within C3aR1 (Cero et al., 2014; Hannedouche et al., 2013).

Spared nerve injury (SNI) is a well characterized model of peripheral nerve injury-induced neuropathic pain (Decosterd & Woolf, 2000). In this injury, the three branches of

the sciatic nerve are exposed. The peroneal and tibial nerves are ligated and cut, and the sural nerve is left intact. Following this injury, subjects develop mechanical hypersensitivity in the ipsilateral hindpaw, in the lateral portion of the hindpaw which is innervated by the sural nerve (Bourquin et al., 2006; Decosterd & Woolf, 2000). This hypersensitivity is reproducible and long-lasting in mice and rats. TLQP-21 modulates nociceptive signaling and nerve injury-induced hypersensitivity through both peripheral and spinal mechanisms (Chen et al., 2013; Fairbanks et al., 2014; Rizzi et al., 2008). Our lab previously demonstrated that TLQP-21 elicits hyperalgesia and participates in SNI-induced hypersensitivity through an unknown mechanism in the spinal cord (Fairbanks et al., 2014).

Microglial signaling is a crucial factor in the response of the central nervous system (CNS) to injury and disease. In the dorsal horn, microglia mediate neuroinflammation in chronic pain states such as neuropathic pain (Ji, Xu, & Gao, 2014; Taves, Berta, Chen, & Ji, 2013). Following SNI, there are a number of immunohistochemical changes in the dorsal horn of the L3/L4 spinal cord, where the axons of the sciatic nerve terminate (Corder et al., 2010; Sorge et al., 2011). Microglial immunoreactivity (Iba1-ir) is increased specifically in the medial and central portion of the dorsal horn in the L3-L4 sections of the spinal cord (Corder et al., 2010). C3aR1 has been localized via *in situ* hybridization to neurons, microglia, and cultured astrocytes (Davoust, Jones, Stahel, Ames, & Barnum, 1999). Additionally, C3aR1 participates in microglial signaling under pathological conditions including neurodegeneration and virus-induced cognitive impairment (Lian et al., 2016; Vasek et al., 2016). Although the complement system has been implicated in mechanisms of neuropathic pain (Griffin et al., 2007; Liu et al., 1995; Twining et al., 2005), the potential relevance of microglial C3aR1 has not been addressed.

In the following experiments, we utilized immunohistochemistry to visualize C3aR1-ir in the spinal cord of naïve mice and determined the localization of C3aR1 protein. Using microglial cultures, we showed that TLQP-21 activated C3aR1 located on microglia. We probed changes in C3aR1 expression following spared nerve injury, and showed that C3aR1 signaling is important in the maintenance of hypersensitivity after injury.

Methods:

Animals: All work with animals adhered to the guidelines of the Committee for Research and Ethical Issues of the International Association for the Study of Pain and was approved by the Institutional Animal Care and Use Committee at the University of Minnesota in accordance with American Veterinary Medical Association guidelines. ICR/CD-1 outbred mice were purchased from Envigo (Indianapolis, USA). C3aR1 knock-out mice on a Balb/cJ background and wild-type Balb/cJ were obtained from Jackson Labs (# 005712).

Spared Nerve Injury (SNI) model: The spared nerve injury model is a well-established model that produces substantial and prolonged changes in mechanical sensitivity and cold responsiveness that closely mimic the cutaneous hypersensitivity associated with clinical neuropathic pain (Decosterd & Woolf, 2000). SNI or sham surgery were performed under isoflurane anesthesia as described (Bourquin et al., 2006). For RNA analysis and immunohistochemistry, SNI was performed at 35 days of age. For qPCR, mice were sacrificed at 2 weeks post-surgery, and fresh tissue was collected for RNA extraction. To assess the time course of C3aR1 expression following peripheral nerve

injury, mice were sacrificed by transcardial perfusion at 3, 14, and 28 days post-surgery.

Von Frey mechanical allodynia testing: Mechanical withdrawal thresholds for the hindpaw were measured at baseline and on Day 42 post-surgery by an experimenter blind to condition. Mice were acclimated at least 30 minutes in the testing environment within a glass cup on a raised metal mesh platform. To evaluate mechanical threshold we utilized a logarithmically increasing set of 8 von Frey filaments (Stoelting, Wood Dale, IL), ranging in gram force from 0.007 to 6.0 g. These were applied perpendicular to the medial hindpaw surface with sufficient force to cause a slight bending of the filament. A positive response was characterized as a rapid withdrawal of the paw away from the stimulus fiber within 4 s. Using the up-down statistical method (Bonin, Bories, & De Koninck, 2014; Chaplan, Bach, Pogrel, Chung, & Yaksh, 1994), the withdrawal threshold was calculated for each mouse and then averaged within the experimental groups.

Real-time quantitative PCR (qPCR): Two weeks post-surgery, spinal cords were removed via hydraulic extrusion. The lumbar enlargements were dissected and split along the midline into ipsilateral and contralateral halves relative to the peripheral injury. After homogenization, RNA was extracted with the Qiagen RNA Easy Lipid Mini Kit (Qiagen) and purified with the TURBO DNA free kit (Thermo Scientific). cDNA was generated with the Roche Transcriptor First Strand cDNA synthesis kit (Roche), and quantitative real-time PCR was performed on a LightCycler 480 machine using primers for C3aR1 and GAPDH and the Roche LightCycler 480 SYBR Green Master Mix (Roche). Primer sequences were: C3aR1: 5-ACAAGTGAGACCAAGAATGACC-3 and 5-GATTCCATCTCAGTGTGCTTG-3. GAPDH: 5-GTGGAGTCATACTGGAACATGTAG-3 and 5-AATGGTGAAGGTCGGTGTG-3. DDCT values were calculated for each condition using sham contralateral as the control group. Fold changes (2^{DDCT}) for each group were

compared with a one-way ANOVA, followed by Tukey's *post hoc* test.

Immunohistochemistry: Mice were deeply anesthetized with isoflurane and perfused via the heart with calcium-free Tyrode's solution (in mM: 116 NaCl, 5.4 KCl, 1.6 MgCl₂·6H₂O, 0.4 MgSO₄·7H₂O, 1.4 NaH₂PO₄, and 26 Na₂HCO₃) followed by fixative (4% paraformaldehyde and 0.2% picric acid in 0.1M phosphate buffer, pH 6.9). Tissues were dissected, incubated in 10% sucrose overnight at 4°C, and then cryostat-sectioned (14 µm) and thaw-mounted on to gelatin-coated slides. Sections were preabsorbed in blocking buffer (PBS containing 0.3% Triton-X 100, 1% BSA, 1% normal donkey serum) for 30 min, incubated in primary antibodies overnight at 4°C, rinsed with PBS 3 x 10 min, incubated in secondary antisera (1:300, Jackson ImmunoResearch, West Grove, CA) for 1 h at room temperature, washed with PBS, and coverslipped using PBS/glycerol containing 0.1% *p*-phenylenediamine (Sigma). Primary antibodies included: rat anti-C3aR1 (1:100, Hycult Biotech), rabbit anti-Iba1 (1:1000; Wako Chemicals), goat anticollagen IV (1:2500, SouthernBiotech), mouse anti-GFAP (1:1000, Sigma), mouse anti-MAP2 (1:5000; Millipore), and rabbit anti-NeuN (1:1000, Cell Signaling). Images were collected with an Olympus FluoView1000 confocal imaging system. Adjustments of contrast and brightness were performed in Adobe Photoshop CS5; images from wild type and knockout mice were adjusted identically. For quantification of colocalization of Iba1 and GFP labeling in Iba1-eGFP mice, images of dorsal horn were collected as z-stacks (6 optical sections, 1 µm apart) and projected in Image J. Three nonadjacent sections of lumbar spinal cord were imaged for each subject (*n* = 3). The projected images were thresholded above the level of background staining intensity, using the same threshold value for all Iba1 and GFP images, respectively. Stacks of corresponding Iba1 and GFP images were created in Image J. Cellular profiles, identified based on the presence of a soma-like structure with associated processes, were outlined

and assessed for presence of Iba1 and GFP labeling. Labeled profiles were counted, and the average number of double-labeled and single-labeled profiles per section was calculated for each subject. For quantitative image analysis of C3aR1-ir, single optical sections of C3aR1/Iba1/MAP2 triple-labeling were collected using constant image acquisition settings. Iba1 staining was used for unbiased selection of the focal plane. Analysis was performed in ImageJ. MAP2 labeling was used for reproducible outlining of a region of dorsal horn that included laminae I–III. To measure the area of C3aR1 and Iba1 labeling, the images were thresholded by a blinded experimenter. Analysis by three different blinded experimenters yielded reproducible results. C3aR1 and Iba1 labeling was expressed as % thresholded area. Data from three nonadjacent L3/L4 sections were averaged from each spinal cord.

Primary microglial cultures: Cortical cells were collected from postnatal day 1–3 mouse pups of both sexes (CD-1, Charles River; Balb c/J wild-type or C3aR1 knock-out, Jackson Laboratory) and plated under conditions that promote survival of microglia and astrocytes but not neurons (Skaper, Argentini, & Barbierato, 2012). Mixed glial cultures were maintained in EMEM 1 10% fetal bovine serum (FBS) 1 1% L-glutamine 1 1% Penstrep (EMEM, 500 mL, Gibco; FBS, Gibco, 26140–079; L-glutamine, 200 mM, Thermo Fisher; Penstrep, Gibco) at 37°C. After approximately 2 weeks, the flasks were shaken at 200 rpm for 1.5 h to detach microglia. Each flask contained cells from approximately two pups and yielded approximately four coverslips. Cells were plated on 25 mm coverslips coated with poly- D-lysine (Sigma) at a density of 45,000 cells per coverslip. Cells were kept at 37°C for 72 h prior to calcium imaging. The primary cultures consisted of approximately 98% microglia.

Calcium imaging: Cultured primary microglia were used 72 h after plating. Coverslips were

incubated with the ratiometric intracellular calcium indicator Fura-2 AM (Invitrogen) at a final concentration of 1.5 mM in HEPES buffer containing 1% bovine serum albumin for 20 min prior to calcium imaging. Coverslips were then transferred to a recording chamber and perfused at a rate of 1.8 mL/min with HEPES–Hank’s buffer (25 mM HEPES, 135 mM NaCl, 2.5 mM CaCl₂, 3.5 mM KCl, 1 mM MgCl₂, and 3.3 mM glucose, pH 7.4 and 335–340 mOsm adjusted with sucrose). A single field of view containing approximately 8 cells was imaged in each coverslip. Experimenters chose fields of view based on microglia cell morphology, such as resting elongated cells and rounded cells. Cells were exposed to 100 mM ATP at 60 s and 10 mM TLQP-21 at 660 s during the recording session. Excitation wavelengths of 340 and 380 were used to measure bound and unbound calcium, respectively, in order to examine calcium flux. Excitation wavelengths and shutter speed were controlled by a DeltaRam X controller and LPS-220B lamp (PTI). ImageMaster 5.0 software (PTI) was used to collect and analyze all images. Ratios of 340/380 were calculated and differences between the amplitude ratios at baseline and at peak after stimulation were measured in each cell within the field of view. Cells were considered responsive to ATP or TLQP-21 if the peak amplitude was twofold greater than noise, defined as the difference between the maximum and minimum baseline values during the 10-s period preceding drug application. Three to five coverslips were tested from three CD-1 WT, three C3aR1 WT, and three C3aR1 KO cultures. Cells were grouped into responders or nonresponders in a contingency table for each treatment and were compared using Fisher’s exact test.

Statistical Analyses: Data are expressed as the mean \pm SEM, with $p < .05$ as significant. p values were determined using t -tests for two-group analysis, and 1- or 2-way ANOVA with repeated measures followed by pairwise comparisons using GraphPad Prism software (version 6; GraphPad Software, San Diego, CA). Proportions of profiles/cells

were compared using Fisher's exact test.

Results:

C3aR1 is expressed in spinal microglia:

Although *C3aR1* mRNA transcripts have been localized to neurons, astrocytes, and microglia in spinal cord (Davoust, Jones, Stahel, Ames, & Barnum, 1999), much less is known about the spinal distribution of C3aR1 protein. To fill this gap, we characterized a C3aR1 antibody with immunohistochemistry of spinal cord sections. Figure 1 demonstrates C3aR1 immunoreactivity (–ir) on fine, short processes and a few cellular profiles throughout the spinal cord, including in the dorsal and ventral horn as well as in the white matter. C3aR1-ir was absent in C3aR1 knockout mice, demonstrating antibody specificity (Figure 1.1a,b). Double labeling for C3aR1 and Iba1, a marker of macrophages and microglia, indicated that C3aR1-ir was almost exclusively associated with microglia (Figure 1.1c–h, arrowheads). Intense C3aR1 labeling was also present in Iba1-positive meningeal/subarachnoid macrophages located within the pia mater or in close apposition to subarachnoid blood vessels, as indicated by their proximity to collagen IV-ir (Urabe et al., 2002) (Figure 1.1c–h, arrows; Figure 1.1i).

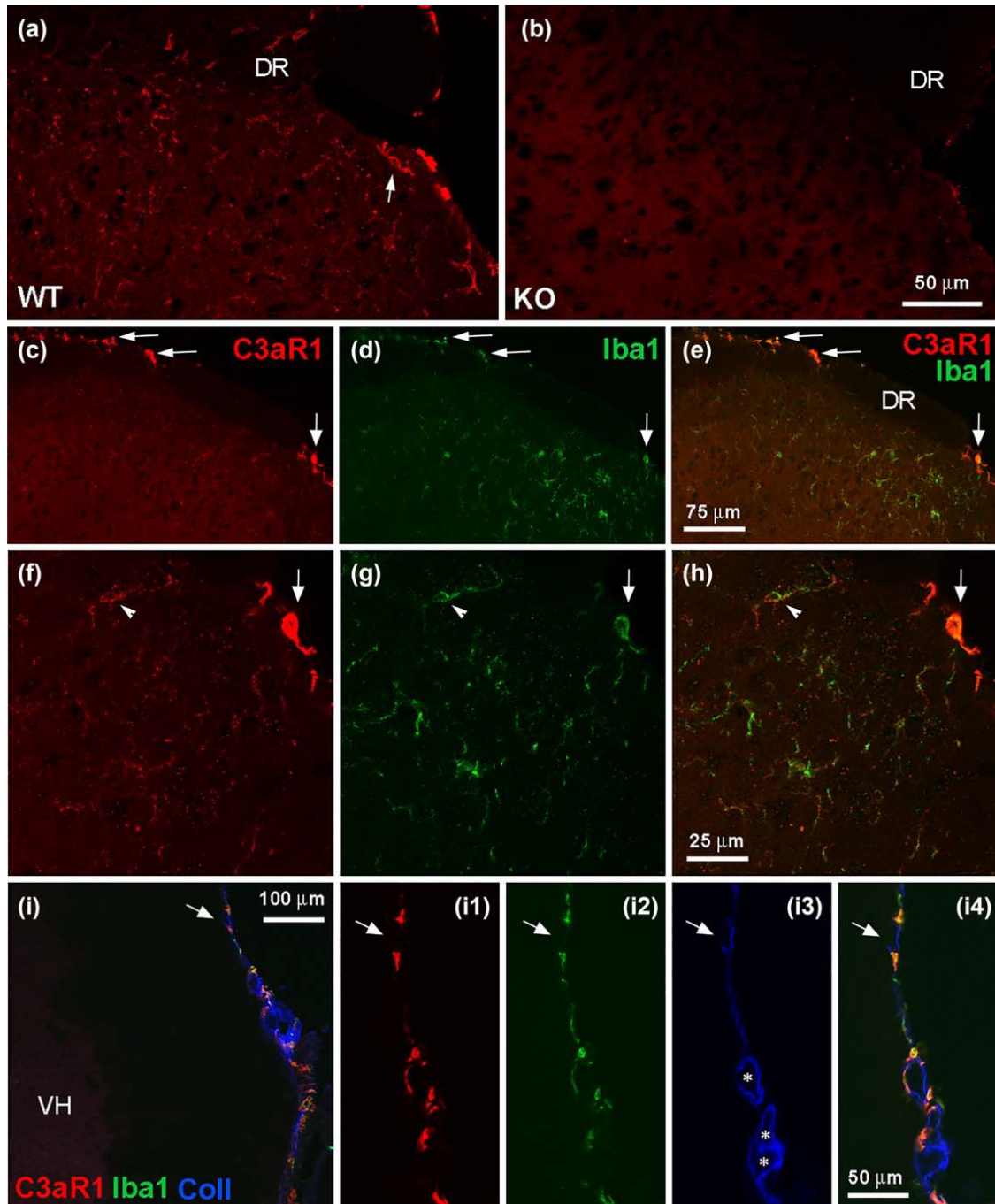


Figure 1.1: Spinal localization of C3aR1. (a, b) C3aR1 immunolabeling in superficial dorsal horn from wild-type (WT) and knock-out (KO) mice (DR indicates dorsal roots). The arrow in A indicates a cellular profile that is outlined by C3aR1 immunoreactivity (–ir). Scale bar: 50 μm . (c–h) Immuno-histochemical analysis of C3aR1-ir (red) and its relationship to

*Iba1-ir (green) in dorsal horn. The dorsolateral region of the spinal cord in c–e is shown at higher magnification in f–h; e and h represent digital merging of c, d and f, g, respectively to show colocalization of labeling. C3aR1 and Iba1-ir overlap in fine processes and cellular profiles in superficial dorsal horn (f–h, arrowheads indicate the same cellular profile). Arrows in c–h indicate C3aR1/Iba1-positive profiles at the spinal cord perimeter. The image shown in f–h represents a projection of 3 optical sections, 1 μ m apart. Scale bars: c–e, 75 μ m; f–h, 25 μ m. (i) C3aR1/Iba1-positive profiles at the spinal cord perimeter are associated with collagen IV (Coll) labeling that delineates the pia mater and subarachnoid blood vessels (VH indicates ventral horn; * indicate subarachnoid blood vessels). The spinal cord perimeter is shown at higher magnification in (I1–4). The arrows indicate the same region in I and I1–4. Scale bars: I, 100 μ m; I1–4, 50 μ m.*

TLQP-21-evoked Ca^{2+} signaling occurs in microglia: imaging in microglial cultures:

Following our localization of C3aR1 to microglia in the spinal cord, we aimed to determine whether TLQP-21 is able to directly activate microglia. We evaluated Ca^{2+} signaling in cortical microglial cultures prepared from neonatal CD-1 mice (P1–3). To restrict our analysis of TLQP-21-evoked responses to viable microglia, we used ATP as a reliable stimulus for microglial Ca^{2+} signaling (Wang, Kim, van Breemen, & McLarnon, 2000). Cells were considered responsive to ATP or TLQP-21 if the peak amplitude was twofold greater than noise. We found that all TLQP-21-responsive cells were ATP-responsive (representative trace shown in Figure 1.2a). As illustrated by the scatterplots

of peak response amplitudes, of 97 cells found to be ATP-responsive, 37 also responded to TLQP-21, while 60 did not (Figure 1.2b). To determine if these responses were mediated by C3aR1 activation, we tested the effects of the R21A analog. In these experiments, of 78 cells found to be ATP-responsive, only 5 responded to R21A, while 73 did not. Statistical analysis indicated that a significantly lower proportion of cells responded to R21A (6%) compared to TLQP-21 (38%) ($p < .0001$, Fisher's exact test).

We next compared TLQP-21 responses in microglial cultures taken from either C3aR1 knock-out (KO) mice or their Balb/cJ wild-type (WT) controls. Figure 1.2c and d show scatterplots of peak response amplitudes for ATP and TLQP-21 for responders and nonresponders in WT and KO microglial cultures. Similar proportions of WT (90%) and KO (87%) cells responded to ATP. In contrast, the proportions of TLQP-21 responsive cells in WT (65%) and KO (5%) cultures differed significantly ($p < .0001$, Fisher's exact test). Taken together, these experiments demonstrate that TLQP-21 directly activates C3aR1- dependent Ca^{2+} signaling in microglia.

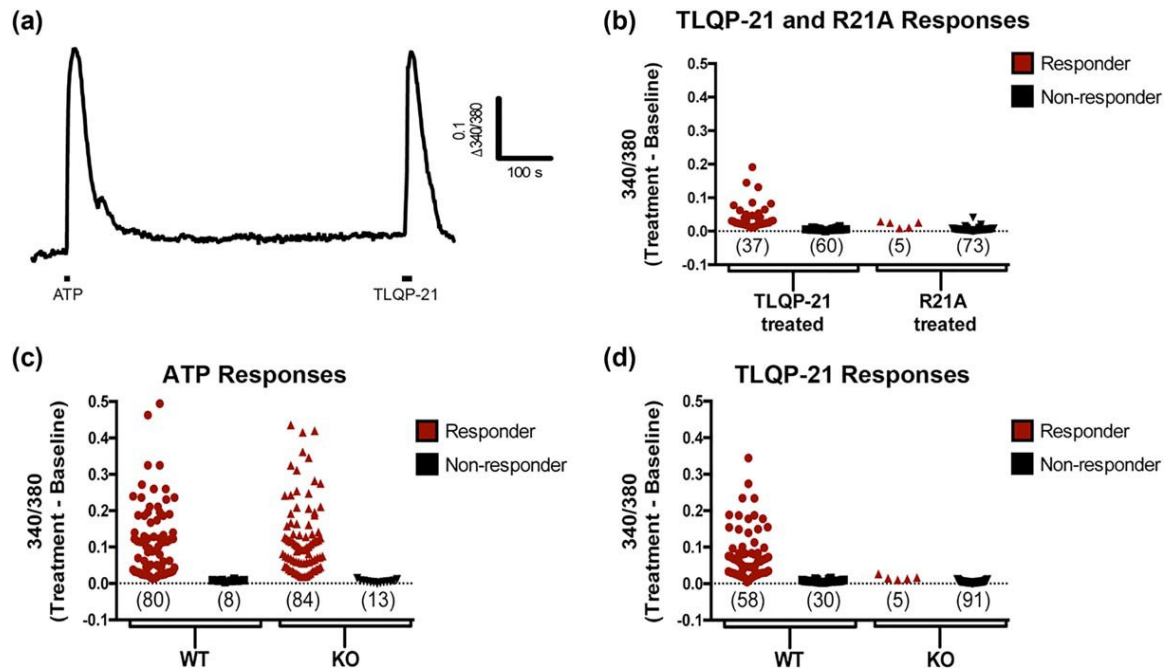


Figure 1.2: TLQP-21 activates C3aR1 in cultured primary microglia. (a) Representative ratiometric (D340/380 nm) traces of ATP (100 μ M) and TLQP-21 (10 μ M)-evoked Ca^{2+} transients in microglial cells isolated from P1–3 neonatal brain from wild-type (WT) mice. (b) Scatter plot of peak response amplitudes to TLQP-21 and R21A in wild-type cultures demonstrates that the proportions of TLQP-21 and R21A responders and nonresponders are significantly different ($p < .0001$, Fisher's exact test). (c) Scatter plot of peak response amplitudes to ATP in cultures from WT and C3aR1 KO mice shows that the proportions of ATP responders and nonresponders in WT and KO cultures are not significantly different. (d) Scatter plot of peak response amplitudes to TLQP-21 in cultures from C3aR1 KO and WT mice shows that the proportions of TLQP-21 responders and nonresponders in WT and KO cultures are significantly different ($p < .0001$, Fisher's exact test).

Each symbol in b–d represents a cell [Color figure can be viewed at wileyonlinelibrary.com]

C3aR1 contributes to peripheral nerve injury-induced hypersensitivity:

Intrathecal administration of TLQP-21 induces a transient, prostaglandin-dependent heat hyperalgesia in the warm water tail immersion assay (Fairbanks et al., 2014). Preliminary data from the lab (collected by KK) found that an antagonist to C3aR1, SB290157, had no behavioral effect when injected alone, but dose-dependently (0.1–1.0 nmol) inhibited the hyperalgesia induced by TLQP-21. We previously used an immunoneutralization approach to demonstrate that TLQP-21 is necessary for nerve injury-induced hypersensitivity (Fairbanks et al., 2014). To determine whether C3aR1 signaling is necessary as well, we evaluated the effect of SB290157 in the SNI model of neuropathic pain. SB290157 (1 nmol, i.t.) reversed mechanical hypersensitivity as compared to vehicle (Figure 1.3c; $p < .01$ at 30 min post-drug, $p < .05$ at 2 h post-drug, two-way repeated measures ANOVA and Bonferroni's *post hoc* test).

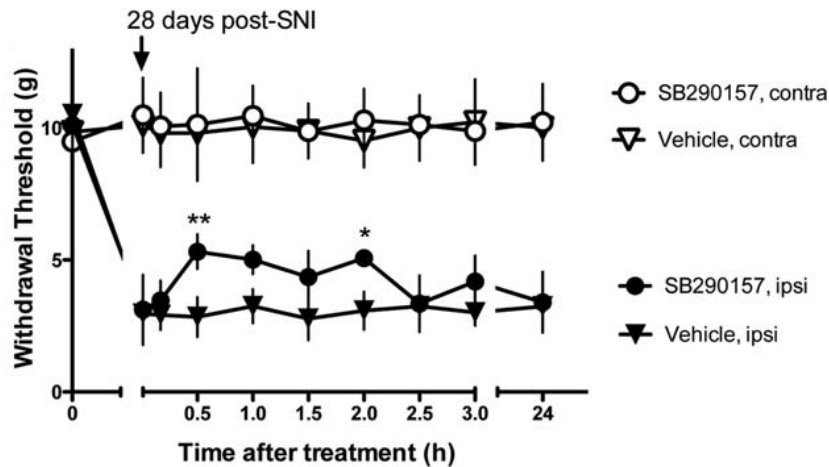


Figure 1.3: *C3aR1* mediates peripheral nerve injury-induced hypersensitivity. The reduction in mechanical withdrawal thresholds after SNI is partially reversed by SB290157. ** $p < .01$ at 30 min, * $p < .05$ at 2 h after drug treatment, two-way repeated ANOVA, followed by Bonferroni post hoc test. Data represent mean \pm SEM

Peripheral nerve injury increases the spinal expression of C3aR1 in a time-dependent manner:

Due to the prominence of immune activation following injury, and the contribution of microglia to neuropathic pain in animal models of peripheral nerve injury, we tested the hypothesis that spared nerve injury (SNI) increases the expression of C3aR1 in the dorsal horn. As illustrated in Figure 1.4a, 14 days after SNI we observed an approximately twofold increase in C3aR1 mRNA in the ipsilateral spinal cord ($2.22 \pm$

0.2) as compared to the contralateral side of SNI mice (1.33 ± 0.25) or the ipsilateral (1.31 ± 0.21) or contralateral (1.07 ± 0.13) spinal cord of sham mice ($p < .001$, $n = 14-16$ mice/ group; one-way ANOVA followed by Tukey's multiple comparisons test). To determine the time course of the increase in spinal C3aR1 expression, we measured the area of C3aR1 labeling in dorsal horn at 3, 14, and 28 days after SNI or sham surgery (Figure 1.4b). The maximum increase in C3aR1-ir, relative to sham, was observed 3 days after nerve injury. Although the labeling progressively decreased at 14 and 28 days post-surgery, C3aR1 expression remained elevated in the medial portion of dorsal horn as compared to control (Figure 1.4c-h).

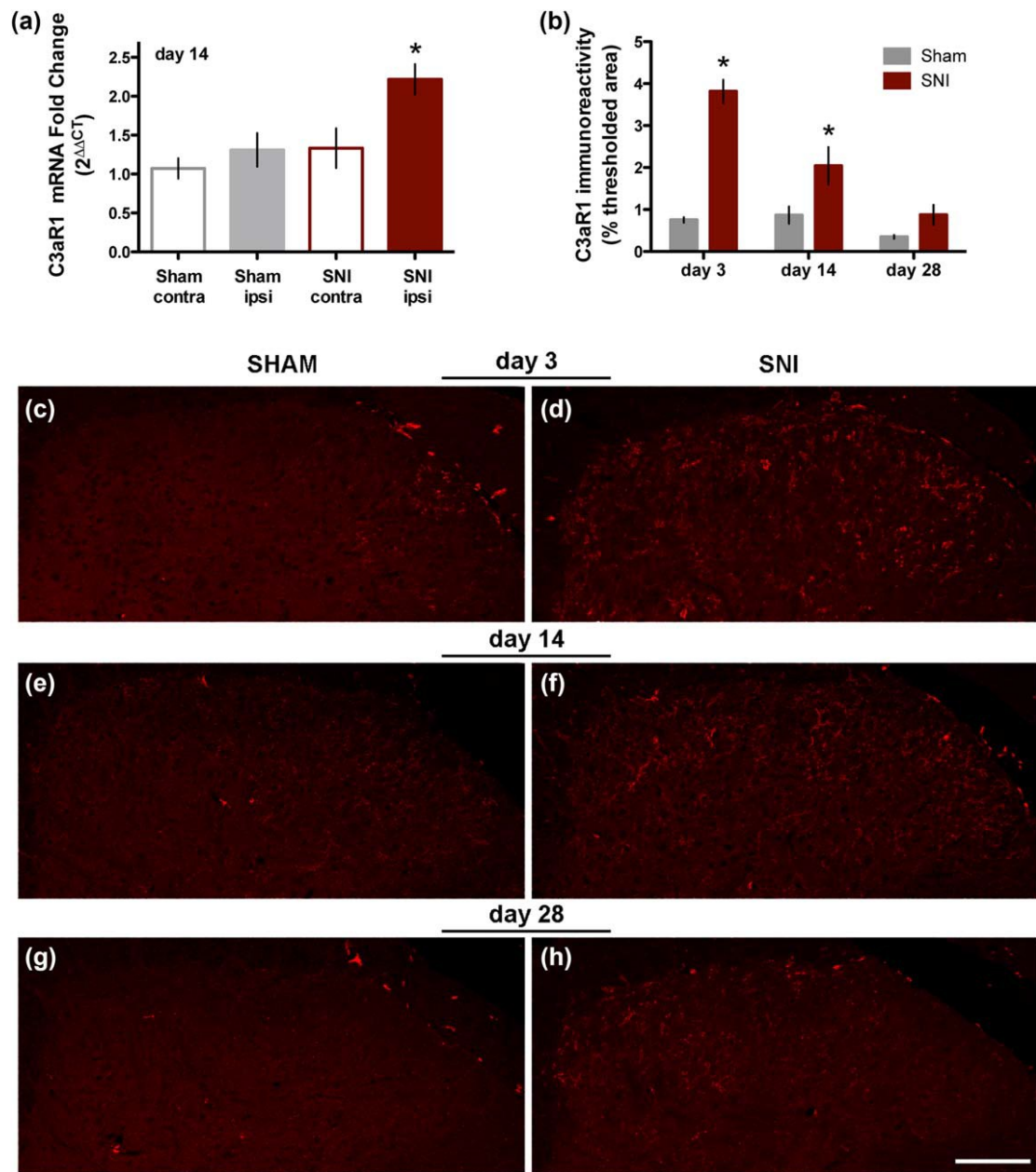


Figure 1.4: Spinal expression of C3aR1 increases after nerve injury. (a) Real-time qPCR analysis demonstrates an increase in expression of C3aR1 mRNA in the ipsilateral spinal cord 14 days after SNI ($n = 10-13$ mice/group. $*p < .05$, one-way ANOVA followed by Tukey's post hoc test; data represent mean \pm SEM). (b) Quantitative analysis of C3aR1 immunolabeling indicates that maximum increase in C3aR1 expression occurs 3 days post-surgery ($p < .1$ at day 3, $p < .05$ at day 14, $p = .06$ at day 28; t test). (c-h)

Representative images illustrate the increase in C3aR1-ir at days 3 (C, sham; D, SNI), 14 (E, sham; F, SNI), and 28 (G, sham; H, SNI) after nerve injury. Scale bar: 100 μ m.

C3aR1 is primarily localized to microglia or macrophages after nerve injury:

Having established that C3aR1 is expressed in microglia in the spinal cord in naïve animals, we next used double-label immunohistochemistry to confirm that C3aR1 immunoreactivity (-ir) is not expressed in neurons or astrocytes in the dorsal horn following SNI. We found that C3aR1-ir was extensively co-localized with Iba1-ir at all time points examined (14 days post-surgery shown in Figure 1.5a). In contrast, C3aR1-ir did not co-localize with either the astrocyte marker GFAP or the neuronal marker NeuN (Figure 1.5b,c). These data indicate that the expression of C3aR1 is limited to microglia, with no evidence of expression in spinal astrocytes or neurons, in the setting of nerve injury.

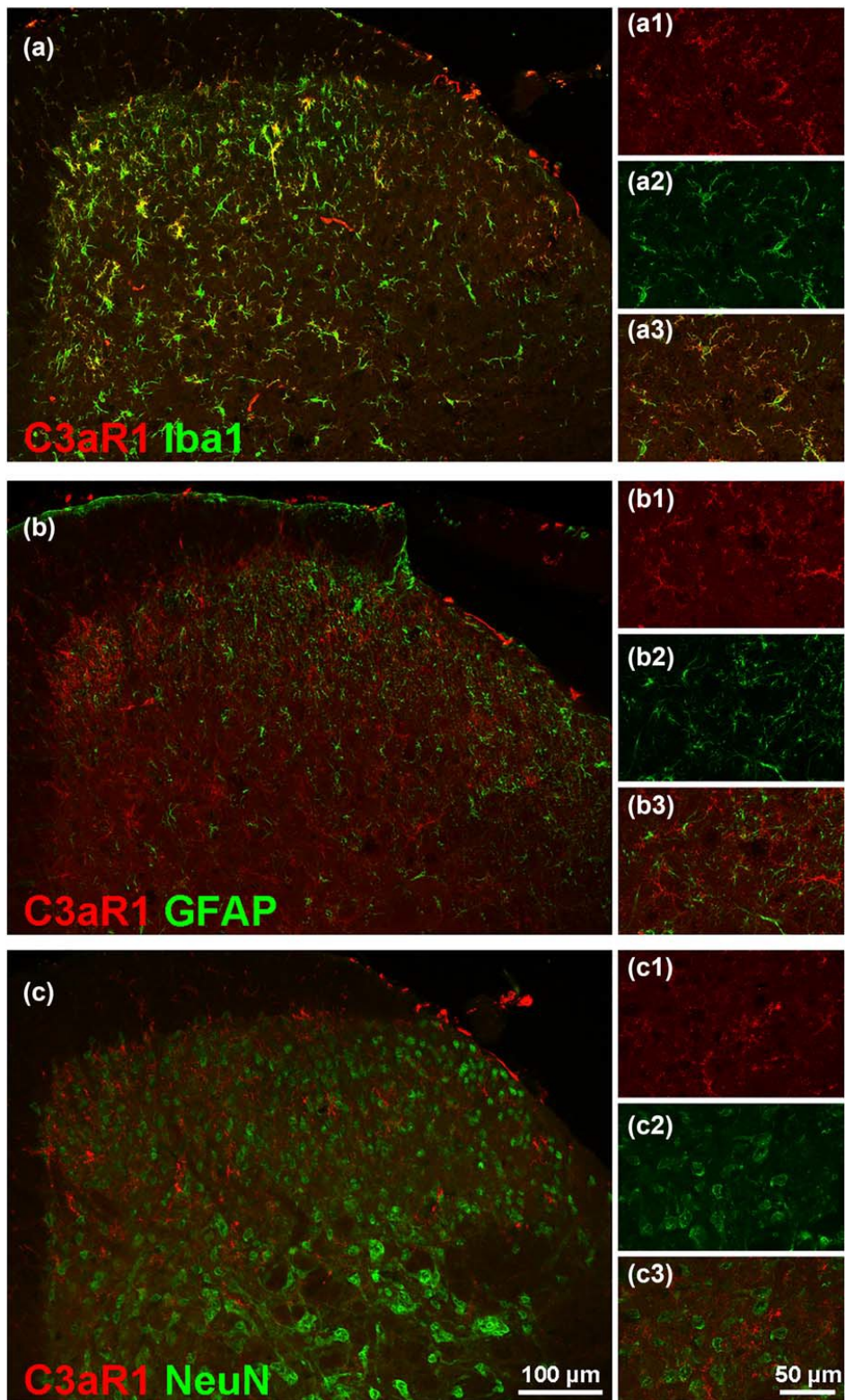


Figure 1.5: Spinal C3aR1-ir is localized in microglia after nerve injury. Double-labeling

for C3aR1 (red) and Iba1 (green, a), GFAP (green, b), and NeuN (green, c) in ipsilateral lumbar dorsal horn of SNI mice 14 days postsurgery. C3aR1-ir in dorsal horn colocalizes with Iba1-ir but not GFAP or NeuN-ir. Scale bar: 100 μ m for a–c, 50 μ m for a1–3, b1–3, c1–3

Discussion

C3aR1 has emerged as a neuro-glial mediator that contributes critically to pathological processes in the CNS by regulating neuroinflammation as well as neuronal structure and function (Lian et al., 2015; Vasek et al., 2016). We previously demonstrated that the newly identified ligand of C3aR1, TLQP-21, elicits hyperalgesia and participates in the development and maintenance of nerve injury-induced hypersensitivity (Fairbanks et al., 2014). Here we examined the interaction of TLQP-21 and C3aR1, and provide the first evidence that microglial C3aR1 mediates the effects of TLQP-21 within the central nervous system.

TLQP-21 directly targets C3aR1 to activate microglia

We provide functional and anatomical evidence that microglia are the predominant cellular target for the effects of TLQP-21. First, we demonstrate extensive C3aR1 co-localization with Iba1-ir microglia in the dorsal horn. Our co-localization analysis of C3aR1, GFAP, and NeuN labeling did not yield evidence for C3aR1 expression in astrocytes or neurons; however, we cannot rule out a secondary contribution of activation in neurons and/or astrocytes. Second, the absence of TLQP-21-elicited Ca^{2+} transients in C3aR1 KO mice and in WT cultures exposed to R21A reinforces the evidence that TLQP-21 signaling

is C3aR1-mediated.

C3aR1 in peripheral injury-induced spinal neuroplasticity

Using immunoneutralization, we previously demonstrated that endogenous spinal TLQP-21 contributes to the development and maintenance of nerve injury-induced hypersensitivity (Fairbanks et al., 2014). We examined the contribution of the receptor to hypersensitivity following SNI, and found that administration of a C3aR1 antagonist was able to attenuate the maintenance of mechanical allodynia. Our studies utilizing microglial cultures identify microglial C3aR1 as the target for TLQP-21. Since the TLQP-21 precursor VGF is upregulated in sensory neurons within 24 h of nerve injury (Riedl et al., 2009), spinal TLQP-21 released from injured sensory neurons is positioned to function as an endogenous danger signal that contributes to spinal neuroinflammation after nerve injury through activation of C3aR1. Little is known about the spinal availability of the originally characterized C3aR1 ligand C3a. Although expression of C3, the precursor of C3a, emerges in spinal microglia three days after peripheral nerve injury (Gattlen et al., 2016; Griffin et al., 2007; Liu et al., 1995; Twining et al., 2005), the generation of C3a or its contribution to hypersensitivity remains to be established.

We examined C3aR1 expression in the lumbar dorsal horn following peripheral nerve injury. Our results indicate a robust and early upregulation of C3aR1 specifically in microglia following peripheral nerve injury. This increase is highest during the acute phases of injury, steadily decreasing over time. These results point to a potentially important role in signaling through C3aR1 immediately following injury. In peripheral nerve injury, the increase in C3aR1 expression occurred in the area innervated by the central terminals of nociceptors for the ipsilateral hindpaw. This increase did not occur on the contralateral spinal cord or in sham controls, indicating a specific increase in complement

activation occurring following the unilateral nerve injury. Moreover, pharmacological inhibition of C3aR1 attenuated the behavioral hypersensitivity associated with SNI. These results provide the first evidence that microglial C3aR1 contributes to neuropathic pain. C3aR1 activation of monocytes induces release of ATP and cytokines (Asgari et al., 2013). Spinal microglia also have the capacity to release ATP (Liu, Kalous, Werry, & Bennett, 2006), and microglial purinergic receptors are heavily implicated in neuropathic pain mechanisms (Beggs, Trang, & Salter, 2012). This leads us to speculate that the potential downstream consequences of C3aR1 signaling following peripheral and central injury include microglial release of ATP and cytokines, including mediators of spinal neuroplasticity such as IL-1b (Clark et al., 2015; Gruber-Schoffnegger et al., 2013).

C3aR1 is expressed in meningeal/subarachnoid macrophages

The present study makes the intriguing and novel observation that C3aR1 is expressed in meningeal/subarachnoid macrophages. It is well documented that macrophages can be found in mouse meninges and human cerebrospinal fluid, and that their number increases in pathological states such as multiple sclerosis (Chinnery, Ruitenbergh, & McMenamin, 2010; Polfliet et al., 2001; Waschbisch et al., 2016). Thus, we suggest that C3aR1 is well-positioned to respond to complement pathway activation within the cerebrospinal fluid (e.g., in response to pathogens). Importantly, VGF fragments have been detected in multiple proteomic studies of human CSF (Bartolomucci et al., 2011). Therefore, we speculate that TLQP-21 acts at C3aR1 on macrophages in the CSF to promote neuroinflammation. Furthermore, since activated macrophages release prostaglandins that may diffuse within the spinal cord (Ulmann, Hirbec, & Rassendren, 2010), C3aR1 receptors on CSF macrophages may provide insight into the mechanisms underlying the prostaglandin-mediated thermal hyperalgesia observed following

intrathecal injection of TLQP-21 (Fairbanks et al., 2014).

In summary, we show that C3aR1 is localized to microglia in both naïve mice, and mice following peripheral nerve injury. For the first time, we localized C3aR1 to subarachnoid macrophages, indicating that these complement receptor-expressing immune cells are located in a prime location for interaction with the spinal cord during neuropathic states. Previous work in our lab found that TLQP-21 evoked heat hyperalgesia is C3aR1-dependent. Following spared nerve injury, an antagonist to C3aR1 was able to transiently attenuate mechanical hypersensitivity. Additionally, we found that TLQP-21 specifically activates C3aR1 located on microglia. The identification of C3aR1 as the target of TLQP-21 suggests a novel interplay of neuronal and immune signaling mediators in CNS diseases. We identified that there is upregulation of C3aR1 in a time-dependent manner following peripheral nerve injury. The early increase of receptor expression indicates a potentially important role of C3aR1 signaling throughout the acute stages of injury.

CHAPTER 2

COMPREHENSIVE CHARACTERIZATION OF SENSORY BEHAVIOR FOLLOWING A MOUSE MODEL OF SPINAL CORD INJURY

Spinal Cord Injury (SCI) is a devastating condition with approximately 18,000 new injuries occurring each year in the U.S. The average age of SCI patients is 43 years old, and 78% of new injuries occur in males (National Spinal Cord Injury Statistical Center, 2019). The most common causes of SCI are vehicular accidents (38.3%), falls (31.6%), and violence (13.8%). The different types of spinal cord injuries are heterogeneous, with a mix of incomplete tetraplegia (47.2%), incomplete paraplegia (20.4%), complete paraplegia (20.2%), and complete tetraplegia (11.5%) (National Spinal Cord Injury Statistical Center, 2019). Complete spinal cord injuries leave patients with loss of motor and sensory function below the level of injury. Incomplete injuries are much more common, where some motor and sensory function is intact below the level of injury. The symptoms these patients experience differs depending on which portion of the spinal cord is affected. For example, a patient with damage mostly to the dorsal portion of the spinal cord is more likely to have sensory deficits or pain rather than motor symptoms. There are a number of chronic symptoms patients with spinal cord injuries experience. These include paralysis, loss of bladder or bowel control, altered sensation in extremities, muscle spasticity, difficulty breathing, chronic pain, and depression (Hagen, 2015; Sezer, 2015).

Due to the lifelong impact of SCI, the economic and social costs to patients with SCI are staggering. Depending on the age at injury and level of the spinal cord, the lifetime costs of injury are between 1.6 and 4.9 million dollars (National Spinal Cord Injury Statistical

Center, 2019). The first year post-injury has the highest cost of treatment, due to the initial hospital stay and immediate rehabilitation. These estimates do not take into account the tens of thousands of dollars lost each year in un-or-under employment. The life expectancy of patients with SCI is reduced, regardless of age at injury or injury level; the percent decrease in life expectancy scales to the severity of the injury (National Spinal Cord Injury Statistical Center, 2019).

The prevalence of chronic pain in SCI patients is between 26%-96% (Dijkers, Bryce, & Zanca, 2009). Between 16%-63% of patients with chronic pain characterize it as severe (Bryce et al., 2012). The ranges are so variable due to the absence of a generalized classification system. There are a variety of types of chronic pain experienced by SCI patients, including nociceptive pain and neuropathic pain (Bryce et al., 2012; Nanna Brix Finnerup & Bastrup, 2012; Gorp, Kessels, Joosten, Kleef, & Patijn, 2014; Istituto & Biomediche, 2013). Nociceptive pain includes musculoskeletal and visceral pain, arising from the activation of nociceptors. Most nociceptive pain does not arise from the injury itself, but instead from the changes to bodily function and lifestyle that occur following a severe spinal cord injury (Bryce et al., 2012). These include difficulties in digestion and bladder function or strenuous use of particular muscles during movement, with or without mobility aides. Neuropathic pain typically includes at-level and below-level pain, and arises from damage to the spinal cord and spinal nerve roots. At-level pain is within the dermatome of injury to the spinal cord or spinal nerve roots, and can extend up to three dermatomes below the injury. Below-level pain is located more than three dermatomes below the injury, and is considered to be directly related to the injured spinal cord, rather than secondary injury. Common characteristics of neuropathic pain following SCI include sensory deficits within the pain distribution, allodynia or hyperalgesia, and descriptors of

the pain including: burning, tingling, pricking, sharp, squeezing, painful cold, and electric shocks.

Neuropathic pain following SCI is particularly severe, long-lasting, and difficult to treat. In approximately 66% of patients with SCI neuropathic pain, current treatments, including pharmacological agents as well as physical therapy and electrical stimulation, fall short of achieving pain relief (Boldt et al., 2014; N. B. Finnerup & Jensen, 2004; Siddall, McClelland, Rutkowski, & Cousins, 2003). To address this critical need for effective pain management, it is important to elucidate the endogenous mechanisms that cause SCI neuropathic pain. The majority of animal studies examining pain behavior following spinal cord injury have been done in rats. Following thoracic contusion spinal cord injury, rats typically develop mechanical allodynia and thermal hyperalgesia (Hains, 2006a; Hama & Sagen, 2007; Peng et al., 2009; Sweitzer et al., 2006; Zhao et al., 2007a). Performing SCI in mice is more complex, due to their smaller size. It is important to utilize this model, as mice provide the potential for genetic manipulation that is more difficult in other species. Prior to the start of these experiments, there were limited studies examining pain-related behavior in mice following spinal cord injury (Hoschouer et al., 2010; Kerr & David, 2007; Meisner et al., 2010a). Our aim was to thoroughly characterize a range of locomotor, pain, and tactile behaviors following SCI utilizing a mild and moderate contusion injury. The following studies are the most thorough characterization of behavior following SCI in mice to date.

Methods:

Spinal cord injury and postoperative care: All studies were approved by the University of Minnesota Institutional Animal Care and Use Committee (IACUC). Thoracic spinal cord injury or sham surgery was performed on male ICR wild-type mice (CrI:CD1(ICR), Charles River, Wilmington, MA, USA) at 5 weeks of age. Prior to surgery, each subject was given 0.5cc of sterile saline subcutaneously in each hindquarter. Briefly, a laminectomy was performed at T9, and the contusion injury was made with either 50 or 75 kdyn of force with the IH-0400 Infinite Horizons Impactor (Precision Systems and Instrumentation, LLC; Lexington, KY, USA) with a 1.3 mm mouse tip. Sham controls had a laminectomy at T9 with no impact, and naïve subjects were housed in separate cages at the same time as their surgical counterparts. Animals received amoxicillin (14 g/L in drinking water) for 7 days after surgery to prevent urinary tract infection as part of standard postoperative care. Urine was expressed manually twice daily for the first 7 days after surgery and daily thereafter until the return of independent urination. Experimental groups were as follows, listed in Table 2.1:

Cohort:	Surgical Procedure	# of Subjects	Impact (kdyn)	Perfused (Day post-surgery)
50 kdyn Cohort 1	Sham	7	0	50 days
	SCI	10	50	50 days
50 kdyn Cohort 2	Naïve	9	N/A	N/A
	Sham	10	0	45 days
	SCI	11	50	45 days
50 kdyn Cohort 3	Naïve	6	N/A	N/A
	SCI	7	50	45 days
75 kdyn Cohort	Naïve	6	N/A	N/A
	SCI	9	75	45 days

Functional assessment: Locomotor recovery following injury was assessed by two observers using the Basso Mouse Scale (BMS) (Basso et al., 2006), on days 1, 3, 5, 7, 14, 21, 28, and 35 days following injury. Briefly, measurements were made on a 9-point scale derived from ankle movements, plantar/dorsal hindpaw stepping, coordination, trunk instability, and tail position. Mice were placed into an open field and monitored for five minutes each, with scores from 0 (complete paralysis) to 9 (normal locomotion) measured for each hindpaw. BMS scores were compared between treatments via repeated-measures analysis of variance.

Behavioral Testing: A number of behavioral tests were performed following sham or thoracic spinal cord injury beginning at 35 days post-injury and concluding at 45 days. These include:

Rotarod: Mice were tested with the rotarod apparatus (Ugo Basile, Gemonio, Italy). Briefly, subjects were placed on an elevated rotating cylinder that increased in RPM continuously over 300 seconds, from 5 RPM to a peak of 50 RPM. RPM at fall was recorded for three consecutive days, beginning at Day 35 post-surgery. No more than four subjects were tested at a time.

Von Frey mechanical allodynia testing: Mechanical withdrawal thresholds for the hindpaw were measured at baseline and on Day 42 post-surgery by an experimenter blind to condition. Mice were acclimated at least 30 minutes in the testing environment within a glass cup on a raised metal mesh platform. To evaluate mechanical threshold we utilized a logarithmically increasing set of 8 von Frey filaments (Stoelting, Wood Dale, IL), ranging in gram force from 0.007 to 6.0 g. These were applied perpendicular to the medial hindpaw

surface with sufficient force to cause a slight bending of the filament. A positive response was characterized as a rapid withdrawal of the paw away from the stimulus fiber within 4 s. Using the up-down statistical method (Bonin et al., 2014; Chaplan et al., 1994), the withdrawal threshold was calculated for each mouse and then averaged within the experimental groups.

Hargreaves thermal hyperalgesia testing: Mice were tested for hindpaw thermal hyperalgesia using the IITC Plantar Test system at intensity: AI 30 (IITC Life Sciences, Woodland Hills, CA). Briefly mice were acclimated to an ambient floor (33°C) and a beam of focused light was aimed at each hindpaw. The length of time until paw withdrawal was measured. A humane cutoff time was automatically calibrated from the intensity settings.

Burrowing behavior: Burrowing is an ethologically relevant behavior for mice, and others have utilized this as a measure of spontaneous pain following injury, which is improved with analgesic administration (R. M.J. Deacon, 2009; Robert M.J. Deacon, 2006; Jirkof, 2014; Jirkof et al., 2010). Briefly, a PVC tube with a cap at one end is elevated on the other end and filled with normal chow, and is placed in the home cage of each individually housed mouse. The amount of material burrowed during a 2-hour period is weighed, and then the remaining material in the tube is weighed. Data shown as $(\text{Material Burrowed})/(\text{Total Material}) \times 100$ to get a burrowing percentage.

Cotton swab test: The cotton swab test is a dynamic stroke assay designed to test light touch sensation (Garrison, Dietrich, & Stucky, 2011). This test utilizes a cotton swab puffed out to 3x its size, and the swab is brushed along the plantar surface five times with a 10-second break between applications, with the number of paw withdrawals recorded.

Results:

We aimed to characterize a number of locomotor and pain-related behaviors following spinal cord injury. The results are collated into different groups, based on when the surgery was performed. This was due to improvement in surgical proficiency over time. Cohorts that occurred within several weeks of one another were combined. Some of this data is from experiments that had receptor knockdown via antisense oligonucleotides; to have enough SCI subjects for intervention they did not have sham controls. This chapter is presenting data from SCI subjects that received no intervention, or ones that received vehicle control injections. The results of the manipulations will be presented in chapter three.

Male ICR mice recover locomotion following mild and moderate thoracic contusion spinal cord injury in a reproducible manner:

Following contusion spinal cord injury, we assessed locomotor recovery with the Basso Mouse Scale (BMS). Testing occurred following SCI on days 1, 3, 5, 7, and then weekly for the remainder of the study. BMS is not designed as a linear scale, but rather follows the stereotypical sequence of recovery that occurs in mice following SCI (Basso et al., 2006). Therefore, recovery over time does not tend to occur in a linear trajectory. Instead, scores tend to rapidly increase in the first few testing days, and then eventually plateau. Scores between (0-3) indicate hindlimb paralysis with variable amounts of ankle movement. Once subjects have reached between (4-6) on the scale, they are plantar stepping with variable coordination and foot placement. The 50 kdyn and 75 kdyn forces

were chosen so that we could characterize both a mild and a moderate-severe injury, in order to assess whether injury severity was a factor in the development of pain-related behaviors. 75 kdyn is considered a moderate-to-severe injury in mice (Kerr & David, 2007; Orr et al., 2017; Zhang et al., 2015). In studies characterizing this injury as severe, mice recovered to an average of 3 on the BMS scale (Kerr & David, 2007). Our 75 kdyn mice recovered to an average between 4 and 5 on the BMS scale, so we categorized this group as moderately injured.

Following mild or moderate injury, mice recover locomotor function in a stereotypical fashion, from low day one scores to a plateau occurring between 28 and 35 days post-SCI. On day one after injury, there are a percentage of each cohort that have scores of 4 or higher, indicating a less severe injury. As surgical proficiency improves, the percentage of mice that had higher scores on day 1 decreased. Throughout the rest of this chapter, results are presented in two ways: 1) all SCI mice for each cohort are averaged regardless of their BMS score on day one post-injury, and 2) SCI subjects are split between low and high day one BMS scores. A low score was between 0-3, and a high score was between 4-9.

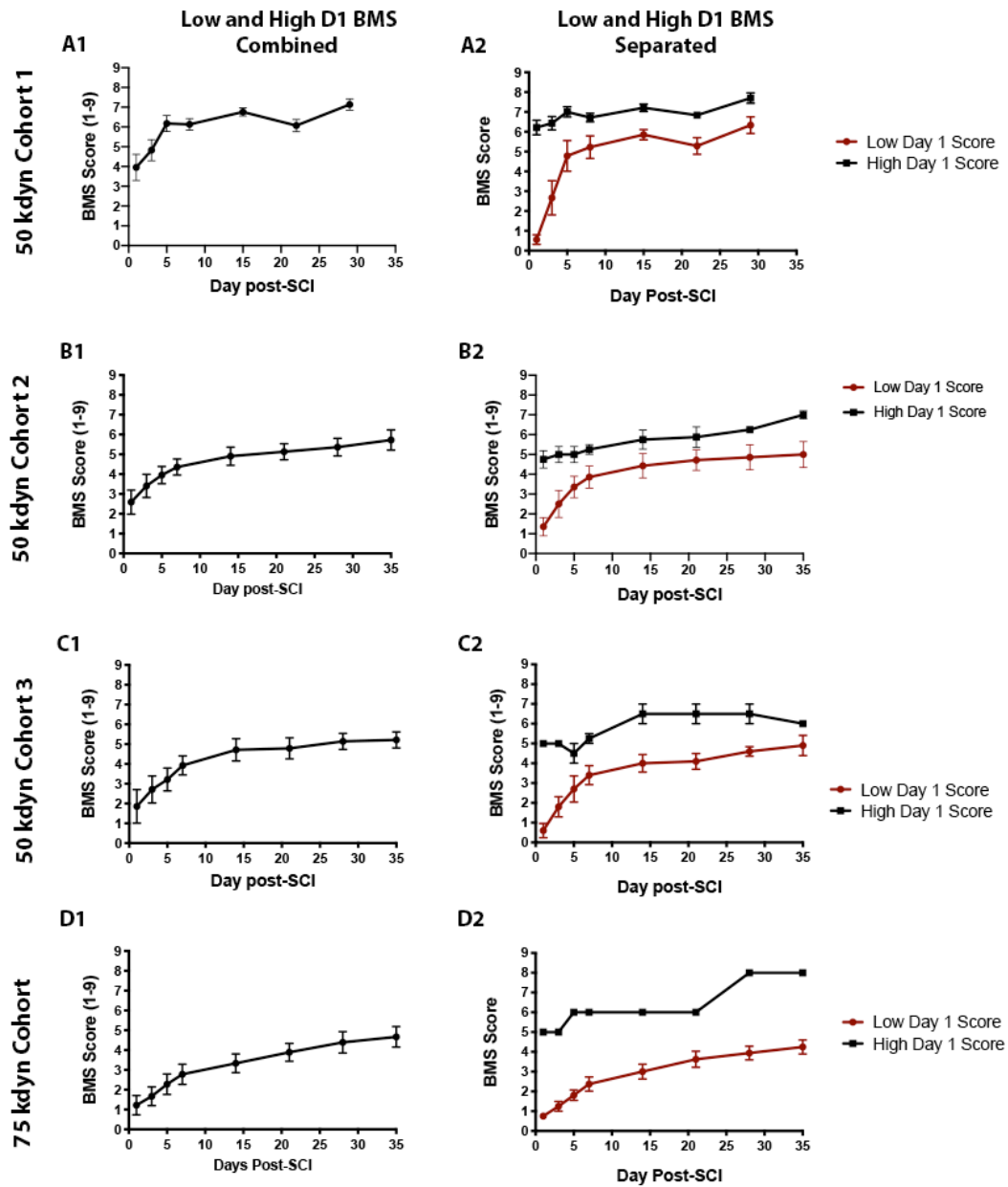
Table 2.2 illustrates the average BMS scores on day 1 and day 35 for the combined and split groups. A two-way ANOVA with repeated measures was run to assess significant differences over time between the low day one and high day one groups. For all 50 kdyn cohorts, there were significant differences between the low and high day one BMS scores over time (p-values and F values reported in Table 2.2). The 75 kdyn group only had one animal with a BMS score of 4 or higher on day one, therefore no significant differences could be calculated between groups. We also examined whether the low and

high day one groups differed specifically on day 35 by utilizing Sidak's multiple comparisons test. There were no significant differences between the low and high day one groups on day 35 for any of the cohorts, indicating that both groups ended up recovering to a similar BMS score prior to the start of behavioral testing (p-values reported in Table 2.2). We also aimed to examine whether there were significant differences between all cohorts, specifically in the combined data. There were no significant differences in the two-way ANOVA (Fig. 2.1e; Time x Cohort, $p = 0.807$, $F(14,168) = 0.664$. Additionally, there were no significant differences at any of the timepoints measured between cohorts (Sidak's multiple comparisons test).

Table 2.2: BMS Scores

BMS Scores		# mice	Day 1	Day 35	ANOVA Results Time x Day 1 Score	Sig diff on day 35?
50 kdyn Cohort 1	Combined	22	3.96 ± 0.66	7.19 ± 0.28		
	Low Day 1	9	0.556 ± 0.242	6.33 ± 0.42	Yes; $p < 0.0001$ $F(6,107) = 16.02$	No $p = 0.148$
	High Day 1	14	6.21 ± 0.37	7.70 ± 0.26		
50 kdyn Cohort 2	Combined	11	2.59 ± 0.61	5.73 ± 0.51		
	Low Day 1	7	1.36 ± 0.46	5.00 ± 0.66	Yes; $p < 0.0001$ $F(7,63) = 3.75$	No $p = 0.164$
	High Day 1	4	4.75 ± 0.43	7.00 ± 0.20		
50 kdyn Cohort 3	Combined	7	1.86 ± 0.85	5.21 ± 0.41		
	Low Day 1	5	0.6 ± 0.37	4.9 ± 0.51	Yes; $p = 0.0040$ $F(7,35) = 3.70$	No $p = 0.559$
	High Day 1	2	5.00 ± 0	6.00 ± 0		
75 kdyn Cohort	Combined	9	1.22 ± 0.49	4.67 ± 0.52		
	Low Day 1	8	0.75 ± 0.16	4.25 ± 0.35	No; $p = 0.406$	Not sufficient for comparison
	High Day 1	1	5.00	8.00		

BMS Scores



E All Cohorts

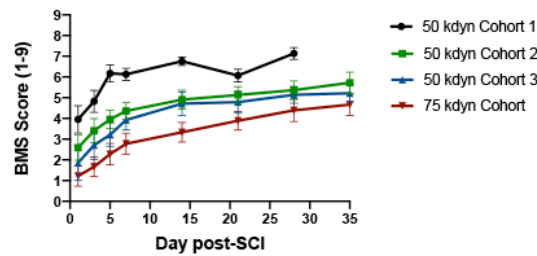


Figure 2.1: Male ICR mice recover locomotion following mild and moderate thoracic contusion spinal cord injury in a reproducible manner: Mice had BMS scores taken on days 1, 3, 5, 7, and then weekly for the remainder of the studies. **A-D(1-3):** All cohorts, regardless of injury severity, exhibit stereotypical locomotor recovery, with lower scores on day one, rapid improvement between day one and day 14, and a plateau between day 28-35. Values on day one and day 35 are reported in Table 2.2. **E:** Comparisons of the combined data for the three 50 kdyn cohorts and the 75 kdyn cohort did not find significant differences between any of them (Two-way ANOVA with Sidak's multiple comparisons ($p=0.807$, $F(14,168)=0.664$)).

Analysis of mild 50 kdyn thoracic contusion spinal cord injury effects on fine motor coordination in male ICR mice:

We analyzed differences in fine motor coordination between sham and SCI mice with the rotarod apparatus. The mice we tested included the first and second 50 kdyn cohorts. There were no differences between the sham and SCI mice in either of the mild 50 kdyn cohorts that were tested (Fig. 2.2(a1,b1); $p=0.835$ and $p=0.097$ respectively, unpaired t-test and one-way ANOVA). When the data was separated into two groups based on the BMS scores at day one, there were no differences between sham or any SCI group (Fig. 2.2(a2,b2); $p=0.704$ and $p=0.409$ respectively, one-way ANOVA with Tukey's *post hoc*). Even though the naïve mice exhibit higher RPM averages than the sham or SCI mice in the second 50 kdyn cohort, the differences were not significant (Tukey's *post hoc*). We aimed to examine whether there were differences in rotarod performance based on the BMS score on day one post-injury. To do this we ran a correlation comparing day one

BMS score to the RPM at fall on testing day (Fig. 2.2(a3-b3)). The two mild injury cohorts had different relationships between day one BMS score and RPM, with the first 50 kdyn cohort having a negative correlation ($r=-0.820$) and the second 50 kdyn cohort having a positive correlation between the two variables ($r=0.532$).

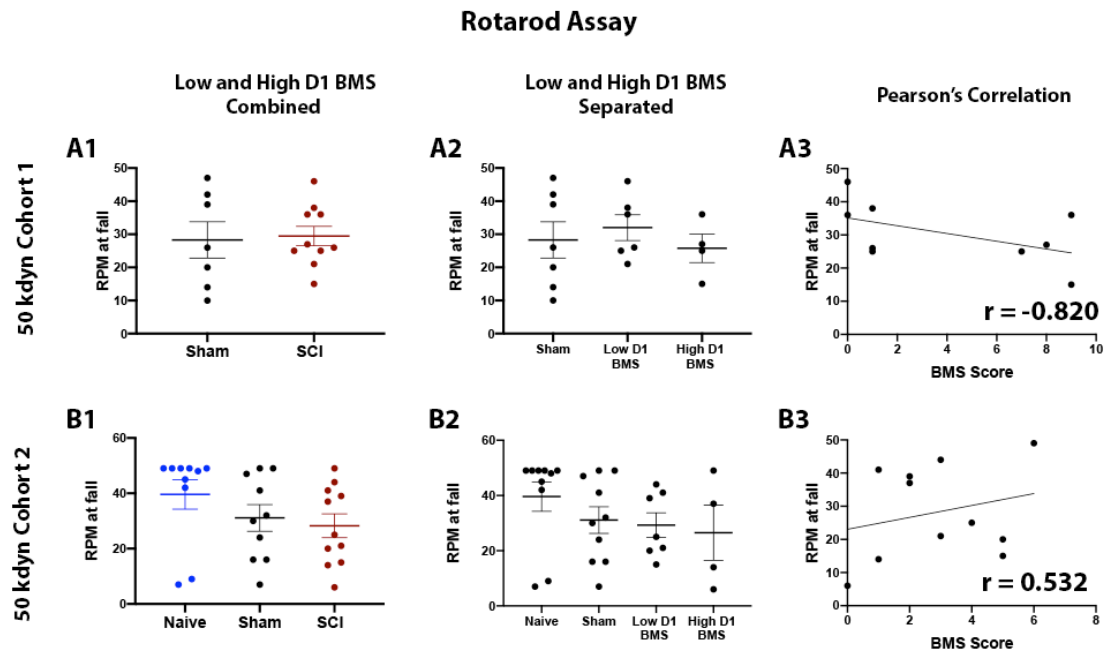


Figure 2.2: Analysis of mild 50 kdyn thoracic contusion spinal cord injury effects on fine motor coordination in male ICR mice: We analyzed differences in fine motor coordination between sham and SCI mice with the rotarod apparatus. RPM at fall was recorded for three consecutive days, beginning at Day 35 post-surgery. **A1-B1:** No significant differences between sham and SCI, or naïve, sham, or SCI in the rotarod test ($p=0.835$ and $p=0.097$ respectively, unpaired t -test and one-way ANOVA). **A2-B2:** SCI subjects were split into two groups based on their day one BMS score. There were no significant differences between sham and SCI, or naïve, sham, or SCI in the rotarod test ($p=0.704$ and $p=0.409$ respectively, one-way ANOVA with Tukey's post hoc) **A3:** There

was a negative correlation between the RPM at fall and the day one BMS score ($r=-0.820$) for the first 50 kdyn cohort, and (b3) a positive correlation between RPM at fall and the day one BMS score ($r=0.532$) for the second 50 kdyn cohort.

Mechanical withdrawal thresholds are not altered following mild and moderate thoracic contusion spinal cord injury in male ICR mice:

We utilized von frey filaments to test mice for mechanical sensitivity following mild and moderate injury. This assay was originally developed to test for pain-related behavior, where subjects with mechanical allodynia exhibit reduced withdrawal thresholds, measured in grams of force (Chaplan et al., 1994). In order to test for mechanical allodynia, the ability to detect stimuli within non-nociceptive ranges must be intact. Previous studies have found that the ability to detect stimuli for mechanical allodynia testing is variable in mice following contusion spinal cord injury (Hoschouer et al., 2010). For these experiments, mice from all three 50 kdyn cohorts and the mice from the 75 kdyn cohort were tested. Our results indicate that regardless of the cohort, our injured subjects did exhibit changes in mechanical sensitivity. For each cohort, SCI mice consistently had higher thresholds than sham controls, and similar withdrawal thresholds to the naïve control mice. For the first and third 50 kdyn cohorts, there were no significant differences between sham and SCI or naïve and SCI subjects (Fig. 2.3(a1,c1); $p = 0.258$ or $p=0.228$ respectively, unpaired t-test). Though the subjects in the low day one BMS score group tended to have higher withdrawal thresholds than the shams or subjects in the high day one score group when separated out, the differences were not significant (Fig. 2.3(a2,c2): $p=0.170$ and $p=0.147$, one-way ANOVA with Tukey's *post hoc*). For the

second 50 kdyn cohort, the sham subjects had significantly reduced withdrawal thresholds compared to the naïve and SCI mice. This indicates that the laminectomy was potentially capable of eliciting mechanical allodynia, and that this did not occur in the SCI subjects (Fig. 2.3b1; $p = 0.0071$, one way ANOVA, tukey's *post hoc*). When the subjects with low and high day one BMS scores were separated, there were significant differences between sham and high day one SCI mice, but not low day one SCI mice ($p=0.009$, one-way ANOVA with Tukey's *post hoc*). The 75 kdyn cohort did not have any differences between naïve and SCI subjects, demonstrating that impact force does not elicit changes in mechanical sensitivity in our hands (Fig. 2.3d1; $p=0.512$, unpaired t-test). This remained true when the subjects with low and high day one scores were separated (Fig. 2.3d2; $p=0.805$, one-way ANOVA with Tukey's *post hoc*). Interestingly, when we ran correlations comparing BMS score on day one to withdrawal threshold, there was a consistent trend for all mild and moderate cohorts. For all cohorts, there was a negative correlation between withdrawal threshold and BMS score on day one, indicating that the more severely injured mice on day one have higher thresholds on testing day, and the less severely injured mice on day one have lower thresholds on testing day (Fig. 2.3(a3-d3): 50 kdyn cohort 1: $r = -0.517$; 50 kdyn cohort 2: $r = -0.194$; 50 kdyn cohort 3: $r = -0.366$; 75 kdyn cohort: $r = -0.184$).

Von Frey Mechanical Allodynia

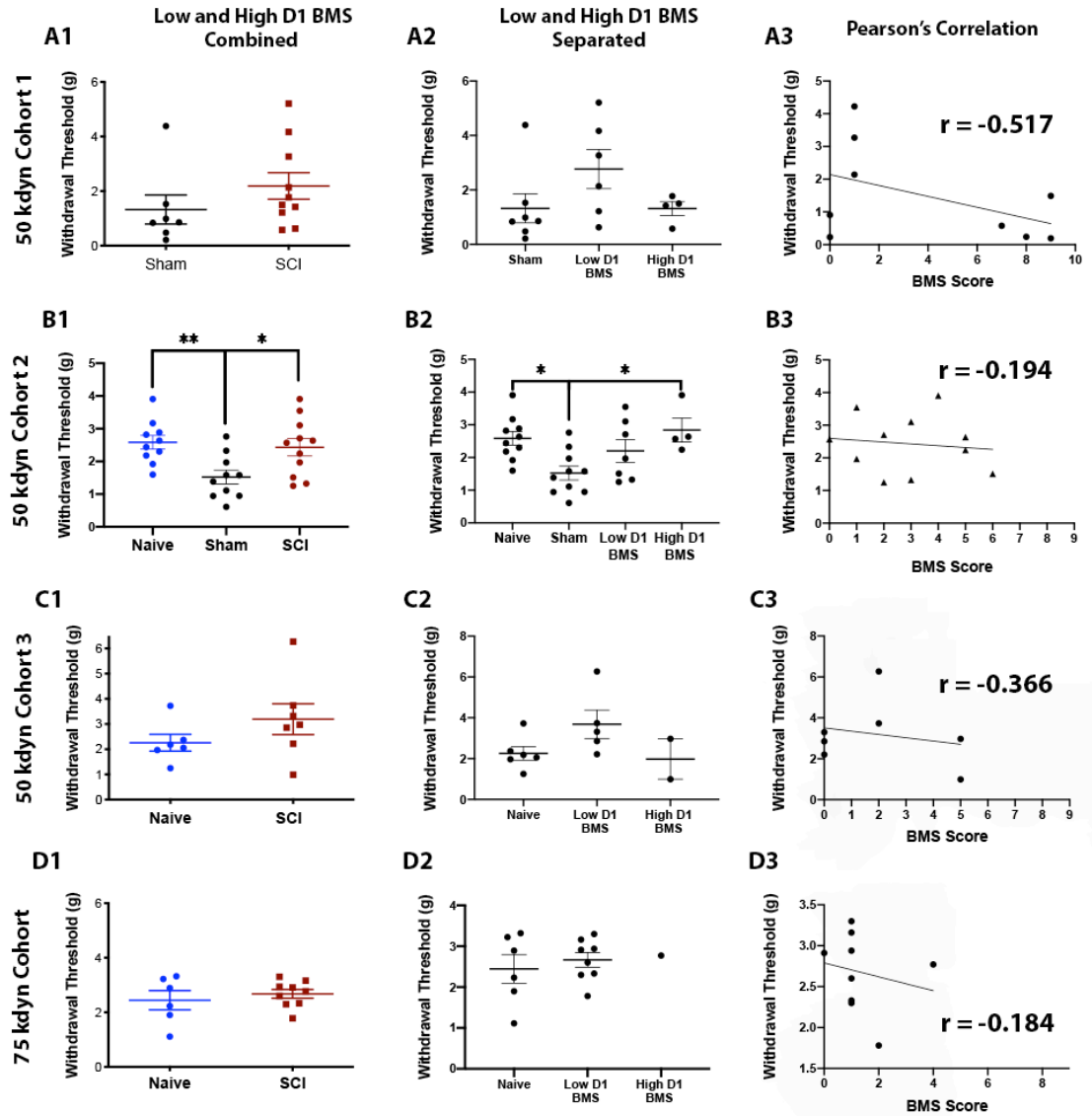


Figure 2.3: Mechanical withdrawal thresholds are not altered following mild and moderate thoracic contusion spinal cord injury in male ICR mice: At six weeks following thoracic contusion SCI, withdrawal thresholds were measured with von frey filaments. **A1,C1:** For the first and third 50 kdyn cohorts, withdrawal thresholds for SCI mice were unchanged compared to sham controls ($p = 0.258$ or $p=0.228$ respectively, unpaired t -

test). **A2,C2:** When the injured subjects were split based on their day one BMS scores, there were no significant differences between groups ($p=0.170$ and $p=0.147$, one-way ANOVA with Tukey's post hoc). **B1:** For the second 50 kdyn cohort, the sham subjects exhibited mechanical allodynia compared to the naïve and SCI mice ($p = 0.0071$, one way ANOVA, tukey's post hoc). **B2:** When the injured subjects were split based on their day one BMS scores, sham had significantly lower thresholds compared to naïve and to the injured subjects with high day one BMS scores ($p=0.009$, one-way ANOVA with Tukey's post hoc) **D1-2:** The moderate 75 kdyn cohort did not have different mechanical thresholds compared to sham controls (combined: $p=0.512$, unpaired t-test; separated: $-p=0.805$, one way ANOVA with Tukey's post hoc). **A3-D3:** For all cohorts, there was a negative correlation between withdrawal threshold and BMS score on day one, indicating that the more severely injured mice on day one have higher thresholds on testing day, and the less severely injured mice on day one have lower thresholds on testing day (Fig. 2.3(a3-d3): 50 kdyn cohort 1: $r = -0.517$; 50 kdyn cohort 2: $r = -0.194$; 50 kdyn cohort 3: $r = -0.366$; 75 kdyn cohort: $r = -0.184$).

Following mild or moderate thoracic contusion spinal cord injury, injury severity measured on day one affects whether male ICR mice develop heat hyperalgesia:

We assessed heat hyperalgesia with the Hargreaves apparatus, which utilizes a radiant heat source aimed toward the hindpaw. Subjects with heat hyperalgesia will exhibit reduced latency to withdraw from the light (Deuis, Dvorakova, & Vetter, 2017; Hargreaves, Dubner, Brown, Flores, & Joris, 1988). We performed this assay with the mice from the second and third 50 kdyn cohorts, and the 75 kdyn cohort. The second 50

kdyn cohort had no significant differences in withdrawal latencies between naïve, sham, or SCI mice regardless of if low and high day one BMS groups were combined or separated (Fig. 2.4(a1,2); $p=0.775$ and $p=0.898$ respectively, one way ANOVA with Tukey's *post hoc*). When the low and high day one groups were combined, the third 50 kdyn cohort had differences approaching significance (Fig 2.4b1; $p=0.083$, unpaired t-test). When day one BMS scores were separated into low and high, the injured subjects with low day one scores had significantly lower withdrawal latencies compared to naïve mice, indicating thermal hyperalgesia (Fig. 2.4b2, $p=0.015$, one-way ANOVA with Tukey's *post hoc*). For the moderate 75 kdyn contusion injury, there were no significant differences between naïve and injured mice (Fig. 2.4d1; $p=0.388$, Welch's t-test separated). The high day one subject in the 75 kdyn cohort was statistically an outlier in the combined group, therefore examining differences based on low or high day one scores for this test are meaningless. We ran correlations comparing BMS score on day 1 to withdrawal latency, and there was a consistent trend for all injuries regardless of impact force. For all cohorts, there was a highly positive correlation between withdrawal latency and BMS score on day one, indicating that the more severely injured mice on day one have lower latencies on testing day, and the less severely injured mice on day one have higher latencies on testing day (Fig. 2.4(a3-c3): 50 kdyn cohort 2: $r = 0.752$; 50 kdyn cohort 3: $r = 0.997$; 75 kdyn cohort: $r = 0.991$). Our results point to thermal hyperalgesia developing in spinal cord injury subjects in a variable manner, with more severely injured mice on day one following SCI being more likely to exhibit reduced withdrawal latencies.

Hargreaves Thermal Hyperalgesia

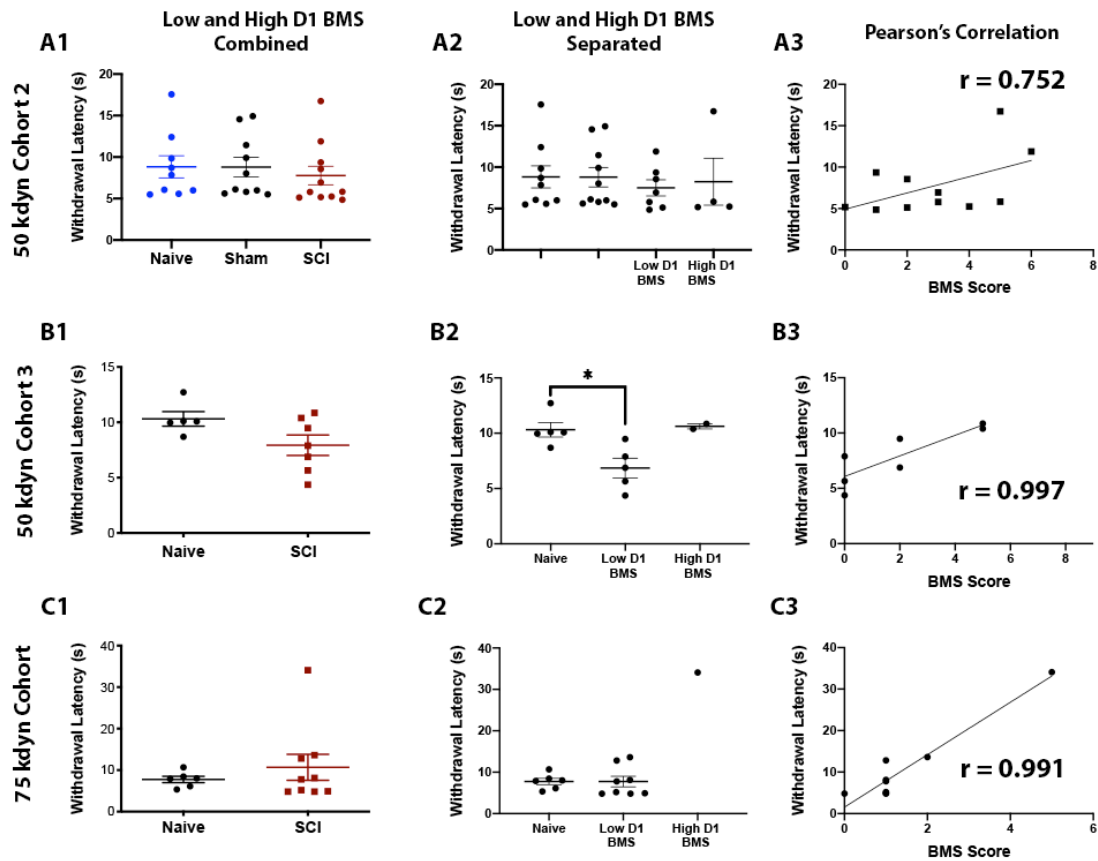


Figure 2.4: Following mild or moderate thoracic contusion spinal cord injury, injury severity measured on day one affects whether male ICR mice develop heat hyperalgesia: **A1-C1:** The mild 50 kdyn and moderate 75 kdyn injuries did not elicit heat hyperalgesia when day one groups are combined (**a1-b1**: $p=0.775$ and 0.083 , one way ANOVA and unpaired t -test respectively; **c1**: $p=0.388$, Welch's t -test). **B2:** Subjects with low day one BMS scores have significantly lower withdrawal thresholds than naïve subjects on testing day ($p=0.015$, one-way ANOVA with Tukey's post hoc). **C1-3:** For all cohorts, there was a highly positive correlation between withdrawal latency and BMS score on day one, indicating that the more severely injured mice on day one have lower

latencies on testing day, and the less severely injured mice on day one have higher latencies on testing day (Fig. 2.4(a3-c3): 50 kdyn cohort 2: $r = 0.752$; 50 kdyn cohort 3: $r = 0.997$; 75 kdyn cohort: $r = 0.991$).

Following mild or moderate thoracic contusion spinal cord injury, injury severity measured on day one affects how much male ICR mice burrow:

Burrowing is an ethologically relevant behavior in mice, most frequently utilized as a model of overall well-being (R. M.J. Deacon, 2009; Robert M.J. Deacon, 2006; Jirkof, 2014). Some have used this as a measure of spontaneous pain following injury, which is improved with analgesic administration (Andrews et al., 2012; Deuis et al., 2017; Jirkof et al., 2010). We tested burrowing behavior in all three 50 kdyn cohorts, and in the 75 kdyn cohort. Our results indicate that in general, burrowing behavior is decreased in SCI mice. Though the trend of decreased burrowing in SCI subjects remains consistent regardless of injury severity, there are no significant differences in burrowing behavior between any of the groups tested when the subjects with low and high day one scores were combined (Fig. 2.5a1-d1; **a1**: $p=0.354$, unpaired t-test; **b1**: $p=0.519$, one way ANOVA with Tukey's *post hoc*; **c1**: $p= 0.109$, Welch's t-test; **d1**: $p=0.164$, unpaired t-test). When subjects with low and high day one BMS scores are separated, there are significant differences that are uncovered. For the first 50 kdyn cohort, there are significant differences between the sham and low day one subjects, and between the low day one and high day one groups ($p= 0.0104$, one-way ANOVA with Tukey's *post hoc*). This indicates that more severely injured subjects on day one end up burrowing less than less severely injured mice, regardless of if they have recovered similar

locomotion by testing day. These trends held for the other 50 kdyn cohorts and the 75 kdyn cohort, even if they were not significantly different (Fig. 2.5b2-d2; $p > 0.05$, one-way ANOVA with Tukey's *post hoc*). Overall our results suggest a trend in reduced burrowing, which we presume might be due to reduced locomotion, reduced level of well-being, or spontaneous pain-behavior. We ran correlations comparing BMS score on day 1 to percent of material burrowed, and there was a consistent trend for all injuries regardless of impact force. For all cohorts, there was a highly positive correlation between burrowing percentage and BMS score on day one, indicating that the more severely injured mice on day one burrow less, and the less severely injured mice on day one burrow more (Fig. 2.4(a3-c3): 50 kdyn cohort 1 : $r = 0.775$; 50 kdyn cohort 2: $r = 0.336$; 50 kdyn cohort 3: $r = 0.995$; 75 kdyn cohort: $r = 0.889$).

Burrowing

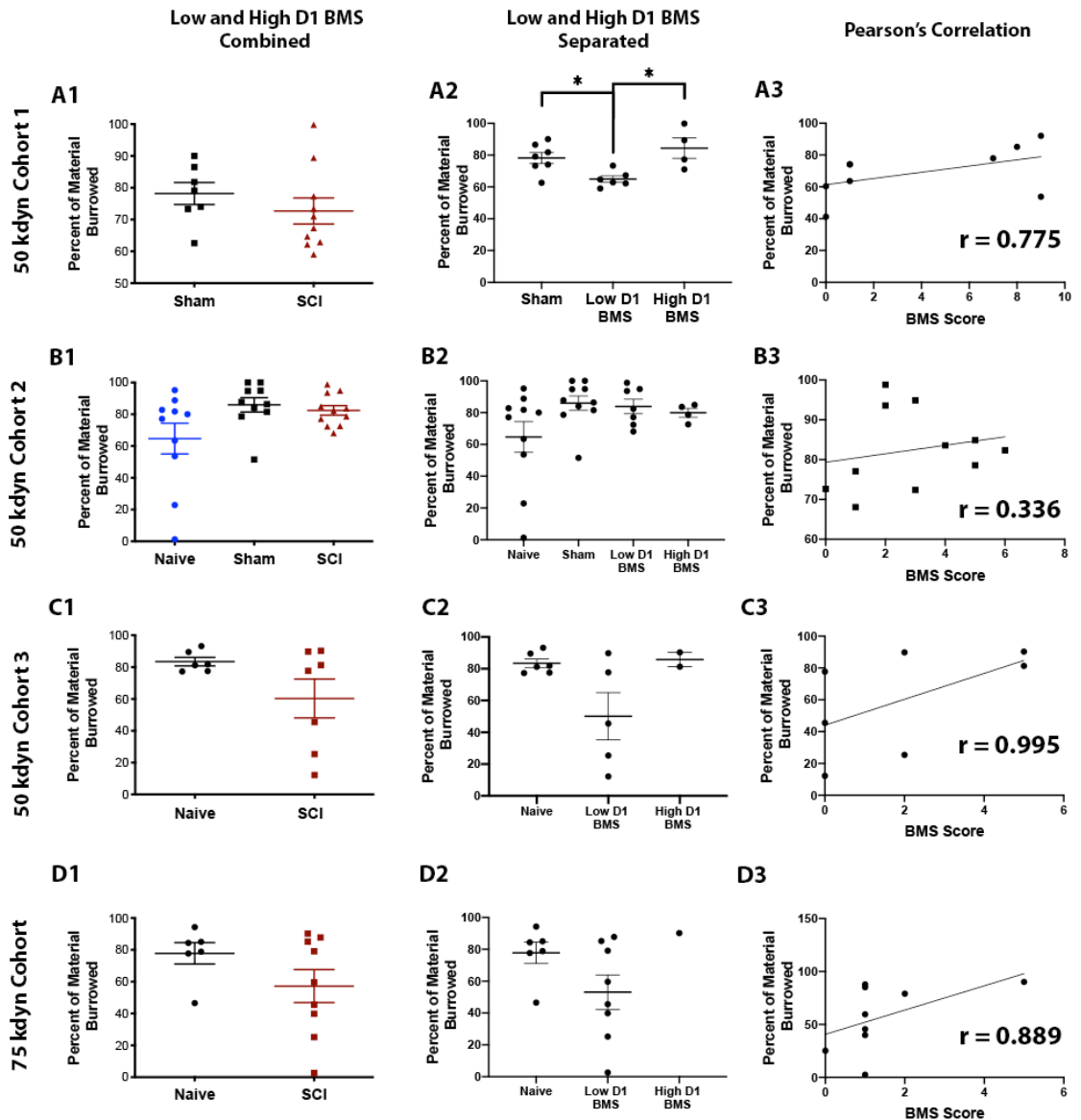


Figure 2.5: Following mild or moderate thoracic contusion spinal cord injury, injury severity measured on day one affects how much male ICR mice burrow: The percentage of material burrowed during the burrowing assay was measured and compared between naïve, sham, and SCI mice. **A1-D1:** Though the trend of decreased burrowing in SCI subjects remains consistent regardless of injury severity, there are no significant

differences in burrowing behavior between any of the groups tested when the subjects with low and high day one scores were combined (**A1**: $p=0.354$, unpaired t-test; **b1**: $p=0.519$, one way ANOVA with Tukey's post hoc; **1**: $p=0.109$, Welch's t-test; **d1**: $p=0.164$, unpaired t-test). **A2**: For the first 50 kdyn cohort, there are significant differences between the sham and low day one subjects, and between the low day one and high day one groups ($p=0.0104$, one-way ANOVA with Tukey's post hoc). **B2-D2**: When low and high day one BMS groups were separated, there was a statistically insignificant trend towards decreased burrowing for more severely injured subjects on day one ($p>0.05$, one-way ANOVA with Tukey's post hoc). **A3-D3**: We ran correlations comparing BMS score on day 1 to percent of material burrowed, and there was a consistent trend for all injuries regardless of impact force. For all cohorts, there was a highly positive correlation between burrowing percentage and BMS score on day one, indicating that the more severely injured mice on day one burrow less, and the less severely injured mice on day one burrow more (Fig. 2.4(a3-c3): 50 kdyn cohort 1 : $r=0.775$; 50 kdyn cohort 2: $r=0.336$; 50 kdyn cohort 3: $r=0.995$; 75 kdyn cohort: $r=0.889$).

Mild and moderate spinal cord injury induces a dramatic loss of light touch sensitivity in male ICR mice:

The cotton swab test is used to examine changes in light touch sensitivity in the hindpaw, specifically sensitivity of low-threshold, rapidly adapting mechanoreceptors (Dhandapani et al., 2018; Garrison et al., 2011). We tested mice from the second and third 50 kdyn cohorts, and from the 75 kdyn cohort. For the second 50 kdyn cohort, the SCI mice had

significantly decreased responses when compared to the naïve or sham mice, which were not different from one another (Fig. 2.6a1; $p=0.0003$, one way ANOVA, Tukeys *post hoc*). These results did not change when subjects were split into low day one and high day one groups; both SCI groups had significantly reduced responses compared to sham and naïve mice (Fig. 2.6a2; $p<0.0001$, one-way ANOVA with Tukey's *post hoc*). The third 50 kdyn SCI mice exhibited significantly decreased percent responses when compared to the naïve controls (Fig. 2.6b1; $p=0.0006$, unpaired t-test). When the subjects were separated based on day one BMS scores, only the group with low day one BMS scores were significantly different than naïve controls (Fig. 2.6b2; $p=0.0008$, one-way ANOVA with Tukey's *post hoc*). The moderate 75kdyn contusion SCI subjects had significantly decreased responses compared to naïve control subjects, regardless of if subjects with low and high day one BMS scores were combined or separated (Fig. 2.6c1-2; $p=0.0115$, Welch's t-test or $p = 0.0040$, one-way ANOVA with Tukey's *post hoc*, respectively). We ran correlations comparing BMS score on day 1 to percent responses, and there was not a consistent trend based on injury severity. (Fig. 2.6(a3-c3): 50 kdyn cohort 2 : $r = -0.472$; 50 kdyn cohort 3: $r = 0.854$; 75 kdyn cohort: $r = -0.284$). Overall, our results indicate that mice that underwent contusion spinal cord injuries exhibit significant decreases in responsiveness to the cotton swab stimulus. This indicates a significant loss of light touch sensitivity occurring in the spinal cord injury subjects, regardless of injury severity.

Cotton Swab Test

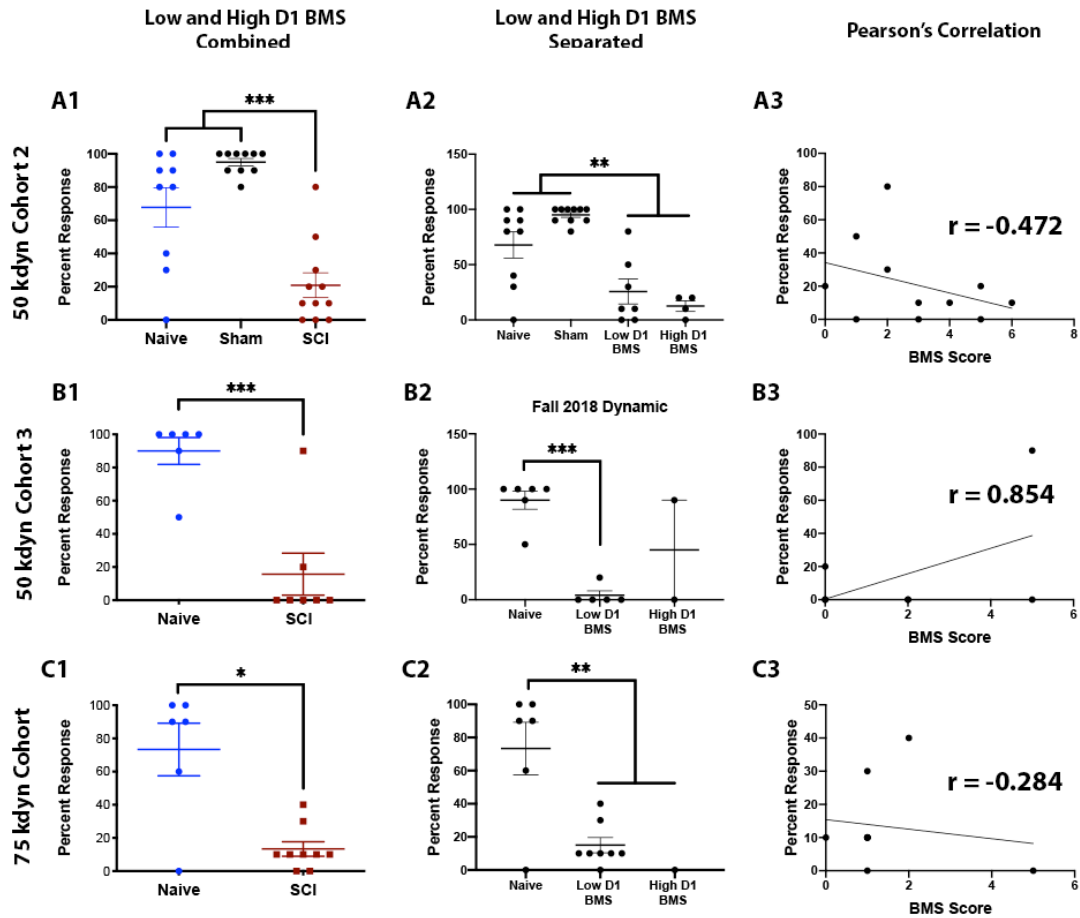


Figure 2.6: Mild and moderate thoracic contusion spinal cord injury induces a dramatic loss of light touch sensitivity in male ICR mice: We utilized the cotton swab test to examine changes in light touch sensitivity in the hindpaw. **A1:** For the second 50 kdyn cohort, SCI mice had significantly decreased responses when compared to the naïve or sham mice, which were not different from one another (Fig. 2.6a1; $p=0.0003$, one way ANOVA, Tukeys post hoc). **A2:** When subjects were split into low day one and high day one groups, both SCI groups had significantly reduced responses compared to sham and naïve mice (Fig. 2.6a2; $p<0.0001$, one-way ANOVA with Tukey's post hoc). **B1:** The third 50 kdyn SCI mice exhibited significantly decreased percent responses when

compared to the naïve controls (Fig. 2.6b1; $p=0.0006$, unpaired t -test). **B2:** For the third 50 kdyn cohort, when the subjects were separated based on day one BMS scores, only the group with low day one BMS scores were significantly different than naïve controls (Fig. 2.6b2; $p=0.0008$, one-way ANOVA with Tukey's post hoc). **C1-2:** The moderate 75 kdyn contusion SCI subjects had significantly decreased responses compared to naïve control subjects, regardless of if subjects with low and high day one BMS scores were combined or separated (Fig. 2.6c1-2; $p=0.0115$, Welch's t -test or $p = 0.0040$, one-way ANOVA with Tukey's post hoc, respectively). **A3-C3:** We ran correlations comparing BMS score on day 1 to percent responses, and there was not a consistent trend based on injury severity. (Fig. 2.6(a3-c3): 50 kdyn cohort 2 : $r = -0.472$; 50 kdyn cohort 3: $r = 0.854$; 75 kdyn cohort: $r = -0.284$).

Discussion

Spinal cord injury is severe, long-lasting, and presents with a myriad of complications. Animals studies have aimed to examine SCI to investigate potential interventions, but many of these experiments have been done in rats. The present study aimed to thoroughly characterize behavior following mild and moderate thoracic contusion SCI in male ICR mice. These studies are the most thorough characterization of sensory behavior following SCI in mice to date, including touch, and evoked or spontaneous pain behaviors. We show for the first time that following SCI, mice exhibit a dramatic loss of light touch sensitivity.

Spinal cord injury induces a significant loss of light touch sensitivity in mice

The cotton swab test was originally designed to complement a light touch punctate assay, intended as a more dynamic light touch stimulus (Garrison et al., 2011). It was developed to study the mechanosensitive ion channel TRPC1, which is primarily located on A-beta and peptidergic IB4-negative C-fibers (Elg, Marmigere, Mattsson, & Ernfors, 2007). The cotton swab assay was utilized to assess if there was an effect of TRPC1 knockdown on sensitivity of large diameter, low-threshold mechanosensory neurons (Garrison et al., 2011). Following knockdown of TRPC1, there were decreased cotton swab responses. Another study examined the effect of ablating TrkB-positive sensory neurons, which are primarily myelinated low-threshold mechanoreceptors that innervate D-hairs and rapidly adapting mechanoreceptors (Dhandapani et al., 2018). Ablation of low-threshold afferents led to decreased cotton swab responses. These studies elucidate the mechanoreceptors that are activated by the cotton swab assay in naïve mice, specifically low threshold, rapidly adapting mechanoreceptors. Following intraplantar CFA or spared nerve injury, mice respond in higher percentages than vehicle-injected or sham mice (Cowie, Moehring, O'Hara, & Stucky, 2018). The cotton swab test is therefore a useful assay to test light touch sensitivity, which is able to detect mechanical allodynia in injury models.

Though this test has been utilized on mice that have had inflammation or peripheral nerve injury, these studies are the first to utilize this assay to test light touch following spinal cord injury. Overall, the cotton swab test uncovered changes in light touch sensitivity that occur following spinal cord injury. SCI was capable of producing a significant decrease in responses when compared to naïve and sham mice. The near-complete absence of

responses to the stimulus seen in the SCI subjects points to a significant loss of their light touch sensitivity, specifically information sent from low-threshold rapidly adapting mechanoreceptors. These mice had the ability to plantar step, and even the most severely injured had withdrawal responses to noxious stimuli. Therefore, we concluded that the lack of withdrawal response to the cotton swab were indicative of reduced sensitivity rather than motor deficits.

The loss of light touch sensitivity is consistent with what would be predicted to occur following dorsal column damage, a component of the contusion spinal cord injury. The dorsal column-medial lemniscal pathway relays information sent from the periphery to the brain. The information carried through this pathway includes touch and proprioceptive information. In humans, spinal cord injury can lead to loss of sensation, with or without pain (Eide et al., 1996). In mice and rats, contusion spinal cord injury leads to a lesion in the spinal cord that encompasses the dorsal columns at the level of injury (Attwell, van Zwieten, Verhaagen, & Mason, 2018; James et al., 2011). This disrupts the flow of touch information being sent from the periphery. Electrophysiological recordings from teased dorsal root fibers found that following SCI, rats have a complete conduction block in ascending dorsal column axons during the acute phases of injury (James et al., 2011). Conduction across the lesion improves slightly over time, but still remains significantly reduced during the chronic phase of injury. Interestingly, though there were still a large number of demyelinated fibers in the dorsal columns during the chronic phase, there was a subpopulation of axons that remained myelinated but were unable to conduct action potentials (James et al., 2011). Our work points to the cotton swab assay being a useful test to measure changes in touch sensitivity following SCI in mice. In addition, due to the

potential presence of intact axons in this area that can be targeted with interventions to regain function, this assay is a potential tool to measure attenuation of these deficits.

3

Severity of injury influences pain-related behaviors following spinal cord injury in mice

Our results examining mechanical sensitivity, thermal hyperalgesia, and burrowing behavior uncover the impact of injury severity following SCI on measures of pain-related behavior. Prior to the start of these studies, there were a limited number of studies that found mice with mechanical allodynia and thermal hyperalgesia following a variety of SCI methods, including clip compression and weight-drop contusion (Hoschouer, Yin, & Jakeman, 2009; Kerr & David, 2007; Meisner, Marsh, & Marsh, 2010b; Tanabe, Ono, Honda, & Ono, 2009). Prior to the conclusion of these studies, several papers were published confirming the development of thermal hyperalgesia following SCI in mice (Castany, Gris, Vela, Verdú, & Boadas-Vaello, 2018; Gensel, Donahue, Bailey, & Taylor, 2019). Consistent with this work, we were able to detect thermal hyperalgesia in our spinal cord injury mice, particularly the subjects with more severe injury on day one. There was a highly positive correlation between BMS score on day one and withdrawal latency, with more injured mice on day one post-SCI exhibiting lower withdrawal latency.

Evaluation of spontaneous or ongoing pain in mice is more difficult than measuring evoked responses, but methods have been adapted to evaluate behavior in models of persistent pain. In peripheral and inflammatory injury models, conditioned place preference has been utilized to assess ongoing pain, by measuring the preference of an injured subject for a chamber paired with a non-opioid analgesic (King et al., 2009; Okun et al., 2011; Sufka, 1994). There are only a handful of studies utilizing conditioned place preference in spinal

cord injury, where they found evidence of ongoing pain in rats (Davoody et al., 2011; Yang et al., 2014). Burrowing is an ethologically relevant behavior that is considered a measure of overall well-being in mice (Robert M.J. Deacon, 2006; Jirkof, 2014). There are several groups that have found reduced burrowing in peripheral models of pain, which is attenuated by administration of an analgesic (Andrews et al., 2012; Deuis et al., 2017; Jirkof et al., 2010). These studies are the first to examine burrowing behavior in mice following spinal cord injury. Our results point to a consistent trend in decreased burrowing in spinal cord injured mice, that is highly correlated to injury severity on day one following SCI. These results are complex to draw conclusions from, due to the nature of spinal cord injury. It is possible that this reduced burrowing is indeed due to ongoing pain, but unless this behavior is reversed through administration of an analgesic, it is impossible to conclude that is the case. It is also possible that overall these mice are feeling ill, and therefore the reduced burrowing is due to a reduction in overall well-being. A complication with testing ongoing pain measures in spinal cord injury is the motor impairment that is a hallmark of the injury. It is possible that reduced burrowing is due primarily to reduced overall movement, even though these mice have recovered locomotion enough to perform the task. Future studies should take this into account when designing methods to probe ongoing pain in mice following spinal cord injury.

We utilized von frey filaments to test mechanical sensitivity, and found that in general, SCI mice had higher thresholds than sham mice and similar thresholds to naïve controls. There was a consistent negative correlation between injury severity on day one post-SCI and withdrawal thresholds, with more severely injured mice having higher thresholds. This is in line with work by Hoschouer et al, where they found that SCI mice had higher hindpaw withdrawal thresholds than control mice, even though they responded to a pin-prick, which

is a noxious mechanical stimuli (Hoschouer et al., 2010). More recent work has found mechanical allodynia in mice following SCI, but importantly these injuries were specifically designed to not cause paresis, with BMS scores on day one hovering around 5.0 on the scale (Castany et al., 2018). These findings are in line with our work and the work by Hoschouer et al, indicating that injury severity is an important consideration when testing for mechanical allodynia in spinal cord injured mice. The Von Frey test was originally developed to assess mechanical allodynia (Chaplan et al., 1994), but in order to measure this, function of low threshold mechanoreceptors must be intact. Our work utilizing the cotton swab assay found a loss of light touch sensitivity, likely caused by a loss of information sent through low threshold rapidly adapting mechanoreceptors due to dorsal column damage. Recent work examining peripheral nerve injury has uncovered a role for the dorsal column pathway in transmitting mechanical allodynia, upending the long-standing idea that pain primarily travels through anterolateral pathways, segregated from touch which is sent through the dorsal columns. Several groups have lesioned the dorsal column pathway following the establishment of mechanical allodynia and thermal hyperalgesia. One group reported a total loss of mechanical allodynia but not hyperalgesia 24 hours after transecting the dorsal columns (H. Sun et al., 2001). Importantly, additional work found that there is recovery of mechanical allodynia several weeks after dorsal column lesion, indicating that though the dorsal columns are involved in transmission of mechanical allodynia, they are not solely responsible for the persistence of this behavior (Saadé et al., 2002). In patients with spinal cord injuries, there are a number that have loss of sensation without pain, pain without loss of sensation, or experience both simultaneously. Studies examining sensation in these patients concluded that central dysesthesia following spinal cord injury isn't solely due to dysfunction of spinothalamic tract, and that there is potential involvement of dorsal column dysfunction as well (Eide et

al., 1996; N. B. Finnerup, Johannesen, Fuglsang-Frederiksen, Bach, & Jensen, 2003). Overall, our results point to the absence of mechanical allodynia in our spinal cord injury mice, but whether this is due to the damaged dorsal columns or these mice do not have allodynia is unclear. Interestingly, in one of our cohorts we were able to elicit lowered withdrawal thresholds in sham control mice, which received the laminectomy without impact. These were significantly lower than both the naïve and the SCI mice, indicating mechanical allodynia. These results point to the importance of including both naïve and sham control mice when examining mechanical sensitivity following spinal cord injury.

Another factor to consider is that the pain-related behaviors we were examining were exclusively looking at below-level pain. Following SCI, many patients have at-level neuropathic pain, described as pain within three dermatomes of the level of injury. There have been limited studies examining at-level pain in mice following spinal cord injury. One group found a marked decrease of responses to noxious pin-prick and non-noxious von frey filaments directly caudal to the injury site on the dorsal trunk (Hoschouer et al., 2010). These areas needed to be shaved, so that the testing site was visible, the area tested was reproducible, and so that responses were not due to activation of mechanoreceptors specifically innervating the hairs.

Conclusions

Overall, our findings point to a dramatic loss of light touch sensitivity following spinal cord injury in male mice, most likely caused by damaged dorsal columns disrupting the flow of information from low-threshold mechanoreceptors. Following spinal cord injury, male mice develop thermal hyperalgesia that is dependent on injury severity, and they burrow less

than sham or naïve controls. Interestingly, our mice did not develop mechanical allodynia following spinal cord injury, and this may also be mediated by the damage to the dorsal columns. These studies are the most thorough characterization of behavior following SCI in mice to date.

CHAPTER 3
ANTISENSE OLIGONUCLEOTIDE-MEDIATED KNOCKDOWN OF COMPLEMENT-3A
RECEPTOR 1:
EFFECT ON PERIPHERAL AND CENTRAL MODELS OF NEUROPATHIC PAIN

The complement pathway is a component of the innate immune system, which is called into action by invading pathogens and endogenous signals indicating injury. The complement 3a receptor (C3aR1) was originally identified as the cognate G-protein coupled receptor for complement component 3a (C3a), a member of the alternative complement pathway (Biryukov & Stoute, 2018; Harboe & Mollnes, 2008; Thurman & Holers, 2006). C3aR1 has been localized via immunohistochemistry to myeloid cells including microglia and macrophages (Doolen et al., 2017), and has been found in neurons and cultured astrocytes via *in situ* hybridization (Davoust et al., 1999). Activation of C3aR1 leads to leukocyte activation and chemotaxis and can mediate apoptotic cell death, demyelination, and activation of resting microglia and astrocytes (Peterson & Anderson, 2014). C3aR1 participates in microglial signaling under pathological conditions including neurodegeneration and virus-induced cognitive impairment (Hong et al., 2016; Lian et al., 2015; Vasek et al., 2016).

In addition to C3a, the receptor has another endogenous ligand, the neuropeptide TLQP-21, and these ligands have a competitive relationship at the same binding site within C3aR1 (Cero et al., 2014; Hannedouche et al., 2013). Our lab has found that TLQP-21 is involved in the development and maintenance of hypersensitivity following peripheral nerve injury, and that this may occur through the activation of microglia by TLQP-21 in a

C3aR1-dependent manner (Doolen et al., 2017; Fairbanks et al., 2014). Upregulation of C3aR1 in microglia has been found following CNS injury, and our lab has shown that C3aR1 is upregulated in lumbar dorsal horn microglia in a time-dependent manner following peripheral nerve injury and spinal cord injury. We previously used an immunoneutralization approach to demonstrate that TLQP-21 contributes to nerve injury-induced hypersensitivity (Fairbanks et al., 2014), and in addition we evaluated the effect of the C3aR1 antagonist SB290157 in the SNI model of neuropathic pain. The antagonist reversed mechanical hypersensitivity as compared to vehicle, but the half-life of the C3aR1 antagonist is approximately 1.5 hours, and therefore any effect of reducing signaling through C3aR1 could only be assessed acutely. The antagonist has exhibited agonist activity in some cells (Mathieu et al., 2005; Therien, Baelder, & Kohl, 2014), and it also binds to several nonspecific targets (Proctor et al., 2004), so evaluation of the behavioral effects of reducing C3aR1 signaling is difficult to separate from off-target effects. Additionally, the only C3aR1 knockout model available is a global knockout, and there are potential compensatory mechanisms occurring throughout development. In order to assess longer-term effects of reducing signaling through C3aR1 in adult mice, the development of antisense oligonucleotides specifically designed to suppress C3aR1 expression provides a promising avenue for long-term gene knockdown.

Antisense oligonucleotides (ASOs) have been one of the most popular methods utilized in scientific research to alter gene expression *in vivo* over the past 25 years. ASOs are synthetically produced short sequences of 13-25 nucleotides in length, designed to hybridize to a target mRNA by aligning complementary base pairs. The ASO binding to the target mRNA creates a DNA/RNA heteroduplex, and ribonuclease H1 (RNase H) is an enzyme that is recruited to degrade these heteroduplexes in both the cytoplasm and

nucleus (Dias & Stein, 2002; Kole, Krainer, & Altman, 2012; Koller & Dean, 2006). Once the mRNA is degraded, the ASO is released from the target and is free to bind to more target mRNA strands, thus one strand of an ASO is able to degrade multiple mRNA target strands. Each target mRNA codes for a specific protein, and the ASO binding to and promoting the degradation of this mRNA disrupts the synthesis of this particular protein. The consequence of ASO administration is selective, efficient, and long-lasting knockdown of a target protein.

Antisense oligonucleotides have therapeutic potential (Evers, Toonen, & van Roon-Mom, 2015), and a number of studies have utilized ASOs to explore knockdown of targets involved in nociception. Chronic constriction injury is a model of peripheral nerve injury-induced neuropathic pain, and it leads to hypersensitivity in mice. Knockdown of NF- κ B, a key mediator of immune activation, via ASOs prior to CCI significantly attenuated the development of mechanical allodynia and thermal hyperalgesia (T. Sun et al., 2006). ASOs have also been utilized in inflammatory pain models, where knockdown of the P2X3 receptor has effectively attenuated CFA-induced thermal hyperalgesia and hindpaw formalin injection-induced nociceptive behaviors (Honore et al., 2002).

Our goal was to examine the consequences of knocking down C3aR1 expression with antisense oligonucleotides in the context of peripheral and central models of hypersensitivity. These studies are the first to examine the consequence of C3aR1 knockdown on pain-related behaviors following injury.

Methods:

C3aR1 antisense oligonucleotide: Antisense oligonucleotides (ASOs) were developed by researchers BF and HK at Ionis Pharmaceuticals. ASOs were designed with five 2'-O-methoxyethyl-modified ribonucleotides on the 5' and 3' ends, and a phosphorothioate backbone aimed at promoting uptake and improving nuclease resistance. The middle targeting oligonucleotides bound to the complementary base pairs of the target mRNA, which recruited RNase H for degradation. The stock solution of ASO was 100 ug/ul, diluted in phosphate buffered saline. ASO was diluted 1:2 in 0.9% sterile saline for intrathecal injections, where 10ul of diluted ASO was injected over 15-30 seconds. The final concentration of ASO injected per subject was 500 ug in 10ul. Vehicle solution for injection was a 1:1 mix of phosphate buffered saline and 0.9% sterile saline. Sequence for C3aR1 ASO: (ACCAAGTTTTTCATCCAATTT). Sequence for control non-targeting ASO: (CCTATAGGACTATCCAGGAA).

Spared Nerve Injury (SNI) model: The spared nerve injury model is a well-established model that produces substantial and prolonged changes in mechanical sensitivity and cold responsiveness that closely mimic the cutaneous hypersensitivity associated with clinical neuropathic pain (Decosterd & Woolf, 2000). SNI or sham surgery were performed under isoflurane anesthesia as described (Bourquin et al., 2006).

Spinal cord injury and postoperative care: All studies were approved by the University of

Minnesota Institutional Animal Care and Use Committee (IACUC). Thoracic spinal cord injury or sham surgery was performed on male ICR wild-type mice (CrI:CD1(ICR), Charles River, Wilmington, MA, USA) at 5 weeks of age. Prior to surgery, each subject was given 0.5cc of sterile saline subcutaneously in each hindquarter. Briefly, a laminectomy was performed at T9, and the contusion injury was made with either 50 or 75 kdyn of force with the IH-0400 Infinite Horizons Impactor (Precision Systems and Instrumentation, LLC; Lexington, KY, USA) with a 1.3 mm mouse tip. Sham controls had a laminectomy at T9 with no impact, and naïve subjects were housed in separate cages at the same time as their surgical counterparts. Animals received amoxicillin (14 g/L in drinking water) for 7 days after surgery to prevent urinary tract infection as part of standard postoperative care. Urine was expressed manually twice daily for the first 7 days after surgery and daily thereafter until the return of independent urination. Animals were assigned to the following groups listed in Table 3.1:

Cohort:	Surgical Procedure	# of Subjects	Impact (kdyn)	Perfused (Day post-surgery)
50 kdyn: 6 Days IHC	Sham	9	0	6 days
	SCI	7	50	6 days
50 kdyn: 50 Days IHC	Sham	10	0	50 days
	SCI	10	50	50 days
50 kdyn: Vehicle vs. C3aR1 ASO	Naïve	9	N/A	N/A
	Sham	10	0	45 days
	SCI	11	50	45 days
50 kdyn: Vehicle vs. Control ASO vs. C3aR1 ASO	Naïve	6	N/A	N/A
	SCI	7	50	45 days
75 kdyn: Vehicle vs. C3aR1 ASO	Naïve	6	N/A	N/A
	SCI	9	75	45 days

Functional assessment: Locomotor recovery following injury was assessed by two observers using the Basso Mouse Scale (BMS) (Basso et al., 2006) on days 1, 3, 5, 7, 14, 21, 28, and 35 days following injury. Briefly, measurements were made on a 9-point scale derived from ankle movements, plantar/dorsal hindpaw stepping, coordination, trunk instability, and tail position. Mice were placed into an open field and monitored for five minutes each, with scores from 0 (complete paralysis) to 9 (normal locomotion) measured for each hindpaw. BMS scores were compared between treatments via repeated-measures analysis of variance.

Behavioral Testing:

A number of behavioral tests were performed following sham or thoracic spinal cord injury beginning at 35 days post-injury and concluding at 45 days. These include:

Rotarod: Mice were tested with the rotarod apparatus (Ugo Basile, Gemonio, Italy). Mice were placed on an elevated rotating cylinder that increased in RPM continuously over 300 seconds, from 5 RPM to a peak of 50 RPM. RPM at fall was recorded for three consecutive days, beginning at Day 35 post-surgery. No more than four mice were tested simultaneously.

Von Frey mechanical allodynia testing: Mechanical withdrawal thresholds for the hindpaw were measured at baseline and on Day 42 post-surgery by an experimenter blind to condition. Mice were acclimated at least 30 minutes in the testing environment within a glass cup on a raised metal mesh platform. To evaluate mechanical threshold we utilized a logarithmically increasing set of 8 von Frey filaments (Stoelting, Wood Dale, IL), ranging in gram force from 0.007 to 6.0 g. These were applied perpendicular to the medial hindpaw

surface with sufficient force to cause a slight bending of the filament. A positive response was characterized as a rapid withdrawal of the paw away from the stimulus fiber within 4 s. Using the up-down statistical method (Bonin et al., 2014; Chaplan et al., 1994), the withdrawal threshold was calculated for each mouse and then averaged within the experimental groups.

Hargreaves thermal hyperalgesia testing: Mice were tested for hindpaw thermal hyperalgesia using the IITC Plantar Test system at intensity: AI 30 (IITC Life Sciences, Woodland Hills, CA). Briefly mice were acclimated to an ambient floor (33°C) and a beam of focused light was aimed at each hindpaw. The length of time until paw withdrawal was measured. A humane cutoff time was automatically calibrated from the intensity settings.

Burrowing behavior: Burrowing is an ethologically relevant behavior for mice (Robert M.J. Deacon, 2006), and others have utilized this as a measure of spontaneous pain following injury, which is improved with analgesic administration (Andrews et al., 2012; Deuis et al., 2017; Jirkof et al., 2010). Briefly, a PVC tube with a cap at one end is elevated on the other end and filled with normal chow, and is placed in the home cage of each individually housed mouse. The amount of material burrowed during a 2-hour period is weighed, and then the remaining material in the tube is weighed. Data shown as $(\text{Material Burrowed})/(\text{Total Material}) \times 100$ to get a burrowing percentage.

Cotton Swab Test: The cotton swab test is a dynamic tactile sensitivity assay designed to test light touch sensitivity (Garrison et al., 2011). This test utilizes a cotton swab puffed out to 3x its size, and the swab is brushed along the plantar surface five times with a 10-second break between applications, with the number of paw withdrawals recorded.

Cold Allodynia: Acetone was loaded into a 1mL syringe, and a bubble of acetone was brought above the tip of the syringe and placed onto the hindpaw without touching the syringe to the paw, a total of three times. The average amount of time each subject spent lifting, flicking, and licking the paw was recorded and averaged across each application.

Results:

We aimed to examine the effects of ASO treatment on hypersensitivity following peripheral and central models of neuropathic pain. For the peripheral model, we utilized the well-established spared nerve injury model (Decosterd & Woolf, 2000), after which the subject has reliable and long-lasting mechanical hypersensitivity arising within a week of injury. For the central model, we utilized spinal cord contusion injury at the level of the thoracic cord, which is a less established pain model that produces mechanical and thermal hypersensitivity in mice in a more variable manner (Hoschouer et al., 2010; Kerr & David, 2007; Meisner et al., 2010a).

Assessment of C3aR1 knockdown:

During the optimization process at Ionis Pharmaceuticals, they were able to produce reliable knockdown of C3aR1 expression (60% reduction on average) in the lumbar spinal cord assessed via qPCR. We confirmed that the C3aR1 ASO in our hands successfully knocks down C3aR1 mRNA in the lumbar, thoracic, and cervical spinal cord, via qPCR (Fig. 3.1 a-c, qPCR performed by BK). In both injury models utilized for

these studies, we assessed the knockdown of the receptor via immunohistochemistry. Our previous work found expression of C3aR1 primarily localized to microglial profiles in the parenchyma, in SNI lumbar spinal cord (Doolen et al., 2017). Additionally, C3aR1 labeling was intense in the subarachnoid macrophages apposed to the cord, located around the entire circumference. Following administration of C3aR1 ASO, we observed knockdown of C3aR1 expression in microglia in the lumbar spinal cord (Fig. 3.1 a-b). In contrast, there is clearly detectable labeling in the subarachnoid macrophages surround the cord, suggesting that there is ineffective knockdown of C3aR1 in these cells. (Fig. 3.1 d-e).

Figure 3.1

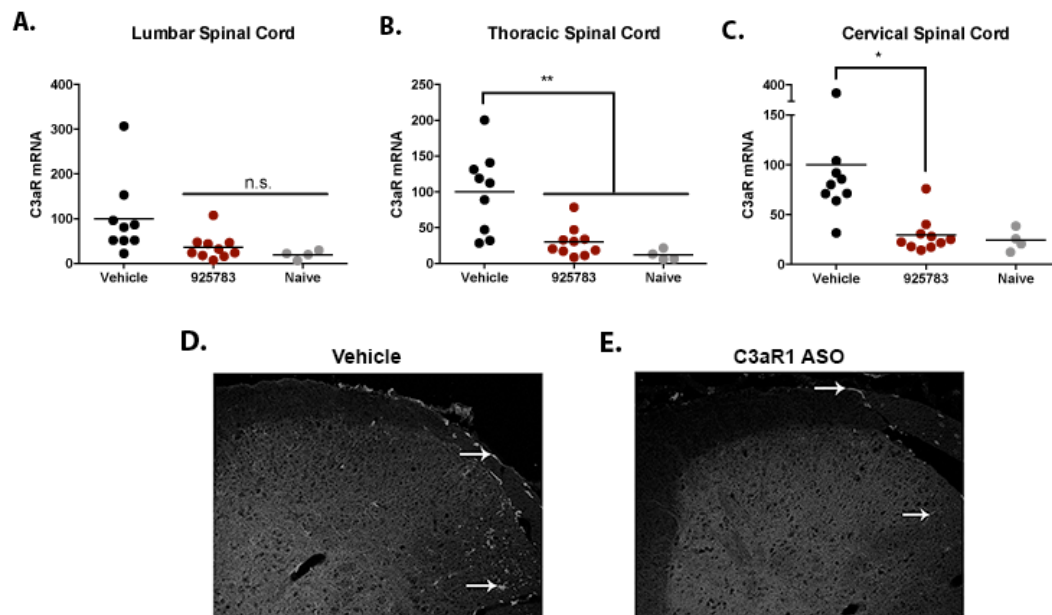


Figure 3.1: Treatment with C3aR1 ASO significantly knocks down expression of C3aR1 in the spinal cord. (A-C) Mice received thoracic contusion spinal cord injury, and C3aR1 ASO or vehicle were injected i.t. on day 70 post-SCI. On day 84 post-SCI, spinal cords were removed and separated into lumbar, thoracic, and cervical sections. Naïve age-matched controls had tissue collected at the same time. C3aR1 mRNA was measured via

qPCR by BK at Ionis Pharmaceuticals. **A.** In the lumbar spinal cord, C3aR1 ASO treated mice had reduced C3aR1 expression, which was not significantly different than naïve control mice. There was significant knockdown of C3aR1 mRNA in the: **B.** thoracic and **C.** cervical spinal cord compared to vehicle controls ($p < 0.001$ and $p < 0.05$ respectively). **(D-E)** Lumbar spinal cord sections of mice that underwent spinal cord injury received i.t. injections of C3aR1 ASO or vehicle 3 days after injury. Red = C3aR1 staining **D.** C3aR1-ir is localized to microglial profiles in the lumbar dorsal horn of SNI mice. **E.** C3aR1 ASO given at 14 days following injury knocks down C3aR1-ir in microglial profiles in the lumbar dorsal horn of SNI mice. **Arrows:** Subarachnoid macrophages in mice that received C3aR1 ASO still express C3aR1-ir at similar levels to vehicle treated mice. Quantification of knockdown not performed.

Peripheral Nerve Injury

Treatment with C3aR1 ASO has no effect on the development or maintenance of hypersensitivity following peripheral nerve injury

Our aim was to examine the effect of knocking down C3aR1 on development and maintenance of SNI-induced hypersensitivity. For the development paradigm, mice received C3aR1 ASO or vehicle 7 days before SNI. They were tested post-injury for differences in development of mechanical allodynia. For the maintenance paradigm, mice were given C3aR1 ASO or vehicle 14 days after SNI. Von Frey thresholds were tested weekly following treatment. In either paradigm, mice that received injection of C3aR1 ASO showed no differences in hypersensitivity compared to vehicle controls (Fig 3.2 a-b; development: $p = 0.982$; maintenance: $p = 0.749$; linear regression analysis for

slope and intercept). This indicates that knockdown of C3aR1 expression in microglia was not sufficient enough to alter the development or maintenance of hypersensitivity following SNI.

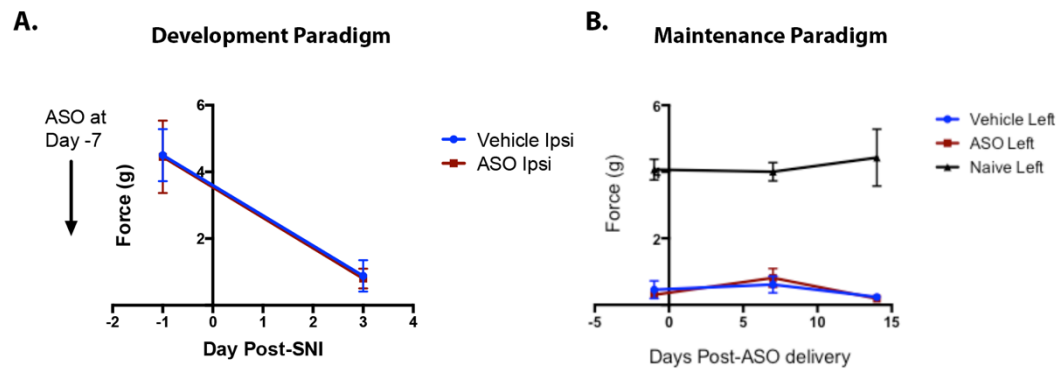


Fig. 3.2: Treatment with C3aR1 ASO has no effect on the development or maintenance of hypersensitivity following peripheral nerve injury. **A.** Development paradigm: Mice received an i.t. Injection of vehicle or C3aR1 ASO 7 days before spared nerve injury, in order to ensure sufficient knockdown prior to surgical manipulation. Mice were given an SNI, and tested for mechanical allodynia with Von Frey filaments three days after injury. There were no significant differences in withdrawal thresholds between vehicle or C3aR1 ASO treated mice ($p=0.982$, linear regression analysis for slope and intercept). **B.** Maintenance paradigm: Mice received SNI and were tested with Von Frey filaments weekly to ensure development of mechanical allodynia. On 14 days post-surgery, mice received i.t. Injections of either vehicle or C3aR1 ASO. Subjects were tested weekly, with no significant differences in withdrawal threshold detected at 7 or 14 days following treatment. ($p=0.749$, linear regression analysis for slope and intercept).

Spinal Cord Injury

Spinal cord injury is a central nervous system injury capable of producing hypersensitivity in mouse and rat models. First, we aimed to examine whether C3aR1 expression is increased following SCI in a similar manner as SNI. We then sought to determine whether treatment with C3aR1 ASO altered the development of injury-related behaviors following SCI. For these experiments, we utilized both a mild and a moderate contusion injury. This was to assess whether severity of injury influenced the effectiveness of C3aR1 knockdown on behavior.

Spinal cord injury increases the spinal expression of C3aR1 in a time-dependent manner:

Our work utilizing spared nerve injury found time-dependent upregulation of C3aR1 specifically in microglia following peripheral nerve injury (Doolen et al., 2017). Following our work characterizing microglial C3aR1 expression at various timepoints after peripheral nerve injury, we aimed to examine whether changes in C3aR1 expression occur following spinal cord injury.

The contusion injury at the level of T9 elicited a mild injury that mice recover from in a stereotypical fashion, and we assessed C3aR1 expression below the level of injury at both the acute and chronic stage. In addition to assessing C3aR1 expression, we also aimed to characterize changes in microglial marker expression by assessing Iba1 immunoreactivity on the same sections. We compared the SCI subjects to the sham controls in order to control for changes in C3aR1 or Iba1 expression due primarily to the

laminectomy. We found time-dependent changes in C3aR1 and Iba1 expression at both the acute and the chronic timepoints after SCI in comparison to sham controls. At six days post-surgery, we saw a significant increase in both C3aR1-ir and Iba1-ir in the lumbar dorsal horn of SCI subjects in comparison to sham controls (Fig. 3.3a1-d1; $p=0.0098$, $p=0.0046$ respectively, unpaired t-test). At fifty days post-surgery, when the subjects are recovered from the acute effects of the injury and have resumed normal locomotion, Iba1 was still significantly increased in SCI mice (Fig. 3.3a2-d2; $p=0.032$, unpaired t-test), whereas C3aR1 was not significantly different in SCI subjects compared to sham controls ($p=0.280$, unpaired t-test).

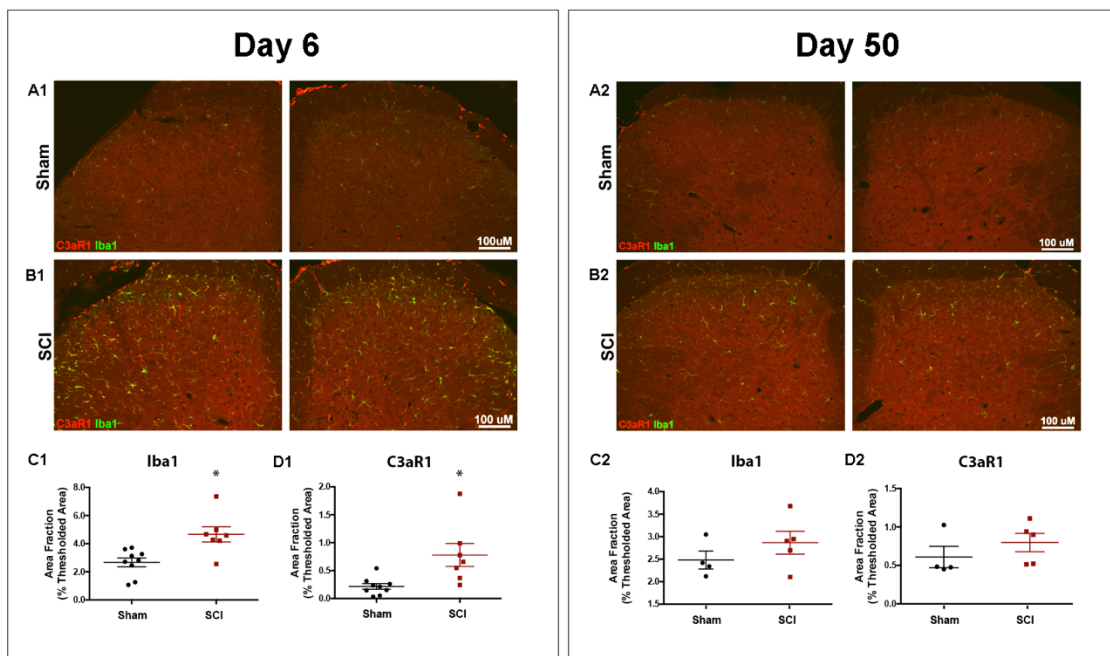


Figure 3.3: Spinal expression of C3aR1 and Iba1 is increased 6 days after spinal cord injury. (a1-b1) Representative images illustrate the increase in C3aR1-ir and Iba1-ir at day 6 post-SCI (A1, sham; B1, SCI). Scale bar: 100 μ m. (c2-d2) Quantitative analysis of C3aR1 and Iba1 immunolabeling indicates a significant increase in C3aR1 expression and Iba1 expression occurs 6 days post-SCI ($p=0.0098$, $p=0.0046$ respectively,

unpaired *t*-test). (a2-b2) Representative images illustrate the increase in Iba1-ir at day 50 post-SCI, whereas C3aR1-ir is equally low in sham and SCI. (A, sham; B, SCI) Scale bar: 100 μ m. (c2-d2) Quantitative analysis of C3aR1 and Iba1 immunolabeling indicates a significant increase in Iba1 expression, that is not present in C3aR1, at 50 days post-SCI ($p=0.032$ and $p=0.280$ respectively, unpaired *t*-test).

We next aimed to identify changes occurring rostral to the injury, specifically in the gracile fasciculus portion of the dorsal columns. We stained for C3aR1 and Iba1 on cervical sections, and imaged the dorsomedial portion of the spinal cord. We visualized C3aR1-ir and Iba1-ir in the dorsal columns of mice that received spinal cord injury (Fig. 3.4a-c: **a**: C3aR1-ir (red) and Iba1-ir (green); **b**: Iba1-ir (white); **c**: C3aR1-ir (white); Scale bar 100 μ m). This indicates that following SCI, long-lasting immune activation occurs in the dorsal columns. Quantification of Iba1 and C3aR1 are in process.

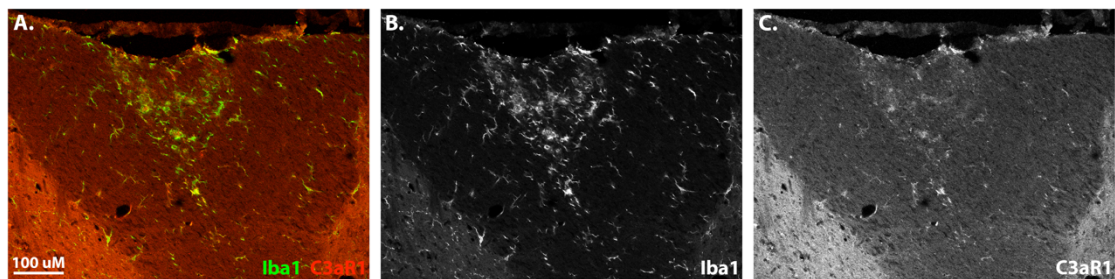


Figure 3.4: Iba1 and C3aR1 are present in the dorsal columns of SCI mice. Immunohistochemistry examining C3aR1 and Iba1 in the dorsomedial cervical spinal cord. a: Representative images of co-labeling of C3aR1-ir (red) and Iba1-ir (green) in the gracile fasciculus of SCI subjects at 45 days following injury. b: Iba1-ir and c: C3aR1-ir

in dorsomedial cervical spinal cord of SCI mice. Scale bar: 100 μ m.

***Treatment with C3aR1 ASO 3 days following a mild 50 kdyn thoracic contusion
SCI has variable effect on behavior in male ICR mice:***

Following intrathecal injection of C3aR1 ASO or vehicle at 3 days following a mild 50 kdyn thoracic contusion SCI, a number of behaviors were monitored. We chose day three following injury in order to knock down receptor expression during the acute phase of injury, which is when we found peak C3aR1 expression. Administering the treatment during the acute phase of injury allowed us to examine the effects of knockdown on development of pain-related behavior. BMS scoring was done on days 1, 3, 5, 7, and then weekly after injury in order to assess locomotor function. Following mild or moderate injury, mice recover locomotor function in a stereotypical fashion, from low day one scores to a plateau occurring between 28 and 35 days post-SCI. On day one after injury, there are a percentage of each cohort that have scores of 4 or higher, indicating a less severe injury. Results are presented in several ways, in one graph combining all subjects for each group, and in another splitting subjects based on their BMS scores on day one post-injury. This was to examine whether there were trends in ASO effects on behavior that were dependent on injury severity. Additionally, we ran Pearson's correlations comparing behavior to BMS scores on day one, to examine the relationships between these variables. There were no significant differences between the locomotor recovery

of subjects that received C3aR1 ASO compared to the vehicle controls, in either the combined or separated analyses. (Fig. 3.5a1-2; combined: $p=0.972$, low day one: $p=0.275$, high day one: $p=0.709$; mixed effects model with Sidak's multiple comparisons test). This indicates the ASO does not impact locomotor recovery following a mild 50 kdyn thoracic contusion injury.

We utilized a number of evoked and spontaneous behavioral tests in order to assess the effects of C3aR1 knockdown on pain-related behaviors.

We assessed the impact of ASO-mediated knockdown of C3aR1 expression on mechanical sensitivity. When high and low day one BMS groups were combined, the sham that received vehicle had significantly lower withdrawal thresholds than both SCI vehicle and SCI ASO groups (Fig. 3.5b1; $p=0.0191$, one-way ANOVA with Tukey's *post hoc*). Interestingly, sham that received ASO were not significantly different than either SCI group. When low and high day one BMS groups were separated, the sham vehicle were significantly lower than both the vehicle and ASO SCI groups that had low day one BMS scores (Fig. 3.5b2; $p=0.0096$, one-way ANOVA with Tukey's *post hoc*). When we ran correlations comparing day one BMS scores to withdrawal threshold, both the vehicle and ASO SCI groups exhibited a negative correlation between BMS day one score and withdrawal thresholds. These were not significantly different from one another (Fig. 3.5b3; vehicle: $r=0.411$; C3aR1 ASO: $r=0.656$).

Burrowing is an ethologically relevant behavior in mice, most frequently utilized as a model of overall well-being (R. M.J. Deacon, 2009; Robert M.J. Deacon, 2006; Jirkof,

2014). Some have used this as a measure of spontaneous pain following injury, which is improved with analgesic administration (Andrews et al., 2012; Deuis et al., 2017; Jirkof et al., 2010). When we tested the effects of ASO on burrowing behavior, there were no significant differences between any group, regardless of surgical group or treatment (Fig. 3.5c1; $p = 0.4356$, one way anova with Tukey's *post hoc*). This remained true when SCI subjects were split into groups based on day one BMS scores (Fig. 3.5c2; $p=0.074$, one-way ANOVA with Tukey's *post hoc*). We ran correlations comparing the relationship between burrowing and injury severity on day one post-SCI, and both vehicle and ASO groups had positive correlations that were not different from one another (Fig. 3.5c3; vehicle: $r=0.800$; C3aR1 ASO: $r=0.746$).

We assessed heat hyperalgesia with the Hargreaves apparatus, which utilizes a radiant heat source aimed toward the hindpaw. Subjects with heat hyperalgesia will exhibit reduced latency to withdraw from the light (Deuis et al., 2017; Hargreaves et al., 1988). When we tested the effects of the C3aR1 ASO on withdrawal latency, there were no significant differences between any group, regardless of surgical group or treatment (Fig. 3.5d1; $p=0.702$, one-way ANOVA with Tukey's *post hoc*). This remained true when SCI subjects were split into groups based on day one BMS scores (Fig. 3.5d2; $p=0.316$, one-way ANOVA with Tukey's *post hoc*). We ran correlations comparing the relationship between withdrawal latency and injury severity on day one post-SCI, and both vehicle and ASO groups had positive correlations that were not different from one another (Fig. 3.5d3; vehicle: $r=0.711$; C3aR1 ASO: $r=0.468$).

The cotton swab test is used to examine light touch sensitivity, specifically testing the presence of information being sent from low-threshold rapidly adapting

mechanoreceptors. When low and high day one BMS groups are combined, both the vehicle and C3aR1 ASO spinal cord injury groups have significantly reduced responses to the cotton swab stimulus compared to the naïve or either sham group. (Fig. 3.5f; $p=0.0013$, one way anova; tukeys *post hoc* test). When subjects are separated based on their day one BMS score, a noteworthy trend emerges. The vehicle SCI group is still reduced compared to the sham or naïve mice, regardless of injury severity. For SCI mice that received ASO, the more injured group on day one is also reduced compared to naïve or sham groups. Interestingly, the SCI mice with high day one BMS scores that received C3aR1 ASO respond to the cotton swab stimulus. They have significantly higher response percentages than the SCI vehicle or low day one ASO group, and are not significantly different than the naïve or sham groups (Fig. 3.5e2; $p<0.0001$; one-way ANOVA with Tukey's *post hoc*). This indicates that the C3aR1 ASO is capable of attenuating the loss of light touch sensitivity in mice that are less injured on day one post-SCI. We ran correlations comparing day one BMS score and percent response to the cotton swab stimulus. In line with the changes seen in the raw data, the relationship between injury severity and cotton swab response are significantly different between vehicle and C3aR1 ASO treatments. There is a slightly negative but nearly absent correlation between injury severity and response to the cotton swab for the SCI mice that received vehicle, indicating that there is no relationship between injury severity and whether the mice will respond to the stimulus (Fig. 3.5e3; $r = -0.099$). In contrast, there is a highly positive correlation between injury severity and percent response in the SCI mice that receive C3aR1 ASO, indicating that less injured mice on day one are more likely to have higher responses to the cotton swab (Fig. 3.5e3; $r = 0.931$).

50 kdyn: Vehicle vs. C3aR1 ASO

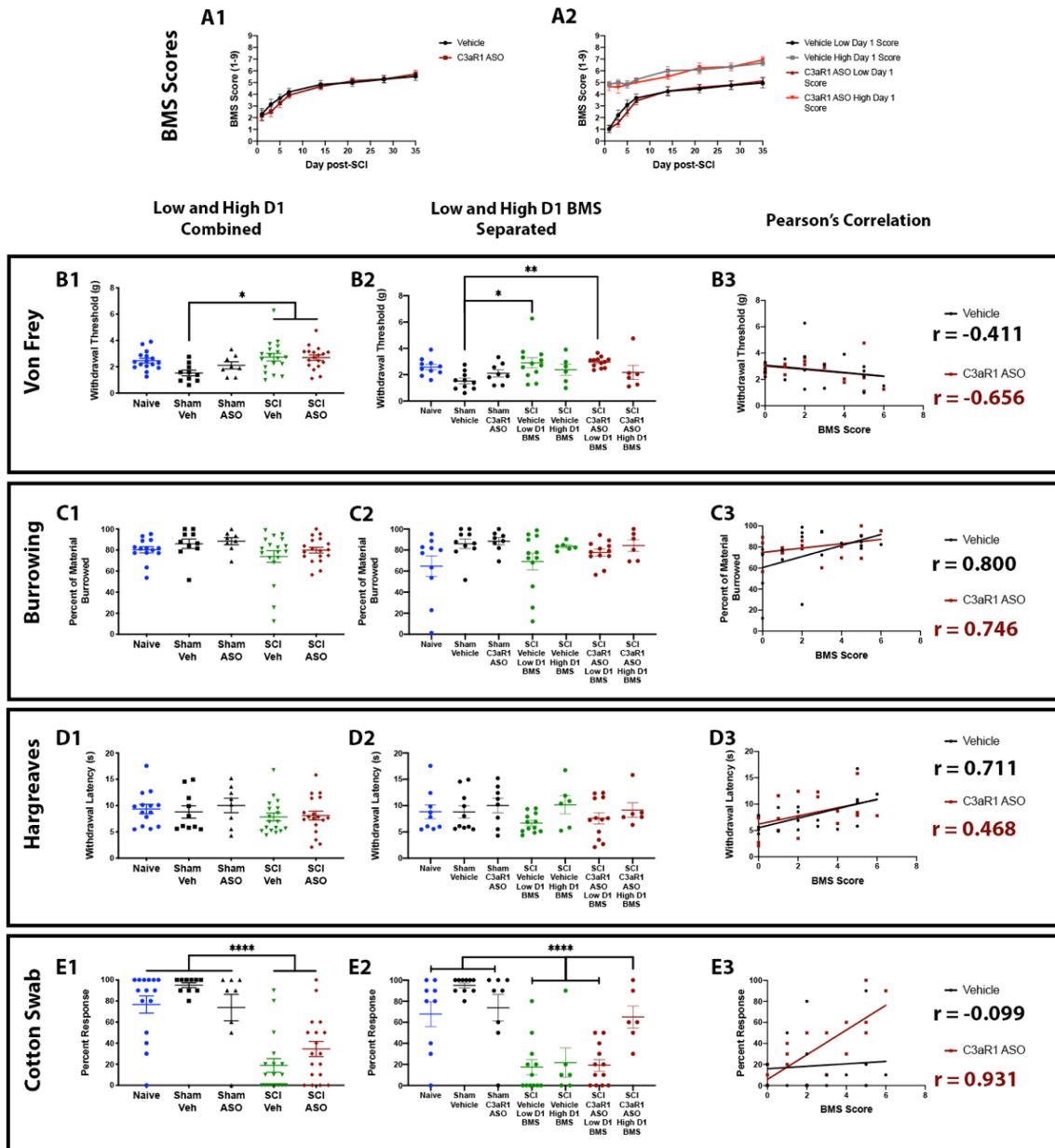


Figure 3.5: Treatment with C3aR1 ASO 3 days following a mild 50 kdyn contusion SCI has variable effect on pain-related behaviors. **A1-2.** BMS locomotor scoring was done on days 1, 3, 5, 7, and then weekly through 28 days. Mice that received C3aR1 ASO recovered locomotor function in a similar manner as vehicle control subjects, regardless of whether high and low day one BMS scores were combined or separated ($p=0.555$ and

$p=0.641$, mixed effects model with Tukeys post hoc). **B1.** When high and low day one BMS groups were combined, the sham that received vehicle had significantly lower withdrawal thresholds than both SCI vehicle and SCI ASO groups ($p=0.0191$, one-way ANOVA with Tukey's post hoc). **B2.** When low and high day one BMS groups were separated, the sham vehicle were significantly lower than both the vehicle and ASO SCI groups that had low day one BMS scores ($p=0.0096$, one-way ANOVA with Tukey's post hoc). **C1-2.** When we tested the effects of ASO on burrowing behavior, there were no significant differences between any group, regardless of surgical group or treatment (Fig. 3.5c1; $p = 0.4356$, one way anova with Tukey's post hoc). This remained true when SCI subjectst were split into groups based on day one BMS scores ($p=0.074$, one-way ANOVA with Tukey's post hoc). **D1-2.** When we tested the effects of the C3aR1 ASO on withdrawal latency, there were no significant differences between any group, regardless of surgical group or treatment ($p=0.702$, one-way ANOVA with Tukey's post hoc). This remained true when SCI subjects were split into groups based on day one BMS scores ($p=0.316$, one-way ANOVA with Tukey's post hoc). **D3.** We ran correlations comparing the relationship between withdrawal latency and injury severity on day one post-SCI, and both vehicle and ASO groups had positive correlations that were not different from one another (vehicle: $r=0.711$; C3aR1 ASO: $r=0.468$). **E1.** When low and high day one BMS groups are combined, both the vehicle and C3aR1 ASO spinal cord injury groups have significantly reduced responses to the cotton swab stimulus compared to the naïve or either sham group. ($p=0.0013$, one way anova; tukeys post hoc test). **E2.** When subjects are separated based on their day one BMS score, the vehicle SCI group is still reduced compared to the sham or naïve mice, regardless of injury severity. For SCI mice that received ASO, the more injured group on day one is also reduced compared to naïve or sham groups. The SCI mice with high day one BMS scores that received C3aR1

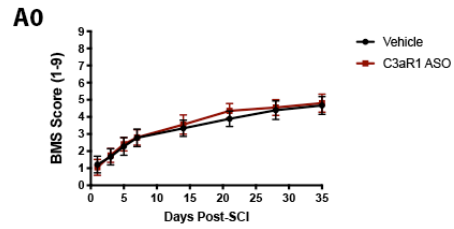
ASO have significantly higher response percentages than the SCI vehicle or low day one ASO group, and are not significantly different than the naïve or sham groups ($p < 0.0001$; one-way ANOVA with Tukey's post hoc).

Treatment with C3aR1 ASO 3 days following moderate 75 kdyn thoracic contusion SCI has a variable effect on behavior in male ICR mice:

We aimed to compare effects of C3aR1 ASO treatment on improvement of pain-related behaviors between mild and moderate spinal cord injury. To do this we tested a number of evoked and spontaneous behaviors in mice that received a moderate 75 kdyn thoracic contusion SCI. BMS scoring was assessed on day 1, 3, 5, 7, and then weekly through 35 days following moderate contusion SCI. There were no significant differences between the locomotor recovery of subjects that received C3aR1 ASO compared to the vehicle controls. (Fig. 3.6a0; $p = 0.841$, two-way ANOVA with Tukey's *post hoc*). There were not enough mice with high day one scores to meaningfully test the differences between groups that had low or high day one BMS scores. Therefore, we combined all subjects and compared the effect of C3aR1 ASO treatment on the behaviors we tested. There were no significant differences in direct comparison of values for Von Frey mechanical thresholds (Fig. 3.6a1; $p = 0.849$, one-way ANOVA, Tukey's *post hoc*), burrowing percentage (Fig. 3.6b1; $p = 0.182$, one-way ANOVA, Tukey's *post hoc*), or thermal withdrawal latencies (Fig. 3.6c1; $p = 0.5309$, One way ANOVA, Tukey's *post hoc*) between any of the groups. In the cotton swab test, we saw a significant decrease of

SCI responses in comparison to naïve controls, regardless of treatment group (Fig. 3.6d1; $p = 0.0015$, one way ANOVA, Tukey's *post hoc*), but there was no effect of C3aR1 ASO on percent responses compared to SCI mice that received vehicle. When we ran correlations comparing BMS scores on day one with each behavior that we tested, there were differences that emerged between vehicle and C3aR1 ASO groups for the Hargreaves assay and the cotton swab test. In the Hargreaves assay, the vehicle group had a highly positive correlation between BMS scores on day one and withdrawal latency, with less severely injured mice having higher withdrawal latencies than more injured subjects (Fig. 3.5c2; vehicle: $r = 0.992$). For the C3aR1 ASO group, there was a negative correlation between BMS score and withdrawal latency, indicating that less injured mice were more likely to have lower withdrawal latencies than their more injured counterparts (Fig. 3.5c2; C3aR1 ASO: $r = -0.711$). In the cotton swab test, the vehicle group had a slightly negative but overall insignificant correlation between BMS scores on day one and percent response, indicating that there was no impact of injury severity on response (Fig. 3.5d2; vehicle: $r = -0.284$). For the C3aR1 ASO group, there was a highly positive correlation between BMS score and percent response, indicating that less injured mice were more likely to respond to the cotton swab stimulus than their more injured counterparts (Fig. 2.5d2; C3aR1 ASO: $r = 0.957$). These results are in line with our findings in the mild 50 kdyn injuries, where the C3aR1 ASO attenuated the loss of light touch sensitivity compared to the low BMS group and the vehicle controls.

75 kdyn: Vehicle vs. C3aR1 ASO



Low and High D1
Combined

Pearson's Correlation

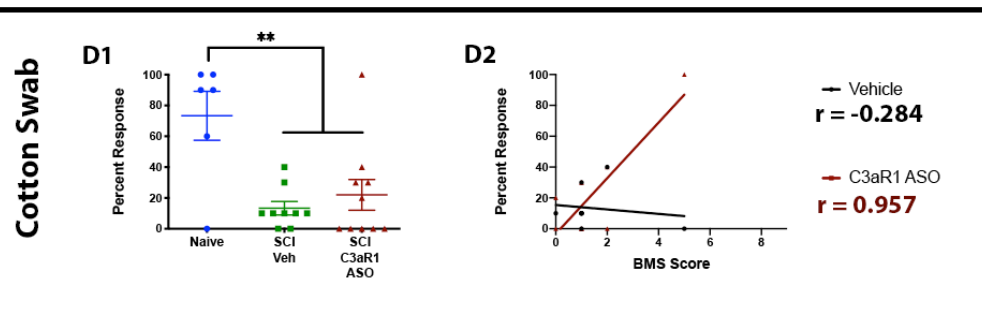
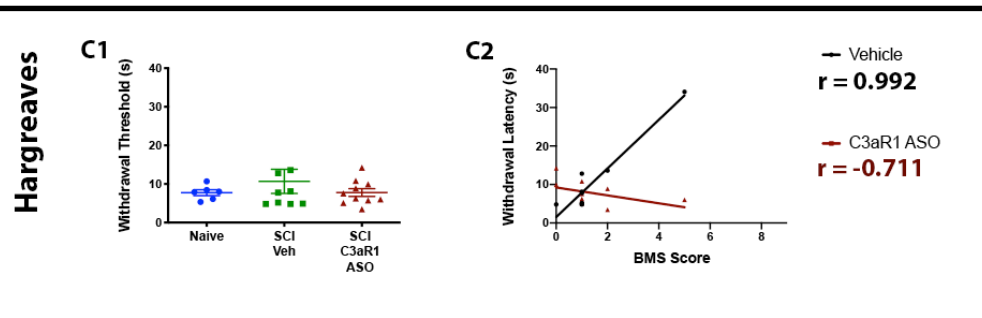
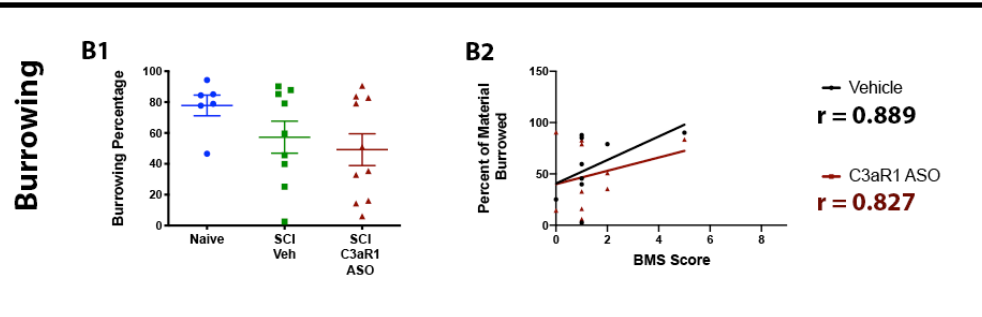
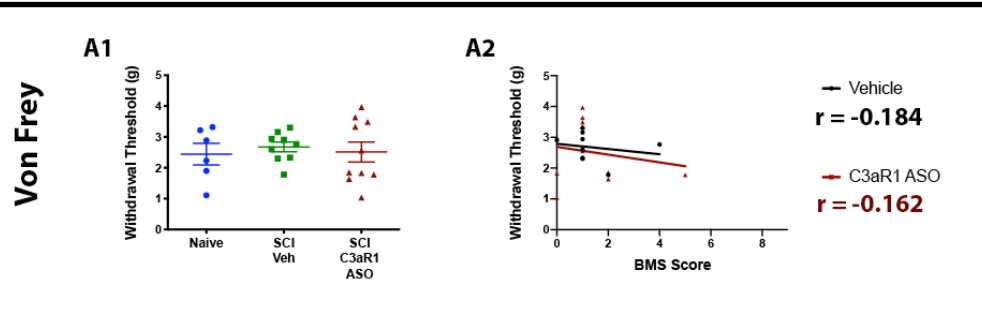


Figure 3.6: Treatment with C3aR1 ASO 3 days following moderate 75 kdyn thoracic contusion SCI has a variable effect on behavior in male ICR mice: **A0.** There were no significant differences between the locomotor recovery of subjects that received C3aR1 ASO compared to the vehicle controls. (Fig. 3.6a0; $p=0.841$, two-way ANOVA with Tukey's post hoc). **A1-C1.** There were no significant differences in direct comparison of values for Von Frey mechanical thresholds (Fig. 3.6a1; $p=0.849$, one-way ANOVA, Tukey's post hoc), burrowing percentage (Fig. 3.6b1; $p=0.182$, one-way ANOVA, Tukey's post hoc), or thermal withdrawal latencies (Fig. 3.6c1; $p=0.5309$, One way ANOVA, Tukey's post hoc) between any of the groups. **D1.** In the cotton swab test, we saw a significant decrease of SCI responses in comparison to naïve controls, regardless of treatment group (Fig. 3.6d1; $p = 0.0015$, one way ANOVA, Tukey's post hoc), but there was no effect of C3aR1 ASO on percent responses compared to SCI mice that received vehicle. **A2-D2.** Correlations were comparing BMS scores on day one with each behavior that we tested, to assess differences between vehicle and C3aR1 ASO groups. *R-values are reported in the figure.*

Control ASO induces upregulation of C3aR1 expression and thermal hypersensitivity in injured subjects:

It was important for us to test whether the ASO itself had non-specific effects that were measurable following spinal cord injury. In order to do so, we utilized a control ASO that had a sequence of nucleotides with no known target in mice or rats. We injected vehicle, control ASO, or C3aR1 ASO in SCI mice at day 3 post-injury. We then assessed a number of evoked and spontaneous behaviors. At 45 days post-injury, we collected

tissue and quantified changes in C3aR1 and Iba1 expression in the lumbar dorsal horn. When subjects were combined regardless of day one BMS score, there were no significant differences in BMS scores, von frey withdrawal thresholds, burrowing percentages, or responses to cotton swab when comparing vehicle, control ASO, or C3aR1 ASO groups (Fig. 3.7a1-c1,e1; BMS: $p=0.555$, two-way ANOVA with Sidak's multiple comparisons test; Von Frey: $p=0.467$, one-way ANOVA with Tukey's *post hoc*; Burrowing: $p=0.248$, one-way ANOVA with Tukey's *post hoc*; cotton swab: $p=0.905$, one-way ANOVA with Tukey's *post hoc*). This remained true when day one BMS groups were separated, even though each treatment had higher percent responses to the cotton swab stimulus in their high day one BMS group (Fig. 3.7a2-c2,e2; von frey: $p=0.156$, one-way ANOVA; burrowing: $p=0.162$, one-way ANOVA; cotton swab: $p<0.0001$, one-way ANOVA with Tukey's *post hoc*). When low and high day one BMS groups are combined, the control ASO group had significantly reduced withdrawal latency in the Hargreaves thermal hyperalgesia assay when compared to both the vehicle and C3aR1 ASO groups, and the naïve controls (Fig 3.7c; $p=0.0061$, one-way ANOVA with tukey's *post hoc*). When subjects with low or high day one BMS scores are separated, the low day one group that received control ASO had significantly reduced thresholds compared to naïve, high day one vehicle, and low day one C3aR1 ASO groups (Fig. 3.7e2; $p = 0.0056$, one-way ANOVA with Tukey's *post hoc*). These results indicate that control ASO is capable of eliciting thermal hyperalgesia, which is more likely to occur in the mice that are more injured on day one post-SCI. Comparisons in the correlation of day one BMS score to the various behaviors did not reveal any significant differences between vehicle and control ASO (Fig. 3.7b3-e3; r values reported in figure). For the burrowing task, the vehicle and control ASO groups had positive correlations between injury severity on day one and burrowing. The C3aR1 ASO group had no correlation between burrowing

percentage and injury severity. (Fig. 3.7c; vehicle: $r = 0.995$; control ASO: $r = 0.861$; C3aR1 ASO: $r = -0.170$).

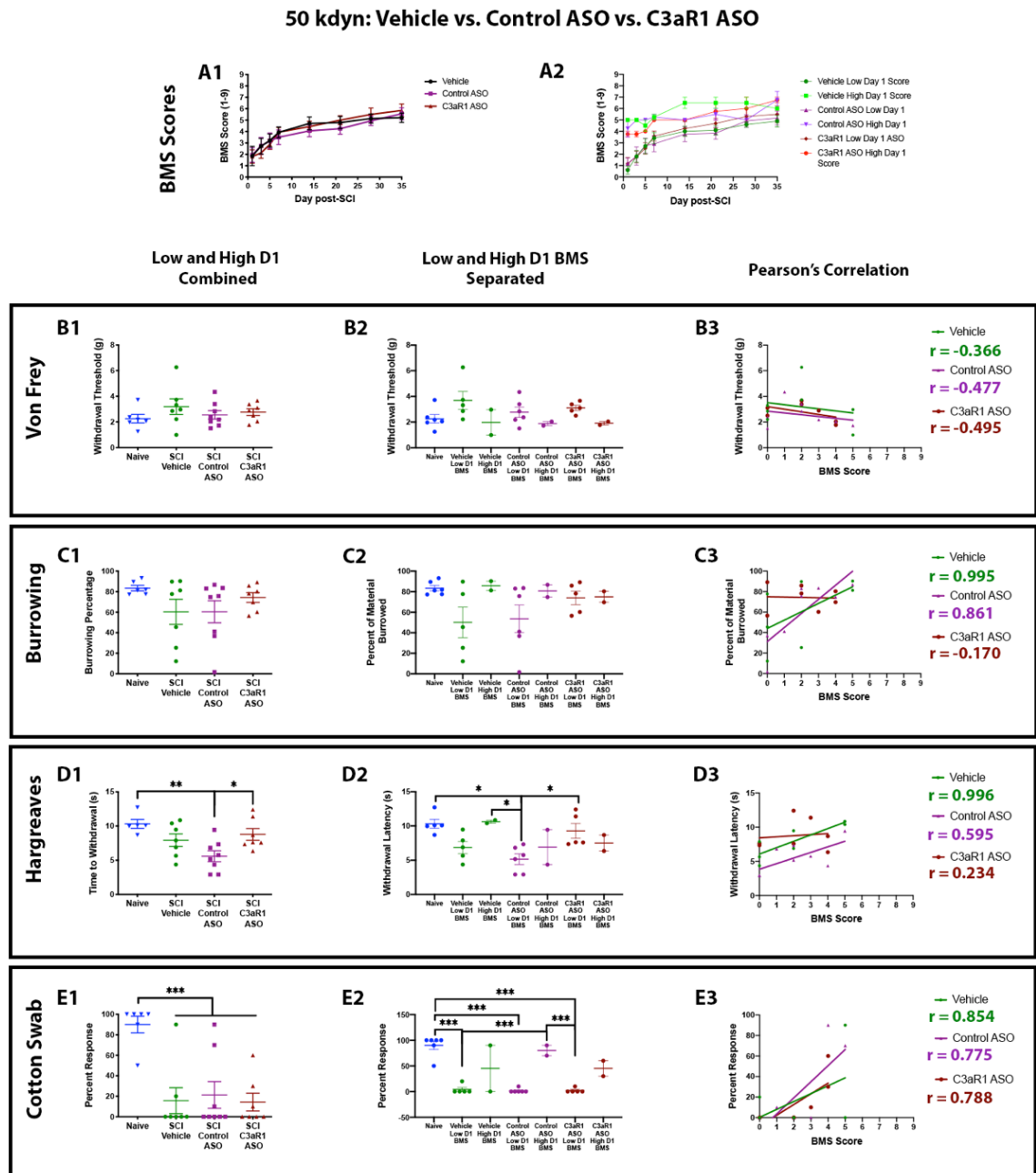


Figure 3.7: Control ASO induces thermal hypersensitivity in injured subjects. **A1.** BMS locomotor scoring was done on days 1, 3, 5, 7, and then weekly through 35 days. Mice

that received control ASO recovered locomotor function the same as vehicle control and C3aR1 ASO subjects ($p=0.555$, two-way ANOVA). **B1.** Burrowing was assessed on day 35-36 post-SCI, and there were no significant differences between control ASO, C3aR1 ASO, and vehicle subjects ($p=0.248$, one-way ANOVA). **C1.** The control ASO group had significantly reduced withdrawal latency in the Hargreaves thermal hyperalgesia assay when compared to both the vehicle and C3aR1 ASO groups, and the naïve controls ($p=0.0061$, one-way ANOVA with tukey's post hoc) **D1.** There were no significant differences in von frey thresholds between groups ($p=0.467$, one-way ANOVA, tukey's post hoc). **E1.** All injured mice exhibited reduced responsiveness in the cotton swab assay. There were no differences between vehicle, control ASO, or C3aR1 ASO subjects ($p=0.905$, one-way ANOVA, tukey's post hoc) **A2-C2,E2:** These trends remained true when day one BMS groups were separated, even though each treatment had higher percent responses to the cotton swab stimulus in their high day one BMS group (Fig. 3.7a2-c2,e2; von frey: $p=0.156$, one-way ANOVA; burrowing: $p=0.162$, one-way ANOVA; cotton swab: $p<0.0001$, one-way ANOVA with Tukey's post hoc). **D2.** When subjects with low or high day one BMS scores are separated, the low day one group that received control ASO had significantly reduced thresholds compared to naïve, high day one vehicle, and low day one C3aR1 ASO groups (Fig. 3.7e2; $p = 0.0056$, one-way ANOVA with Tukey's post hoc). **B3-E3.** Comparisons in the correlation of day one BMS score to the various behaviors did not reveal any significant differences between vehicle and control ASO (Fig. 3.7b3-e3; r values reported in figure).

We collected tissue at 45 days post-SCI and did immunohistochemistry on lumbar spinal cord sections. We specifically quantified C3aR1 and Iba1 expression and compared each treatment group. We saw a significant increase in C3aR1-ir in control ASO subjects in comparison to naïve, SCI vehicle, and SCI C3aR1 ASO mice (Fig. 3.8a; $p < 0.0001$, one way ANOVA with tukey's *post hoc*). There were no changes in Iba1-ir in control ASO compared to any of the other groups (Fig. 3.8b; $p = 0.117$, one-way ANOVA with tukey's *post hoc*).

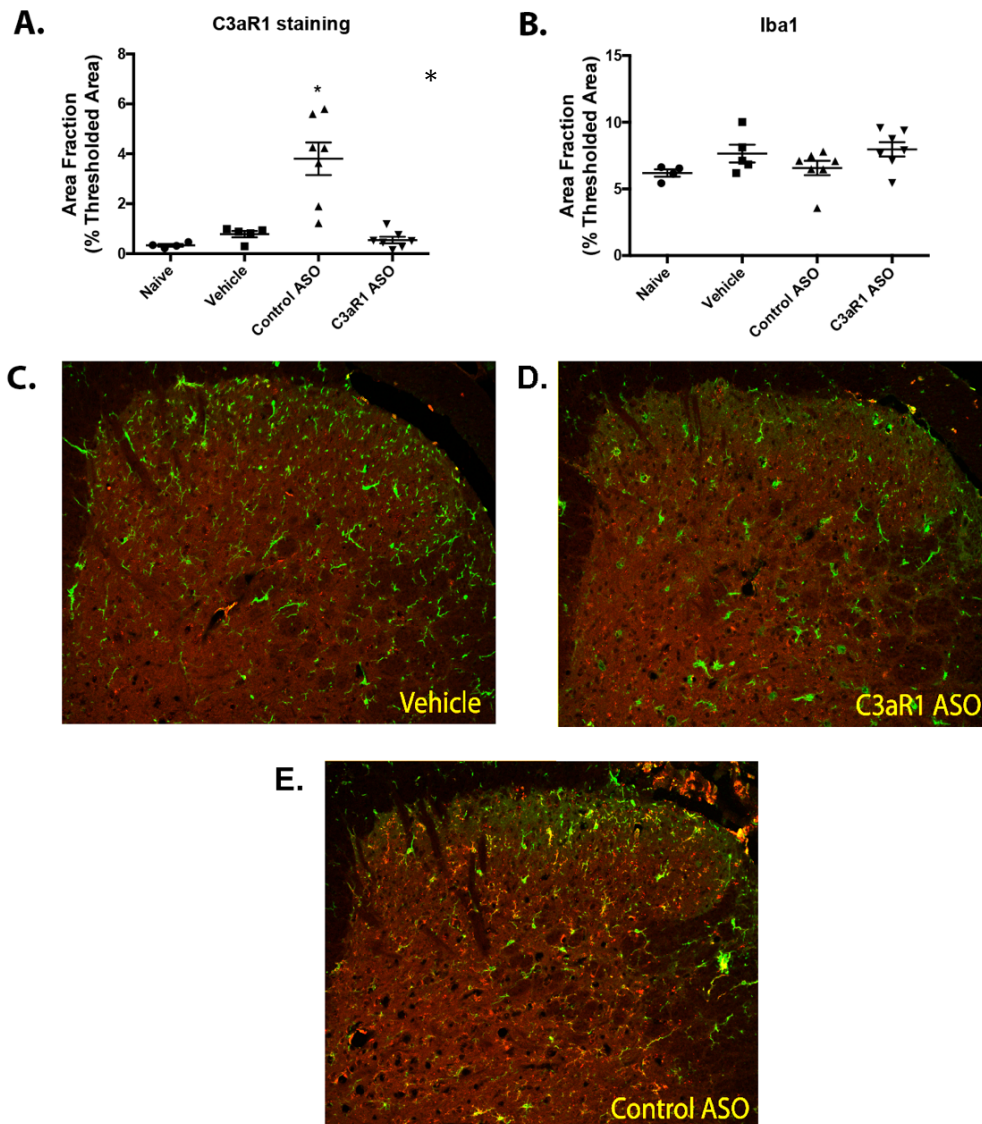


Figure 3.8: Control ASO-induced changes in expression of C3aR1 in injured subjects.

A. Quantification of C3aR1-ir and Iba1-ir in the lumbar dorsal horn. Control ASO induces significant upregulation in spinal cord injury subjects compared to naïve subjects, and SCI subjects that received vehicle or C3aR1 ASO ($p < 0.0001$, one way ANOVA with tukey's post hoc). **B.** There were no significant differences in Iba1-ir between any treatment group (; $p = 0.117$, one-way ANOVA with tukey's post hoc). **(C-E)** Immunohistochemistry staining in the lumbar dorsal horn of SCI mice that were treated

with vehicle, control ASO, or C3aR1 ASO. Red =C3aR1, Green =Iba1, 20x.

Discussion

In these studies, we sought to determine the effect of ASO-mediated knockdown of C3aR1 expression in a peripheral and central model of neuropathic pain. We utilized a number of evoked and spontaneous pain-related behaviors, in addition to immunohistochemistry, in order to examine these effects.

Effective knockdown of C3aR1 expression with antisense oligonucleotides

Prior to our experiments, the C3aR1 ASO was optimized at Ionis Pharmaceuticals, including *in vivo* examination of gene knockdown in the spinal cord following intrathecal injection (data not shown). In order to assess effectiveness of the C3aR1 ASO in our hands, we collected tissue at two weeks following administration. Naïve mice have low endogenous expression of C3aR1, so we tested the efficiency of the ASO in mice that had spinal cord injuries. We confirmed through qPCR (performed by BK) that C3aR1 was knocked down in the lumbar, thoracic, and cervical sections of the spinal cord. We performed immunohistochemistry to assess C3aR1 and Iba1 expression following SNl and SCI. We found that C3aR1-ir is knocked down in parenchymal microglia in both models. This knockdown of C3aR1 does not seem to affect the presence of Iba1-ir, suggesting that there are not any nonspecific effects on microglia. In contrast, there was clearly detectable C3aR1 labeling in the subarachnoid macrophages that surround the

spinal cord, suggesting that there is ineffective knockdown of C3aR1 in these cells. This is most likely due in part to the exceptionally high expression level of C3aR1 in subarachnoid macrophages in comparison to microglia. In addition, these cells are abundant around the entire circumference of the spinal cord. Both of these factors make effective knockdown harder to achieve. These cells are an important consideration when assessing the efficacy of the knockdown capability of this particular ASO, which has a 60% knockdown efficiency, measured by Ionis during the optimization process. Based on the near complete knockdown of C3aR1 in the parenchyma seen via immunohistochemistry, it is possible that the remaining 40% of C3aR1 expression detected in the spinal cord is from subarachnoid macrophages that remain attached to the spinal cord tissue assessed via qPCR. It is currently unknown what the functional relevance of these cells are in pain-related behavior. Therefore we do not know the contribution of these cells to the behavioral phenotypes we examined following C3aR1 ASO in these models.

C3aR1 ASO is ineffective at disrupting the development or maintenance of mechanical hypersensitivity following peripheral nerve injury

In our previous work utilizing the C3aR1 antagonist SB290157, we saw a transient attenuation of the maintenance of mechanical allodynia following peripheral nerve injury for approximately two hours post intrathecal or intraperitoneal injection. In contrast, C3aR1 ASO administration either before peripheral nerve injury or after the establishment of mechanical allodynia was unable to disrupt the development or maintenance of hypersensitivity. There are a few potential reasons that the antagonist might be working more effectively than the C3aR1 ASO at disrupting pain-related behaviors. Firstly, the

antagonist is known to have a number of off-target effects that might be disrupting other inflammatory mediators to attenuate hypersensitivity (Proctor et al., 2004). Additionally, the antagonist is likely binding to and antagonizing C3aR1 located on subarachnoid macrophages. These cells still have C3aR1 expression following C3aR1 ASO, therefore their activity might be a contributing factor to the remaining pain behavior seen in these mice.

Spinal cord injury in male mice increases C3aR1 expression in a time-dependent manner

Our work in SNI found time-dependent upregulation of C3aR1 specifically in microglia following peripheral nerve injury (Doolen et al., 2017). We aimed to examine whether changes in microglial C3aR1 expression in the spinal cord occur following SCI, a central model of neuropathic pain. Notably, C3aR1 upregulation has been reported after SCI (Chen et al., 2013). It was important for us to examine expression levels after injury prior to assessing the effects of C3aR1 knockdown on pain-related behavior after SCI. Following SCI, microglia at the injury site are rapidly activated and produce various pro-inflammatory signaling mediators (David & Kroner, 2011; Huang et al., 2013; Pineau, Sun, Bastien, & Lacroix, 2010). Activated microglia appear to contribute to SCI-induced chronic pain, since microglial inhibitor treatment or microglial depletion reverses this pain phenotype (Hains, 2006b; Zhao, Waxman, & Hains, 2007b). Our results indicate a robust and early upregulation of C3aR1 specifically in microglia following spinal cord injury. This increase in microglial C3aR1 was highest during the acute phases of injury, steadily decreasing over time. These results point to a potentially important role in signaling through C3aR1 immediately following injury. The increase in C3aR1 expression we visualized occurred as many as 8-9 spinal cord sections below injury, which indicates widespread neuroinflammation throughout the length of the spinal cord following thoracic

injury. At 50 days following spinal cord injury, the expression of C3aR1 had returned to sham levels, whereas the marker for microglia remained elevated. This indicates that neuroinflammation may persist throughout the chronic phase of injury, through mechanisms other than complement activation. Previous work has shown that decreasing components of the alternative complement system, such as Factor B or C3, prior to spinal cord injury was associated with increased tissue sparing, decreased inflammatory cell infiltration, and improvement in functional recovery (Qiao et al., 2010, 2006). Our findings in light of the existing literature led us to conclude that any intervention we tried should occur during the acute phase of injury, preferably as close to the date of injury as was feasible.

In chapter two, we examined sensory changes that occur following spinal cord injury. Using the cotton swab assay, we found a dramatic loss of light touch sensitivity. This was most likely mediated through a conduction block of low threshold mechanoreceptors, due to damage in the dorsal columns. In addition to examining C3aR1 and Iba1 expression below the level of injury, we also looked at cervical sections to assess changes in receptor expression occurring in the dorsal columns. We visualized C3aR1-ir and Iba1-ir in the gracile fasciculus of the cervical spinal cord of SCI mice. Following spinal cord injury, damage to the dorsal portion of the cord causes axonal degeneration in the dorsal columns (James et al., 2011). Following the induction of demyelination, there is rapid and robust accumulation of activated microglia and macrophages at the site of the injured axons (Cao & He, 2013; Hiremath et al., 1998; Remington, Babcock, Zehntner, & Owens, 2007). These microglia are responsible for clearing debris, to remove damaged tissue and aide in remyelination (Glezer, Simard, & Rivest, 2007; Lampron et al., 2015). The robust and long-lasting immune activation

occurring in the gracile fasciculus is a potential contributor to the altered sensitivity we see in our SCI mice.

Treatment with C3aR1 ASO 3 days following a mild or moderate thoracic contusion SCI does not impact development of pain-related behavior in male ICR mice:

For our intervention during an acute timepoint following SCI, we did not see any changes in evoked or spontaneous measures of pain-related behavior. We assessed mechanical sensitivity with von frey filaments, thermal hyperalgesia with the Hargreaves apparatus, and spontaneous pain/wellness with the burrowing assay. There is inherent variability in whether SCI leads to pain-related behavior following SCI in mice. Our work covered in chapter two found that injury severity influences the development of many of these pain-related behaviors. When we ran correlations comparing injury severity to behavior, there were differences in Hargreaves latency between SCI mice treated with C3aR1 ASO compared to the vehicle control, but only in the moderate 75 kdyn cohort. Overall, we did not find a significant impact of the C3aR1 ASO on pain-related behaviors after SCI. The variability in injury severity and whether mice develop hypersensitivity following SCI should be kept in mind as a potential complication to effectively assessing the efficacy of the ASO.

Spinal cord injury induces a loss of light touch sensitivity that is partially attenuated by administration of C3aR1 ASO during the acute phase of injury

In mice and rats, contusion spinal cord injury leads to a lesion in the spinal cord that encompasses the dorsal columns at the level of injury (Attwell et al., 2018; James et al., 2011). This disrupts the flow of touch information being sent from the periphery, which we have detected in our SCI mice. When comparing responses in mice that received vehicle or C3aR1 ASO, we found that the vehicle group had significantly lower thresholds than naïve mice, sham vehicle mice, and sham that received C3aR1 ASO. SCI mice that received C3aR1 ASO have higher response percentages than their vehicle counterparts, but it wasn't until we separated out subjects high and low day one BMS scores that we found a significant effect. The C3aR1 antisense significantly attenuated the loss of light touch sensitivity specifically in the mice that were less injured on day one. When we correlated injury severity to cotton swab responses, we found in both the mild and moderate cohorts, that SCI mice that receive vehicle have no correlation between injury severity and whether they respond to the stimulus. This is in contrast to the C3aR1 ASO group, which has a highly positive correlation between injury severity and percent response, indicating that less injured mice were more likely to respond to the cotton swab stimulus compared to their more injured counterparts.

Electrophysiological recordings from teased dorsal root fibers found that following SCI, rats have a complete conduction block in ascending dorsal column axons during the acute phases of injury (James et al., 2011). Conduction across the lesion improves slightly over time, but still remains significantly reduced during the chronic phase of injury. Interestingly, though there were still a large number of demyelinated fibers in the dorsal columns during the chronic phase, there was a subpopulation of axons that remained myelinated but were unable to conduct action potentials (James et al., 2011). As a whole, our results point to a potentially protective role of knocking down the C3aR1 receptor in the context of spinal

cord injury, specifically in mice that are less severely injured, but further examination of this is necessary.

Non-targeting Control ASO induces thermal hyperalgesia and C3aR1 upregulation following SCI

In order to examine potential target-independent effects of the ASO, we utilized a control ASO that has no known target in mice. Our results point to potential immune activation elicited by the control ASO, which is capable of causing thermal hypersensitivity and dramatic increases in C3aR1 expression. These changes were long-lasting, still present at six weeks post-ASO treatment. Unpublished work from Ionis Pharmaceuticals has found that there are some control ASOs that are capable of increasing the amount of C3 mRNA, the precursor to C3a, one of the ligands for C3aR1 (unpublished, data not shown). Though there was not an increase of Iba1 expression in the lumbar cord of the control ASO subjects, it is still likely that the increase in C3aR1 was due to immune activation. Iba1 stands for ionized calcium binding adaptor molecule 1 (Ito et al., 1998), and in mammalian cells it is an actin-binding protein expressed in microglia and macrophages (Sasaki, Ohsawa, Kanazawa, Kohsaka, & Imai, 2001). Iba1 enhances membrane ruffling and Rac signaling, is involved in phagocytosis, and can enhance lymphocyte migration (Ohsawa, Imai, Kanazawa, Sasaki, & Kohsaka, 2000). C3aR1 is chiefly located on microglia and macrophages, the immune cells of the spinal cord and surrounding tissues. Activation of C3aR1 by its ligand elicits calcium transients in microglia, and following injury the receptor is specifically upregulated in immune cells (Doolen et al., 2017). These findings point to the importance of choosing control ASOs

that do not elicit immune activation, and additionally uncovers that C3aR1 is a potentially useful marker to examine for whether an ASO elicits an immune response.

In summary, we show that the C3aR1 ASO developed by Ionis Pharmaceuticals effectively knocks down expression of C3aR1, at both the mRNA and protein level. The knockdown of C3aR1 is near-complete in microglia in the parenchyma of the spinal cord, but is less robust in subarachnoid macrophages apposed to the spinal cord. Knocking down C3aR1 expression did not alter the development or maintenance of hypersensitivity behaviors in either injury model. There were promising results pointing to a potentially protective effect of knocking down the C3aR1 receptor during the acute phase of spinal cord injury. We found that knockdown attenuated the loss of light touch sensitivity seen in spinal cord injury animals. Lastly our findings utilizing the control ASO point to C3aR1 as a potentially important marker to screen for when assessing whether an ASO causes immune activation.

OVERALL DISCUSSION

Summary of Findings

The research in this dissertation is the first to examine the involvement of the complement-3a receptor (C3aR1) in peripheral and central neuropathic pain. In chapter one, it was found that microglial C3aR1 is upregulated following peripheral injury, and the receptor is involved in hypersensitivity partially mediated by the neuropeptide TLQP-21. Chapter two presented the most thorough characterization of sensory changes that occur following spinal cord injury in male mice to date. For the first time, it was found that spinal cord injury induces a loss of light-touch sensitivity in male mice, whereas pain behavior was influenced by injury severity. In chapter three, a novel antisense oligonucleotide was used to knock down C3aR1 expression in peripheral nerve injury and spinal cord injury. The C3aR1 ASO had variable results, but had a potentially protective role in spinal cord injury. Additionally, it was found that C3aR1 is a marker that should be examined in future screens for ASO-mediated neuroinflammation. This work highlights the potential relevance of C3aR1 as a therapeutic target following injury, and uncovers the complex role complement receptor-mediated immune signaling has in neuropathic pain.

Significance

The work from this thesis fits into a broad field of research studying neuroimmune interactions in chronic pain. Microglia in the spinal cord are constantly surveying the environment to respond to endogenous signals indicating injury, and complement system recruitment is a key component to this response (Hong et al., 2016; Schafer et al., 2012; Vasek et al., 2016). There are currently a large number of preclinical, clinical trials, and existing therapies that target components of the complement system to treat a number of disorders (Ricklin & Lambris, 2016; Ricklin, Mastellos, Reis, & Lambris, 2017). The most widely used therapy is an antibody to C5, called eculizumab, used to treat the orphan disease atypical haemolytic uraemic syndrome, a deadly disease affecting kidney function. Clinical trials are underway targeting C3 and C3 convertase, which is responsible for the breakdown of C3 into C3a and C3b. These therapies are being developed for use in transplant patients, and lung disorders. Though microglia are considered a key component of the development and maintenance of neuropathic and inflammatory pain, the current therapies aimed at reducing microglial signaling are limited. The most widely used existing therapy for antagonizing microglia is minocycline, but a number of off-target effects and unwanted symptoms reduce the desirability of using minocycline to treat chronic pain (Haight, Forman, Cordonnier, James, & Tawfik, 2019). Specifically targeting complement activation, particular reducing signaling through C3aR1, remains a promising avenue to reduce microglial signaling while avoiding side effects and the vulnerabilities inherent in reducing widespread immune function.

Limitations

The inspiration for this thesis was shaped by previous work from the Vulchanova lab on the neuropeptide precursor VGF, and the biologically active C-terminal peptides. Once the receptor for TLQP-21 was found to be C3aR1, it became possible to study this ligand and receptor interaction. Much of the previous work focused on reducing TLQP-21 signaling, and then measuring the behavioral effects (Fairbanks et al., 2014). The work presented in this thesis targeted the receptor's involvement in neuropathic pain, but C3aR1 has another ligand, C3a, that is an important signaling factor in the complement cascade (Mathern & Heeger, 2015). C3a and its precursor C3 has been implicated in inflammatory and neuropathic pain (Jang et al., 2010; Levin et al., 2008). It is currently unknown what the relative contribution of TLQP-21 versus C3a are in any C3aR1 activation occurring following peripheral or central nervous system injury. Therefore it was impossible to decipher if there was a primary signaling mediator that was specifically affected by knocking down C3aR1, or if TLQP-21 and C3a were equally impacted.

The biggest limitation of the experiments presented in this thesis was the variability of the spinal cord injuries. The complexity of the surgery and inconsistencies between injuries is a known issue in the spinal cord injury field. This variability is a double-edged sword. Having a heterogeneous population to study more closely recapitulates the individual variability present in the human population. This is important for assessment of broadly beneficial therapies. A drawback of this heterogeneity is that it can be difficult to parse the effects of various interventions. The importance of proper surgical training, in addition to having appropriate controls and an adequately powered experimental design is vital.

Another limitation that we encountered throughout our experiments was effectively reducing signaling through C3aR1. Our experiments in chapter one utilized the antagonist SB290157, which is known to have agonist activity in tissues with high expression of C3aR1 (Mathieu et al., 2005; Therien et al., 2014). It also antagonizes other unknown targets (Proctor et al., 2004). We encountered this issue in experiments not presented in this thesis, where the antagonist had activity in a global C3aR1 knockout mouse (unpublished work). We aimed to explore reducing C3aR1 signaling without off-target effects by using a novel antisense oligonucleotide targeting C3aR1 for knockdown. Though the ASO completely knocked down C3aR1 expression in parenchymal microglia, the subarachnoid macrophages still exhibit expression. The functional relevance of this cell population in pain-related behavior is currently unknown. A floxed tdTomato-C3aR reporter knock-in mouse was developed, which has the potential of knocking down C3aR1 expression depending on which Cre mouse line it is crossed with (Quell et al., 2017). Using a CX3CR1-CreER mouse, C3aR1 would be able to be deleted specifically from microglia and macrophages. This would be a potential way to examine complete knockdown of C3aR1 that can be turned on in an adult mouse to avoid compensatory mechanisms that take place during development.

Future Directions

Much of the work presented in this thesis has been examining how reducing signaling through C3aR1, primarily located on microglia, can influence the development of neuropathic pain. One area of research that still needs to be covered are the molecular consequences of microglial C3aR1 activation in this process. Activation of C3aR1 can

mediate apoptotic cell death, demyelination, and activation of resting microglia and astrocytes. What proinflammatory factors are released by microglia upon activation of C3aR1? Additionally, what are the consequences of this on neuronal activity? Microglia are capable of releasing ATP, proinflammatory cytokines and chemokines, and other pronociceptive products (Hawthorne & Popovich, 2011; Imura et al., 2013; H. Liu et al., 2016). Our hypothesis is that activation of microglial C3aR1 leads to neuronal hyperexcitability, contributing to central sensitization and the generation of neuropathic pain. There are a few ways to probe this question, including stimulating microglial cultures with C3a and TLQP-21 and measuring cytokines released via ELISAs. This alone would be insufficient to answer the question though, as microglial cultures lack the complex cellular environment present in the dorsal horn. Calcium imaging and/or electrophysiology in spinal cord slices and *in vivo* in intact spinal cord is capable of probing the short-term consequences of microglial C3aR1 activation on neuronal activity. Preliminary work from the Vulchanova lab has found using *in vivo* electrophysiology recordings that bathing the exposed lumbar dorsal horn with TLQP-21 is capable of significantly increasing the number of wide dynamic range (WDR) neurons that responded to pinch over saline controls (unpublished). What would be interesting to examine is whether C3aR1 ASO knockdown of parenchymal microglia abolished this effect, or if this increase in WDR responses are primarily due to the subarachnoid macrophages that retain C3aR1 expression even after treatment with C3aR1 ASO.

Another area of research that can be explored following this thesis work is the function of C3aR1 expressing subarachnoid macrophages. There are very few studies examining non-parenchymal macrophages, searching for their function in the central nervous system. A recent study examined molecular signatures of these cells, which they dubbed border-

associated macrophages, or BAMs (Van Hove et al., 2019). They found that non-parenchymal macrophages are extremely heterogeneous, with tissue markers varying widely based on whether these macrophages were isolated from dura mater, choroid plexus, or subdural meninges. These diverse molecular signatures pointed toward specialization of these cells based on location, which potentially impacts their function. Those studies were examining BAMs of the brain, whereas our work found these C3aR1 expressing macrophages surrounding the spinal cord. Future work can probe the molecular signatures of these cells to uncover their heterogeneity and gain insight into their potential function depending on what they express. Once more information is known regarding these cells, peripherally-restricted knockdown of specific subpopulations of cells can probe their involvement in pathological processes.

Another future direction that can build upon the work presented in this thesis is to examine further the role of C3aR1 in damage following spinal cord injury. We found a potentially protective role of C3aR1 knockdown on the loss of light touch after SCI, specifically in mice with higher locomotor scores on day one. Work by James et al found a subset of still myelinated but functionally silent set of axons in the dorsal columns that were capable of being recruited to conduct action potentials when the lesion area was cooled. Future work could record from SCI mice and see if subjects that receive C3aR1 ASO exhibit increased conduction across the lesion than vehicle controls. Additionally, the spinal cords from SCI mice that received vehicle or C3aR1 ASO are going to be examined for differences in demyelinated regions and myelin breakdown products.

Overall, the work in this thesis highlights the potential relevance of C3aR1 as a therapeutic target following injury, and uncovers the complex role complement receptor-mediated immune signaling has in neuropathic pain.

CITATIONS

- Andrews, N., Legg, E., Lisak, D., Issop, Y., Richardson, D., Harper, S., ... Rice, A. S. C. (2012). Spontaneous burrowing behaviour in the rat is reduced by peripheral nerve injury or inflammation associated pain. *European Journal of Pain*. <https://doi.org/10.1016/j.ejpain.2011.07.012>
- Attwell, C. L., van Zwieten, M., Verhaagen, J., & Mason, M. R. J. (2018). The Dorsal Column Lesion Model of Spinal Cord Injury and Its Use in Deciphering the Neuron-Intrinsic Injury Response. *Developmental Neurobiology*. <https://doi.org/10.1002/dneu.22601>
- Austin, P. J., & Moalem-Taylor, G. (2010). The neuro-immune balance in neuropathic pain: Involvement of inflammatory immune cells, immune-like glial cells and cytokines. *Journal of Neuroimmunology*. <https://doi.org/10.1016/j.jneuroim.2010.08.013>
- Bangert, C., Brunner, P. M., & Stingl, G. (2011). Immune functions of the skin. *Clinics in Dermatology*. <https://doi.org/10.1016/j.clindermatol.2011.01.006>
- Bartolomucci, A., La Corte, G., Possenti, R., Locatelli, V., Rigamonti, A. E., Torsello, A., ... Moles, A. (2006). TLQP-21, a VGF-derived peptide, increases energy expenditure and prevents the early phase of diet-induced obesity. *Proceedings of the National Academy of Sciences*. <https://doi.org/10.1073/pnas.0606102103>
- Bartolomucci, Alessandro, Possenti, R., Mahata, S. K., Fischer-Colbrie, R., Loh, Y. P., & Salton, S. R. J. (2011). The extended granin family: Structure, function, and biomedical implications. *Endocrine Reviews*. <https://doi.org/10.1210/er.2010-0027>
- Basso, D. M., Fisher, L. C., Anderson, A. J., Jakeman, L. B., Mctigue, D. M., & Popovich, P. G. (2006). Basso Mouse Scale for Locomotion Detects Differences in Recovery after Spinal Cord Injury in Five Common Mouse Strains. *Journal of Neurotrauma*, 23(5), 635–659. <https://doi.org/10.1089/neu.2006.23.635>
- Benoliel, R., Svensson, P., Evers, S., Wang, S.-J., Barke, A., Korwisi, B., ... Treede, R.-D. (2019). The IASP classification of chronic pain for ICD-11. *PAIN*. <https://doi.org/10.1097/j.pain.0000000000001435>
- Berić, A., Dimitrijević, M. R., & Lindblom, U. (1988). Central dysesthesia syndrome in spinal cord injury patients. *Pain*. [https://doi.org/10.1016/0304-3959\(88\)90155-8](https://doi.org/10.1016/0304-3959(88)90155-8)
- Biryukov, S., & Stoute, J. A. (2018). The complement system. In *Complement Activation in Malaria Immunity and Pathogenesis*. https://doi.org/10.1007/978-3-319-77258-5_1
- Boldt, I., Eriks-Hoogland, I., Brinkhof, M. W. G., de Bie, R., Joggi, D., & von Elm, E. (2014). Non-pharmacological interventions for chronic pain in people with spinal cord injury. *Cochrane Database of Systematic Reviews*. <https://doi.org/10.1002/14651858.CD009177.pub2>
- Bonin, R. P., Bories, C., & De Koninck, Y. (2014). A simplified up-down method (SUDO)

- for measuring mechanical nociception in rodents using von Frey filaments. *Molecular Pain*. <https://doi.org/10.1186/1744-8069-10-26>
- Bourquin, A. F., Süveges, M., Pertin, M., Gilliard, N., Sardy, S., Davison, A. C., ... Decosterd, I. (2006). Assessment and analysis of mechanical allodynia-like behavior induced by spared nerve injury (SNI) in the mouse. *Pain*. <https://doi.org/10.1016/j.pain.2005.10.036>
- Bryce, T. N., Biering-Sørensen, F., Finnerup, N. B., Cardenas, D. D., Defrin, R., Lundeberg, T., ... Dijkers, M. (2012). International Spinal Cord Injury Pain Classification: Part I. Background and description. *Spinal Cord*, 50(6), 413–417. <https://doi.org/10.1038/sc.2011.156>
- Cao, L., & He, C. (2013). Polarization of macrophages and microglia in inflammatory demyelination. *Neuroscience Bulletin*. <https://doi.org/10.1007/s12264-013-1324-0>
- Castany, S., Gris, G., Vela, J. M., Verdú, E., & Boadas-Vaello, P. (2018). Critical role of sigma-1 receptors in central neuropathic pain-related behaviours after mild spinal cord injury in mice. *Scientific Reports*, 8(1), 1–13. <https://doi.org/10.1038/s41598-018-22217-9>
- Cero, C., Vostrikov, V. V., Verardi, R., Severini, C., Gopinath, T., Braun, P. D., ... Bartolomucci, A. (2014). The TLQP-21 peptide activates the G-protein-coupled receptor C3aR1 via a folding-upon-binding mechanism. *Structure*. <https://doi.org/10.1016/j.str.2014.10.001>
- Chaplan, S. R., Bach, F. W., Pogrel, J. W., Chung, J. M., & Yaksh, T. L. (1994). Quantitative assessment of tactile allodynia in the rat paw. *Journal of Neuroscience Methods*.
- Chen, K., Deng, S., Lu, H., Zheng, Y., Yang, G., Kim, D., & Cao, Q. (2013). *RNA-Seq Characterization of Spinal Cord Injury Transcriptome in Acute / Subacute Phases: A Resource for Understanding the Pathology at the Systems Level*. 8(8), 1–19. <https://doi.org/10.1371/journal.pone.0072567>
- Cheriyian, T., Ryan, D. J., Weinreb, J. H., Cheriyian, J., Paul, J. C., Lafage, V., ... Errico, T. J. (2014). Spinal cord injury models: A review. *Spinal Cord*, 52(8), 588–595. <https://doi.org/10.1038/sc.2014.91>
- Corder, G., Siegel, A., Intondi, A. B., Zhang, X., Zadina, J. E., & Taylor, B. K. (2010). *A Novel Method to Quantify Histochemical Changes Throughout the Mediolateral Axis of the Substantia Gelatinosa After Spared Nerve Injury: Characterization with TRPV1 and Substance P*. 11(4), 388–398. <https://doi.org/10.1016/j.jpain.2009.09.008>
- Cowie, A. M., Moehring, F., O'Hara, C., & Stucky, C. L. (2018). Optogenetic Inhibition of CGRPα Sensory Neurons Reveals Their Distinct Roles in Neuropathic and Incisional Pain. *The Journal of Neuroscience*, 38(25), 5807–5825. <https://doi.org/10.1523/jneurosci.3565-17.2018>

- Cui, J. G., Holmin, S., Mathiesen, T., Meyerson, B. A., & Linderöth, B. (2000). Possible role of inflammatory mediators in tactile hypersensitivity in rat models of mononeuropathy. *Pain*. [https://doi.org/10.1016/S0304-3959\(00\)00331-6](https://doi.org/10.1016/S0304-3959(00)00331-6)
- D'Mello, R., & Dickenson, A. H. (2008). Spinal cord mechanisms of pain. *British Journal of Anaesthesia*. <https://doi.org/10.1093/bja/aen088>
- David, S., & Kroner, A. (2011). Repertoire of microglial and macrophage responses after spinal cord injury. *Nature Reviews Neuroscience*, 12(7), 388–399. <https://doi.org/10.1038/nrn3053>
- Davoody, L., Quiton, R. L., Lucas, J. M., Ji, Y., Keller, A., & Masri, R. (2011). Conditioned place preference reveals tonic pain in an animal model of central pain. *Journal of Pain*. <https://doi.org/10.1016/j.jpain.2011.01.010>
- Davoust, N., Jones, J., Stahel, P. F., Ames, R. S., & Barnum, S. R. (1999). Receptor for the C3a anaphylatoxin is expressed by neurons and glial cells. *GLIA*. [https://doi.org/10.1002/\(SICI\)1098-1136\(199905\)26:3<201::AID-GLIA2>3.0.CO;2-M](https://doi.org/10.1002/(SICI)1098-1136(199905)26:3<201::AID-GLIA2>3.0.CO;2-M)
- Deacon, R. M.J. (2009). Burrowing: A sensitive behavioural assay, tested in five species of laboratory rodents. *Behavioural Brain Research*. <https://doi.org/10.1016/j.bbr.2009.01.007>
- Deacon, Robert M.J. (2006). Burrowing in rodents: A sensitive method for detecting behavioral dysfunction. *Nature Protocols*. <https://doi.org/10.1038/nprot.2006.19>
- Decosterd, I., & Woolf, C. J. (2000). Spared nerve injury: An animal model of persistent peripheral neuropathic pain. *Pain*. [https://doi.org/10.1016/S0304-3959\(00\)00276-1](https://doi.org/10.1016/S0304-3959(00)00276-1)
- Deuis, J. R., Dvorakova, L. S., & Vetter, I. (2017). Methods Used to Evaluate Pain Behaviors in Rodents. *Frontiers in Molecular Neuroscience*. <https://doi.org/10.3389/fnmol.2017.00284>
- Dhandapani, R., Arokiaraj, C. M., Taberner, F. J., Pacifico, P., Raja, S., Nocchi, L., ... Heppenstall, P. A. (2018). Control of mechanical pain hypersensitivity in mice through ligand-targeted photoablation of TrkB-positive sensory neurons. *Nature Communications*, 9(1). <https://doi.org/10.1038/s41467-018-04049-3>
- Dias, N., & Stein, C. A. (2002). Antisense oligonucleotides: basic concepts and mechanisms. *Molecular Cancer Therapeutics*.
- Dijkers, M., Bryce, T., & Zanca, J. (2009). *Prevalence of chronic pain after traumatic spinal cord injury: A systematic review*. 46(1), 13–30. <https://doi.org/10.1682/JRRD.2008.04.0053>
- Doolen, S., Cook, J., Riedl, M., Kitto, K., Kohsaka, S., Honda, C. N., ... Vulchanova, L. (2017). Complement 3a receptor in dorsal horn microglia mediates pronociceptive neuropeptide signaling. *GLIA*. <https://doi.org/10.1002/glia.23208>
- Dubin, A. E., & Patapoutian, A. (2010). Nociceptors: The sensors of the pain pathway.

- Journal of Clinical Investigation*. <https://doi.org/10.1172/JCI42843>
- Eide, P. K., Jørum, E., & Stenehjem, A. E. (1996). Somatosensory findings in patients with spinal cord injury and central dysaesthesia pain. *Journal of Neurology Neurosurgery and Psychiatry*, 60(4), 411–415. <https://doi.org/10.1136/jnnp.60.4.411>
- Elg, S., Marmigere, F., Mattsson, J. P., & Ernfors, P. (2007). Cellular subtype distribution and developmental regulation of TRPC channel members in the mouse dorsal root ganglion. *Journal of Comparative Neurology*. <https://doi.org/10.1002/cne.21351>
- Evers, M. M., Toonen, L. J. A., & van Roon-Mom, W. M. C. (2015). Antisense oligonucleotides in therapy for neurodegenerative disorders. *Advanced Drug Delivery Reviews*. <https://doi.org/10.1016/j.addr.2015.03.008>
- Fairbanks, C. A., Peterson, C. D., Speltz, R. H., Riedl, M. S., Kitto, K. F., Dykstra, J. A., ... Vulchanova, L. (2014). The VGF-derived peptide TLQP-21 contributes to inflammatory and nerve injury-induced hypersensitivity. *Pain*, 155(7), 1229–1237. <https://doi.org/10.1016/j.pain.2014.03.012>
- Finnerup, N. B., & Jensen, T. S. (2004). Spinal cord injury pain - Mechanisms and treatment. *European Journal of Neurology*. <https://doi.org/10.1046/j.1351-5101.2003.00725.x>
- Finnerup, N. B., Johannesen, I. L., Fuglsang-Frederiksen, A., Bach, F. W., & Jensen, T. S. (2003). Sensory function in spinal cord injury patients with and without central pain. *Brain*. <https://doi.org/10.1093/brain/awg007>
- Finnerup, Nanna Brix, & Bastrup, C. (2012). Spinal cord injury pain: Mechanisms and management. *Current Pain and Headache Reports*, 16(3), 207–216. <https://doi.org/10.1007/s11916-012-0259-x>
- Garrison, S. R., Dietrich, A., & Stucky, C. L. (2011). TRPC1 contributes to light-touch sensation and mechanical responses in low-threshold cutaneous sensory neurons. *Journal of Neurophysiology*, 107(3), 913–922. <https://doi.org/10.1152/jn.00658.2011>
- Gaskin, D. J., & Richard, P. (2012). The economic costs of pain in the United States. *Journal of Pain*. <https://doi.org/10.1016/j.jpain.2012.03.009>
- Gehrmann, J., Matsumoto, Y., & Kreutzberg, G. W. (1995). Microglia: Intrinsic immune effector cell of the brain. *Brain Research Reviews*. [https://doi.org/10.1016/0165-0173\(94\)00015-H](https://doi.org/10.1016/0165-0173(94)00015-H)
- Gensel, J. C., Donahue, R. R., Bailey, W. M., & Taylor, B. K. (2019). Sexual Dimorphism of Pain Control: Analgesic Effects of Pioglitazone and Azithromycin in Chronic Spinal Cord Injury. *Journal of Neurotrauma*, 5, 1–5. <https://doi.org/10.1089/neu.2018.6207>
- Glezer, I., Simard, A. R., & Rivest, S. (2007). Neuroprotective role of the innate immune system by microglia. *Neuroscience*. <https://doi.org/10.1016/j.neuroscience.2007.02.055>

- Gorp, S. Van, Kessels, A. G., Joosten, E. A., Kleef, M. Van, & Patijn, J. (2014). *Pain prevalence and its determinants after spinal cord injury: A systematic review*. 1–10. <https://doi.org/10.1002/ejp.522>
- Grice, E. A., & Segre, J. A. (2011). The skin microbiome. *Nature Reviews Microbiology*. <https://doi.org/10.1038/nrmicro2537>
- Guo, Q., Li, S., Liang, Y., Zhang, Y., Zhang, J., Wen, C., ... Su, B. (2010). Effects of C3 deficiency on inflammation and regeneration following spinal cord injury in mice. *Neuroscience Letters*. <https://doi.org/10.1016/j.neulet.2010.08.056>
- Hagen, E. M. (2015). Acute complications of spinal cord injuries. *World Journal of Orthopedics*. <https://doi.org/10.5312/wjo.v6.i1.17>
- Haight, E. S., Forman, T. E., Cordonnier, S. A., James, M. L., & Tawfik, V. L. (2019). Microglial Modulation as a Target for Chronic Pain. *Anesthesia & Analgesia*, 128(4), 737–746. <https://doi.org/10.1213/ANE.0000000000004033>
- Hains, B. C. (2006a). Activated Microglia Contribute to the Maintenance of Chronic Pain after Spinal Cord Injury. *Journal of Neuroscience*, 26(16), 4308–4317. <https://doi.org/10.1523/JNEUROSCI.0003-06.2006>
- Hains, B. C. (2006b). Activated Microglia Contribute to the Maintenance of Chronic Pain after Spinal Cord Injury. *Journal of Neuroscience*. <https://doi.org/10.1523/JNEUROSCI.0003-06.2006>
- Hama, A., & Sagen, J. (2007). Antinociceptive effect of cannabinoid agonist WIN 55,212-2 in rats with a spinal cord injury. *Experimental Neurology*. <https://doi.org/10.1016/j.expneurol.2006.09.002>
- Hannedouche, S., Beck, V., Leighton-Davies, J., Beibel, M., Roma, G., Oakeley, E. J., ... Bassilana, F. (2013). Identification of the C3a receptor (C3AR1) as the target of the VGF-derived peptide TLQP-21 in rodent cells. *Journal of Biological Chemistry*. <https://doi.org/10.1074/jbc.M113.497214>
- Harboe, M., & Mollnes, T. E. (2008). The alternative complement pathway revisited. *Journal of Cellular and Molecular Medicine*. <https://doi.org/10.1111/j.1582-4934.2008.00350.x>
- Hargreaves, K., Dubner, R., Brown, F., Flores, C., & Joris, J. (1988). A new and sensitive method for measuring thermal nociception in cutaneous hyperalgesia. *Pain*.
- Hawthorne, A. L., & Popovich, P. G. (2011). Emerging Concepts in Myeloid Cell Biology after Spinal Cord Injury. *Neurotherapeutics*. <https://doi.org/10.1007/s13311-011-0032-6>
- Helle, K. B. (2004). The granin family of uniquely acidic proteins of the diffuse neuroendocrine system: Comparative and functional aspects. *Biological Reviews of the Cambridge Philosophical Society*. <https://doi.org/10.1017/S146479310400644X>

- Hiremath, M. M., Saito, Y., Knapp, G. W., Ting, J. P. Y., Suzuki, K., & Matsushima, G. K. (1998). Microglial/macrophage accumulation during cuprizone-induced demyelination in C57BL/6 mice. *Journal of Neuroimmunology*. [https://doi.org/10.1016/S0165-5728\(98\)00168-4](https://doi.org/10.1016/S0165-5728(98)00168-4)
- Hong, S., Beja-Glasser, V. F., Nfonoyim, B. M., Frouin, A., Li, S., Ramakrishnan, S., ... Stevens, B. (2016). Complement and microglia mediate early synapse loss in Alzheimer mouse models. *Science*. <https://doi.org/10.1126/science.aad8373>
- Honore, P., Kage, K., Mikusa, J., Watt, A. T., Johnston, J. F., Wyatt, J. R., ... Lynch, K. (2002). Analgesic profile of intrathecal P2X3 antisense oligonucleotide treatment in chronic inflammatory and neuropathic pain states in rats. *Pain*. [https://doi.org/10.1016/S0304-3959\(02\)00032-5](https://doi.org/10.1016/S0304-3959(02)00032-5)
- Hoschouer, E. L., Basso, D. M., & Jakeman, L. B. (2010). Aberrant sensory responses are dependent on lesion severity after spinal cord contusion injury in mice. *Pain*. <https://doi.org/10.1016/j.pain.2009.11.023>
- Hoschouer, E. L., Yin, F. Q., & Jakeman, L. B. (2009). L1 cell adhesion molecule is essential for the maintenance of hyperalgesia after spinal cord injury. *Experimental Neurology*. <https://doi.org/10.1016/j.expneurol.2008.10.025>
- Huang, C., Han, X., Li, X., Lam, E., Peng, W., & Lou, N. (2013). *NIH Public Access*. 32(10), 3333–3338. <https://doi.org/10.1523/JNEUROSCI.1216-11.2012.Critical>
- Hunsberger, J. G., Newton, S. S., Bennett, A. H., Duman, C. H., Russell, D. S., Salton, S. R., & Duman, R. S. (2007). Antidepressant actions of the exercise-regulated gene VGF. *Nature Medicine*, 13(12), 1476–1482. <https://doi.org/10.1038/nm1669>
- Imura, Y., Morizawa, Y., Komatsu, R., Shibata, K., Shinozaki, Y., Kasai, H., ... Koizumi, S. (2013). *Microglia Release ATP by Exocytosis*. <https://doi.org/10.1002/glia.22517>
- International Association for the Study of Pain. (2017). IASP Terminology.
- Istituto, I., & Biomediche, S. (2013). *Neuropathic pain following spinal cord injury : what we know about mechanisms* ,. 3257–3261.
- Ito, D., Imai, Y., Ohsawa, K., Nakajima, K., Fukuuchi, Y., & Kohsaka, S. (1998). Microglia-specific localisation of a novel calcium binding protein, Iba1. *Molecular Brain Research*. [https://doi.org/10.1016/S0169-328X\(98\)00040-0](https://doi.org/10.1016/S0169-328X(98)00040-0)
- Jaggi, A. S., Jain, V., & Singh, N. (2011). Animal models of neuropathic pain. *Fundamental and Clinical Pharmacology*. <https://doi.org/10.1111/j.1472-8206.2009.00801.x>
- James, N. D., Bartus, K., Grist, J., Bennett, D. L. H., McMahon, S. B., & Bradbury, E. J. (2011). Conduction Failure following Spinal Cord Injury: Functional and Anatomical Changes from Acute to Chronic Stages. *Journal of Neuroscience*. <https://doi.org/10.1523/jneurosci.4306-11.2011>

- Jang, J. H., Clark, J. D., Li, X., Yorek, M. S., Usachev, Y. M., & Brennan, T. J. (2010). Nociceptive sensitization by complement C5a and C3a in mouse. *Pain*. <https://doi.org/10.1016/j.pain.2009.11.021>
- Jensen, T. S., & Finnerup, N. B. (2014). Allodynia and hyperalgesia in neuropathic pain: Clinical manifestations and mechanisms. *The Lancet Neurology*. [https://doi.org/10.1016/S1474-4422\(14\)70102-4](https://doi.org/10.1016/S1474-4422(14)70102-4)
- Ji, R. R., Kohno, T., Moore, K. A., & Woolf, C. J. (2003). Central sensitization and LTP: Do pain and memory share similar mechanisms? *Trends in Neurosciences*. <https://doi.org/10.1016/j.tins.2003.09.017>
- Jirkof, P. (2014). Burrowing and nest building behavior as indicators of well-being in mice. *Journal of Neuroscience Methods*, 234, 139–146. <https://doi.org/10.1016/j.jneumeth.2014.02.001>
- Jirkof, P., Cesarovic, N., Rettich, A., Nicholls, F., Seifert, B., & Arras, M. (2010). Burrowing Behavior as an Indicator of Post-Laparotomy Pain in Mice. *Frontiers in Behavioral Neuroscience*, 4(October), 1–9. <https://doi.org/10.3389/fnbeh.2010.00165>
- Johannes, C. B., Le, T. K., Zhou, X., Johnston, J. A., & Dworkin, R. H. (2010). The Prevalence of Chronic Pain in United States Adults: Results of an Internet-Based Survey. *Journal of Pain*. <https://doi.org/10.1016/j.jpain.2010.07.002>
- Kerr, B. J., & David, S. (2007). Pain behaviors after spinal cord contusion injury in two commonly used mouse strains. *Experimental Neurology*. <https://doi.org/10.1016/j.expneurol.2007.04.014>
- King, T., Vera-Portocarrero, L., Gutierrez, T., Vanderah, T. W., Dussor, G., Lai, J., ... Porreca, F. (2009). Unmasking the tonic-aversive state in neuropathic pain. *Nature Neuroscience*. <https://doi.org/10.1038/nn.2407>
- Kole, R., Krainer, A. R., & Altman, S. (2012). RNA therapeutics: Beyond RNA interference and antisense oligonucleotides. *Nature Reviews Drug Discovery*. <https://doi.org/10.1038/nrd3625>
- Koller, E., & Dean, N. M. (2006). Antisense Oligonucleotides. In *Cell Biology, Four-Volume Set*. <https://doi.org/10.1016/B978-012164730-8/50183-0>
- Kreutzberg, G. W. (1996). Microglia: A sensor for pathological events in the CNS. *Trends in Neurosciences*. [https://doi.org/10.1016/0166-2236\(96\)10049-7](https://doi.org/10.1016/0166-2236(96)10049-7)
- Kupper, T. S., & Fuhlbrigge, R. C. (2004). Immune surveillance in the skin: Mechanisms and clinical consequences. *Nature Reviews Immunology*. <https://doi.org/10.1038/nri1310>
- Lacroix-Fralish, M. L., Austin, J. S., Zheng, F. Y., Levitin, D. J., & Mogil, J. S. (2011). Patterns of pain: Meta-analysis of microarray studies of pain. *Pain*. <https://doi.org/10.1016/j.pain.2011.04.014>

- Lampron, A., Larochelle, A., Laflamme, N., Préfontaine, P., Plante, M.-M., Sánchez, M. G., ... Rivest, S. (2015). Inefficient clearance of myelin debris by microglia impairs remyelinating processes. *The Journal of Experimental Medicine*. <https://doi.org/10.1084/jem.20141656>
- Levi, A., Ferri, G. L., Watson, E., Possenti, R., & Salton, S. R. J. (2004). Processing, distribution, and function of VGF, a neuronal and endocrine peptide precursor. *Cellular and Molecular Neurobiology*.
<https://doi.org/10.1023/B:CEMN.0000023627.79947.22>
- Levin, M. E., Jin, J. G., Ji, R. R., Tong, J., Pomonis, J. D., Lavery, D. J., ... Chiang, L. W. (2008). Complement activation in the peripheral nervous system following the spinal nerve ligation model of neuropathic pain. *Pain*. <https://doi.org/10.1016/j.pain.2007.11.005>
- Lian, H., Yang, L., Cole, A., Sun, L., Chiang, A. C. A., Fowler, S. W., ... Zheng, H. (2015). NFκB-Activated Astroglial Release of Complement C3 Compromises Neuronal Morphology and Function Associated with Alzheimer's Disease. *Neuron*. <https://doi.org/10.1016/j.neuron.2014.11.018>
- Lin, W.-J., Jiang, C., Sadahiro, M., Bozdagi, O., Vulchanova, L., Alberini, C. M., & Salton, S. R. (2015). VGF and Its C-Terminal Peptide TLQP-62 Regulate Memory Formation in Hippocampus via a BDNF-TrkB-Dependent Mechanism. *Journal of Neuroscience*. <https://doi.org/10.1523/jneurosci.0584-15.2015>
- Liu, H., Leak, R. K., & Hu, X. (2016). Neurotransmitter receptors on microglia. *Stroke and Vascular Neurology*, 1(2), 52–58. <https://doi.org/10.1136/svn-2016-000012>
- Liu, T., Van Rooijen, N., & Tracey, D. J. (2000). Depletion of macrophages reduces axonal degeneration and hyperalgesia following nerve injury. *Pain*. [https://doi.org/10.1016/S0304-3959\(99\)00306-1](https://doi.org/10.1016/S0304-3959(99)00306-1)
- Mathern, D. R., & Heeger, P. S. (2015). Molecules great and small: The complement system. *Clinical Journal of the American Society of Nephrology*. <https://doi.org/10.2215/CJN.06230614>
- Mathieu, M. C., Sawyer, N., Greig, G. M., Hamel, M., Kargman, S., Ducharme, Y., ... Therien, A. G. (2005). The C3a receptor antagonist SB 290157 has agonist activity. *Immunology Letters*. <https://doi.org/10.1016/j.imlet.2005.03.003>
- Meisner, J. G., Marsh, A. D., & Marsh, D. R. (2010a). Loss of GABAergic Interneurons in Laminae I–III of the Spinal Cord Dorsal Horn Contributes to Reduced GABAergic Tone and Neuropathic Pain after Spinal Cord Injury. *Journal of Neurotrauma*, 27(4), 729–737. <https://doi.org/10.1089/neu.2009.1166>
- Meisner, J. G., Marsh, A. D., & Marsh, D. R. (2010b). Loss of GABAergic Interneurons in Laminae I–III of the Spinal Cord Dorsal Horn Contributes to Reduced GABAergic Tone and Neuropathic Pain after Spinal Cord Injury. *Journal of Neurotrauma*. <https://doi.org/10.1089/neu.2009.1166>

- Melzack, R., & Wall, P. D. (1965). Pain mechanisms: a new theory. *Science (New York, N.Y.)*.
- Millan, M. J. (1999). The induction of pain: An integrative review. *Progress in Neurobiology*. [https://doi.org/10.1016/S0301-0082\(98\)00048-3](https://doi.org/10.1016/S0301-0082(98)00048-3)
- Moss, A., Ingram, R., Koch, S., Theodorou, A., Low, L., Baccei, M., ... Fitzgerald, M. (2008). Origins, actions and dynamic expression patterns of the neuropeptide VGF in rat peripheral and central sensory neurones following peripheral nerve injury. *Molecular Pain*. <https://doi.org/10.1186/1744-8069-4-62>
- Nahin, R. L. (2015). Estimates of Pain Prevalence and Severity in Adults: United States, 2012. *Journal of Pain*. <https://doi.org/10.1016/j.jpain.2015.05.002>
- National Spinal Cord Injury Statistical Center. (2019). Spinal Cord Injury Facts and Figures at a Glance. *The Journal of Spinal Cord Medicine*, 37(3), 355–356. Retrieved from <http://www.ncbi.nlm.nih.gov/pubmed/26793805> <http://www.pubmedcentral.nih.gov/articlerender.fcgi?artid=PMC4064586>
- Ohsawa, K., Imai, Y., Kanazawa, H., Sasaki, Y., & Kohsaka, S. (2000). Involvement of Iba1 in membrane ruffling and phagocytosis of macrophages/microglia. *Journal of Cell Science*.
- Okun, A., DeFelice, M., Eyde, N., Ren, J., Mercado, R., King, T., & Porreca, F. (2011). Transient inflammation-induced ongoing pain is driven by TRPV1 sensitive afferents. *Molecular Pain*. <https://doi.org/10.1186/1744-8069-7-4>
- Orr, M. B., Simkin, J., Bailey, W. M., Kadambi, N. S., McVicar, A. L., Veldhorst, A. K., & Gensel, J. C. (2017). Compression Decreases Anatomical and Functional Recovery and Alters Inflammation after Contusive Spinal Cord Injury. *Journal of Neurotrauma*, 34(15), 2342–2352. <https://doi.org/10.1089/neu.2016.4915>
- Pannell, M., Labuz, D., Celik, M., Keye, J., Batra, A., Siegmund, B., & Machelska, H. (2016). Adoptive transfer of M2 macrophages reduces neuropathic pain via opioid peptides. *Journal of Neuroinflammation*. <https://doi.org/10.1186/s12974-016-0735-z>
- Peirs, C., & Seal, R. P. (2016). Neural circuits for pain: Recent advances and current views. *Science*. <https://doi.org/10.1126/science.aaf8933>
- Peng, W., Cotrina, M. L., Han, X., Yu, H., Bekar, L., Blum, L., ... Nedergaard, M. (2009). Systemic administration of an antagonist of the ATP-sensitive receptor P2X7 improves recovery after spinal cord injury. *Proceedings of the National Academy of Sciences*, 106(30), 12489–12493. <https://doi.org/10.1073/pnas.0902531106>
- Peterson, S. L., & Anderson, A. J. (2014). Complement and spinal cord injury: Traditional and non-traditional aspects of complement cascade function in the injured spinal cord microenvironment. *Experimental Neurology*, 258, 35–47. <https://doi.org/10.1016/j.expneurol.2014.04.028>

- Pineau, I., Sun, L., Bastien, D., & Lacroix, S. (2010). *Brain , Behavior , and Immunity Astrocytes initiate inflammation in the injured mouse spinal cord by promoting the entry of neutrophils and inflammatory monocytes in an IL-1 receptor / MyD88-dependent fashion*. 24, 540–553. <https://doi.org/10.1016/j.bbi.2009.11.007>
- Price, T. J., Cervero, F., & de Koninck, Y. (2005). Role of cation-chloride-cotransporters (CCC) in pain and hyperalgesia. *Current Topics in Medicinal Chemistry*.
- Price, T. J., & Prescott, S. A. (2015). Inhibitory regulation of the pain gate and how its failure causes pathological pain. *PAIN*. <https://doi.org/10.1097/j.pain.0000000000000139>
- Proctor, L. M., Arumugam, T. V., Shiels, I., Reid, R. C., Fairlie, D. P., & Taylor, S. M. (2004). Comparative anti-inflammatory activities of antagonists to C3a and C5a receptors in a rat model of intestinal ischaemia/reperfusion injury. *British Journal of Pharmacology*. <https://doi.org/10.1038/sj.bjp.0705819>
- Qiao, F., Atkinson, C., Kindy, M. S., Shunmugavel, A., Morgan, B. P., Song, H., & Tomlinson, S. (2010). The alternative and terminal pathways of complement mediate post-traumatic spinal cord inflammation and injury. *American Journal of Pathology*, 177(6), 3061–3070. <https://doi.org/10.2353/ajpath.2010.100158>
- Qiao, F., Atkinson, C., Song, H., Pannu, R., Singh, I., & Tomlinson, S. (2006). Complement plays an important role in spinal cord injury and represents a therapeutic target for improving recovery following trauma. *American Journal of Pathology*. <https://doi.org/10.2353/ajpath.2006.060248>
- Quell, K. M., Karsten, C. M., Kordowski, A., Almeida, L. N., Briukhovetska, D., Wiese, A. V., ... Köhl, J. (2017). Monitoring C3aR Expression Using a Floxed tdTomato-C3aR Reporter Knock-in Mouse. *The Journal of Immunology*. <https://doi.org/10.4049/jimmunol.1700318>
- Ransohoff, R. M., & Brown, M. A. (2012). Innate immunity in the central nervous system. *Journal of Clinical Investigation*. <https://doi.org/10.1172/JCI58644>
- Reichling, D. B., & Levine, J. D. (2009). Critical role of nociceptor plasticity in chronic pain. *Trends in Neurosciences*. <https://doi.org/10.1016/j.tins.2009.07.007>
- Remington, L. T., Babcock, A. A., Zehntner, S. P., & Owens, T. (2007). Microglial recruitment, activation, and proliferation in response to primary demyelination. *American Journal of Pathology*. <https://doi.org/10.2353/ajpath.2007.060783>
- Ren, K., & Dubner, R. (2010). Interactions between the immune and nervous systems in pain. *Nature Medicine*. <https://doi.org/10.1038/nm.2234>
- Ricklin, D., & Lambris, J. D. (2016). New milestones ahead in complement-targeted therapy. *Seminars in Immunology*. <https://doi.org/10.1016/j.smim.2016.06.001>
- Ricklin, D., Mastellos, D. C., Reis, E. S., & Lambris, J. D. (2017). The renaissance of

- Riedl, M. S., Braun, P. D., Kitto, K. F., Roiko, S. A., Anderson, L. B., Honda, C. N., ... Vulchanova, L. (2009). Proteomic Analysis Uncovers Novel Actions of the Neurosecretory Protein VGF in Nociceptive Processing. *Journal of Neuroscience*. <https://doi.org/10.1523/jneurosci.1127-09.2009>
- Ringkamp, M., & Meyer, R. A. (2010). Physiology of Nociceptors. In *The Senses: A Comprehensive Reference*. <https://doi.org/10.1016/B978-012370880-9.00146-8>
- Saadé, N. E., Baliki, M., El-Khoury, C., Hawwa, N., Atweh, S. F., Apkarian, A. V., & Jabbur, S. J. (2002). The role of the dorsal columns in neuropathic behavior: Evidence for plasticity and non-specificity. *Neuroscience*. [https://doi.org/10.1016/S0306-4522\(02\)00417-7](https://doi.org/10.1016/S0306-4522(02)00417-7)
- Salton, S. R., Fischberg, D. J., & Dong, K. W. (1991). Structure of the gene encoding VGF, a nervous system-specific mRNA that is rapidly and selectively induced by nerve growth factor in PC12 cells. *Molecular and Cellular Biology*.
- Sasaki, Y., Ohsawa, K., Kanazawa, H., Kohsaka, S., & Imai, Y. (2001). Iba1 is an actin-cross-linking protein in macrophages/microglia. *Biochemical and Biophysical Research Communications*. <https://doi.org/10.1006/bbrc.2001.5388>
- Sauer, R. S., Hackel, D., Morschel, L., Sahlbach, H., Wang, Y., Mousa, S. A., ... Rittner, H. L. (2014). Toll like receptor (TLR)-4 as a regulator of peripheral endogenous opioid-mediated analgesia in inflammation. *Molecular Pain*. <https://doi.org/10.1186/1744-8069-10-10>
- Schaefer, L. (2014). Complexity of danger: The diverse nature of damage-associated molecular patterns. *Journal of Biological Chemistry*. <https://doi.org/10.1074/jbc.R114.619304>
- Schafer, D. P., Lehrman, E. K., Kautzman, A. G., Koyama, R., Mardinly, A. R., Yamasaki, R., ... Stevens, B. (2012). Microglia sculpt postnatal neural circuits in an activity and complement-dependent manner. *Neuron*. <https://doi.org/10.1016/j.neuron.2012.03.026>
- Sezer, N. (2015). Chronic complications of spinal cord injury. *World Journal of Orthopedics*. <https://doi.org/10.5312/wjo.v6.i1.24>
- Siddall, P. J., McClelland, J. M., Rutkowski, S. B., & Cousins, M. J. (2003). A longitudinal study of the prevalence and characteristics of pain in the first 5 years following spinal cord injury. 103, 249–257. <https://doi.org/10.1016/S0>
- Sorge, R. E., LaCroix-Fralish, M. L., Tuttle, A. H., Sotocinal, S. G., Austin, J.-S., Ritchie, J., ... Mogil, J. S. (2011). Spinal Cord Toll-Like Receptor 4 Mediates Inflammatory and Neuropathic Hypersensitivity in Male But Not Female Mice. *Journal of Neuroscience*. <https://doi.org/10.1523/JNEUROSCI.3859-11.2011>

- Staniland, A. A., Clark, A. K., Wodarski, R., Sasso, O., Maione, F., D'Acquisto, F., & Malcangio, M. (2010). Reduced inflammatory and neuropathic pain and decreased spinal microglial response in fractalkine receptor (CX3CR1) knockout mice. *Journal of Neurochemistry*. <https://doi.org/10.1111/j.1471-4159.2010.06837.x>
- Stein, C., Clark, J. D., Oh, U., Vasko, M. R., Wilcox, G. L., Overland, A. C., ... Spencer, R. H. (2009). Peripheral mechanisms of pain and analgesia. *Brain Research Reviews*. <https://doi.org/10.1016/j.brainresrev.2008.12.017>
- Sufka, K. J. (1994). Conditioned place preference paradigm: a novel approach for analgesic drug assessment against chronic pain. *Pain*. [https://doi.org/10.1016/0304-3959\(94\)90130-9](https://doi.org/10.1016/0304-3959(94)90130-9)
- Sun, H., Ren, K., Zhong, C. M., Ossipov, M. H., Malan, T. P., Lai, J., & Porreca, F. (2001). Nerve injury-induced tactile allodynia is mediated via ascending spinal dorsal column projections. *Pain*. [https://doi.org/10.1016/S0304-3959\(00\)00392-4](https://doi.org/10.1016/S0304-3959(00)00392-4)
- Sun, T., Song, W. G., Fu, Z. J., Liu, Z. H., Liu, Y. M., & Yao, S. L. (2006). Alleviation of neuropathic pain by intrathecal injection of antisense oligonucleotides to p65 subunit of NF- κ B. *British Journal of Anaesthesia*. <https://doi.org/10.1093/bja/ael209>
- Sweitzer, S. M., Pahl, J. L., & DeLeo, J. A. (2006). Propentofylline attenuates vincristine-induced peripheral neuropathy in the rat. *Neuroscience Letters*. <https://doi.org/10.1016/j.neulet.2006.02.058>
- Tanabe, M., Ono, K., Honda, M., & Ono, H. (2009). Gabapentin and pregabalin ameliorate mechanical hypersensitivity after spinal cord injury in mice. *European Journal of Pharmacology*. <https://doi.org/10.1016/j.ejphar.2009.03.020>
- Tang, D., Kang, R., Coyne, C. B., Zeh, H. J., & Lotze, M. T. (2012). PAMPs and DAMPs: Signal 0s that spur autophagy and immunity. *Immunological Reviews*. <https://doi.org/10.1111/j.1600-065X.2012.01146.x>
- Taupenot, L., Harper, K. L., & O'Connor, D. T. (2003). The chromogranin-secretogranin family. *The New England Journal of Medicine*. <https://doi.org/10.1056/NEJMra021405>
- Thakker-Varia, S., Krol, J. J., Nettleton, J., Bilimoria, P. M., Bangasser, D. A., Shors, T. J., ... Alder, J. (2007). The Neuropeptide VGF Produces Antidepressant-Like Behavioral Effects and Enhances Proliferation in the Hippocampus. *Journal of Neuroscience*. <https://doi.org/10.1523/jneurosci.1898-07.2007>
- Therien, A. G., Baelder, R., & Kohl, J. (2014). Agonist Activity of the Small Molecule C3aR Ligand SB 290157. *The Journal of Immunology*. <https://doi.org/10.4049/jimmunol.174.12.7479>
- Thurman, J. M., & Holers, V. M. (2006). The central role of the alternative complement

pathway in human disease. *Journal of Immunology* (Baltimore, Md. : 1950).

- Treede, R.-D., Rief, W., Barke, A., Aziz, Q., Bennett, M. I., Benoliel, R., ... Wang, S.-J. (2015). A classification of chronic pain for ICD-11. *PAIN*. <https://doi.org/10.1097/j.pain.0000000000000160>
- Uematsu, S., & Akira, S. (2008). Pathogen recognition by innate immunity. *Skin Research*.
- Van Hove, H., Martens, L., Scheyltjens, I., De Vlamincx, K., Pombo Antunes, A. R., De Prijck, S., ... Movahedi, K. (2019). A single-cell atlas of mouse brain macrophages reveals unique transcriptional identities shaped by ontogeny and tissue environment. *Nature Neuroscience*. <https://doi.org/10.1038/s41593-019-0393-4>
- Vasek, M. J., Garber, C., Dorsey, D., Durrant, D. M., Bollman, B., Soung, A., ... Klein, R. S. (2016). A complement-microglial axis drives synapse loss during virus-induced memory impairment. *Nature*. <https://doi.org/10.1038/nature18283>
- Yang, Q., Wu, Z., Hadden, J. K., Odem, M. A., Zuo, Y., Crook, R. J., ... Walters, E. T. (2014). Persistent Pain after Spinal Cord Injury Is Maintained by Primary Afferent Activity. *Journal of Neuroscience*. <https://doi.org/10.1523/jneurosci.5316-13.2014>
- Zeilhofer, H. U., Benke, D., & Yevenes, G. E. (2011). Chronic Pain States: Pharmacological Strategies to Restore Diminished Inhibitory Spinal Pain Control. *Annual Review of Pharmacology and Toxicology*. <https://doi.org/10.1146/annurev-pharmtox-010611-134636>
- Zhang, B., Bailey, W. M., Kopper, T. J., Orr, M. B., Feola, D. J., & Gensel, J. C. (2015). Azithromycin drives alternative macrophage activation and improves recovery and tissue sparing in contusion spinal cord injury. *Journal of Neuroinflammation*, 12(1), 1–13. <https://doi.org/10.1186/s12974-015-0440-3>
- Zhao, P., Waxman, S. G., & Hains, B. C. (2007a). Extracellular Signal-Regulated Kinase-Regulated Microglia-Neuron Signaling by Prostaglandin E2 Contributes to Pain after Spinal Cord Injury. *Journal of Neuroscience*, 27(9), 2357–2368. <https://doi.org/10.1523/jneurosci.0138-07.2007>
- Zhao, P., Waxman, S. G., & Hains, B. C. (2007b). Modulation of Thalamic Nociceptive Processing after Spinal Cord Injury through Remote Activation of Thalamic Microglia by Cysteine Cysteine Chemokine Ligand 21. *Journal of Neuroscience*, 27(33), 8893–8902. <https://doi.org/10.1523/jneurosci.2209-07.2007>
- Zhuang, Z. Y., Kawasaki, Y., Tan, P. H., Wen, Y. R., Huang, J., & Ji, R. R. (2007). Role of the CX3CR1/p38 MAPK pathway in spinal microglia for the development of neuropathic pain following nerve injury-induced cleavage of fractalkine. *Brain, Behavior, and Immunity*. <https://doi.org/10.1016/j.bbi.2006.11.003>